
# Relació estructura-funció en la família de transportadors d'aminoàcids heteromultimèrics. Identificació d'una nova família de transportadors lisosomals

Raúl Estévez Povedano

UNITAT DE BIOQUÍMICA I BIOLOGIA MOLECULAR
DEPARTAMENT DE BIOQUÍMICA I BIOLOGIA MOLECULAR
FACULTAT DE BIOLOGIA
UNIVERSITAT DE BARCELONA

# RELACIÓ ESTRUCTURA-FUNCIÓ EN LA FAMÍLIA DE TRANSPORTADORS D'AMINOÀCIDS HETEROMULTIMÈRICS IDENTIFICACIÓ D'UNA NOVA FAMÍLIA DE TRANSPORTADORS LISOSOMALS

**RAÚL ESTÉVEZ POVEDANO**

Barcelona, desembre de 1999

PHYSIOLOGICAL REVIEWS
Vol. 78, No. 4, October 1998
*Printed in U.S.A.*

# Molecular Biology of Mammalian Plasma Membrane Amino Acid Transporters

MANUEL PALACÍN, RAÚL ESTÉVEZ, JOAN BERTRAN, AND ANTONIO ZORZANO

*Departament de Bioquímica i Biologia Molecular, Facultat de Biologia, Universitat de Barcelona, and Departament de Criobiologia i Terapia Cellular, Institut de Recerca Oncològica, Barcelona, Spain*



**Palacín, Manuel, Raúl Estévez, Joan Bertran, and Antonio Zorzano.** Molecular Biology of Mammalian Plasma Membrane Amino Acid Transporters. *Physiol. Rev.* 78: 969–1054, 1998.—Molecular biology entered the field of mammalian amino acid transporters in 1990–1991 with the cloning of the first GABA and cationic amino acid transporters. Since then, cDNA have been isolated for more than 20 mammalian amino acid transporters. All of them belong to four protein families. Here we describe the tissue expression, transport characteristics, structure-function relationship, and the putative physiological roles of these transporters. Wherever possible, the ascription of these transporters to known amino acid transport systems is suggested. Significant contributions have been made to the molecular biology of amino acid transport in mammals in the last 3 years, such as the construction of knockouts for the CAT-1 cationic amino acid transporter and the EAAT2 and EAAT3 glutamate transporters, as well as a growing number of studies aimed to elucidate the structure-function relationship of the amino acid transporter. In addition, the first gene (*rBAT*) responsible for an inherited disease of amino acid transport (cystinuria) has been identified. Identifying the molecular structure of amino acid transport systems of high physiological relevance (e.g., system A, L, N, and $x_c^-$) and of the genes responsible for other aminoacidurias as well as revealing the key molecular mechanisms of the amino acid transporters are the main challenges of the future in this field.

## I. INTRODUCTION

Amino acid transport across the plasma membrane mediates and regulates the flow of these ionic nutrients into cells and, therefore, participates in interorgan amino acid nutrition. In addition, for specific amino acids that act as neurotransmitters, synaptic modulators, or neurotransmitter precursors, transport across the plasma membrane ensures reuptake from the synaptic cleft, maintenance of a tonic level of their extracellular concentration, and supply of precursors in the central nervous system (for review, see Refs. 93, 96, 97, 505). Transfer of amino acids across the hydrophobic domain of the plasma membrane is mediated by proteins that recognize, bind, and transport these amino acids from the extracellular medium into the cell, or vice versa. In the early 1960s, after the pioneer work of Halvor N. Christensen's group, different substrate specificity transport systems for amino acids in mammalian cells (mainly erythrocytes, hepatocytes, and fibroblasts) were identified (reviewed in Ref. 96), and general properties of mammalian amino acid transport were revealed: stereospecificity (transport is faster for L-stereoisomers) and broad substrate specificity (several amino acids share a transport system). Since these initial studies, the main functional criteria used to define amino acid transporters have been *1*) the type of amino acid (acidic, zwitterionic, or basic as well as other characteristics of the side chain) the protein moves across the membrane, according to substrate specificity and kinetic properties, and *2*) the thermodynamic properties of the transport (whether the transporter is equilibrative or drives the organic substrate uphill). This functional classification

has been retained to date, since structural information on higher eukaryote amino acid transporters is incomplete.

Isolation of the first brain GABA transporter (184) in 1990 and the identification of the first cationic amino acid transporter in 1991 (281, 590) represent the starting points for the cloning of mammalian amino acid transporter genes. Several strategies have been used to identify mammalian amino acid transporters. During the 1980s, several groups attempted the purification of these transporters by different methods. Purification strategies have yielded few structural data, although for a couple of transporters related to neurotransmission (the GABA transporter GAT-1 and the glutamate transporter GLT-1), these data allowed microsequencing or generation of specific antibodies that have been used to isolate cDNA clones (184, 424). Alternative strategies and serendipity allowed the identification of up to 22 cDNA (including splice variants, but not species counterparts) for mammalian amino acid transporters or related proteins (see sect. II). This structural information is not complete. The genes identified seem to correspond to eight classic transport systems and their variants, whereas another eight of the major amino acid transport systems are unknown at the molecular level (see Table 1). An excellent review by Kilberg's group (342) describes the molecular biology of the amino acid transporters cloned up to 1995.

The molecular identification of amino acid transporters or related proteins leads to ongoing studies on the structure-function relationship and the molecular genetics of the pathology associated with these transporters. In this review, attention is paid to the molecular biology, structure-function relationship, physiological role, and human genetics of amino acid transporters. Regulation of plasma membrane amino acid transport in mammals is beyond the scope of the present review and has been extensively reviewed (96, 278, 350).

## A. Amino Acid Transport Systems in the Plasma Membrane of Mammalian Cells

Functional studies based on saturability of transport, substrate specificity, kinetic behavior, mode of energization, and mechanisms of regulation performed in perfused organs, isolated cells, and purified plasma membranes led to the identification of a mutiplicity of transport agencies in the plasma membrane of mammalian cells (for review, see Refs. 26, 94–96). The properties of some of the best-characterized amino acid transport systems are summarized in Table 1. From these studies it is evident that a particular transport system carries different amino acids and that amino acid transport systems show overlapping specificities. Different cells contain a distinct set of transport systems in their plasma membranes, as a combination of common or almost ubiquitous (e.g., systems A, ASC, L, $y^+$ and $X^-_{AG}$) and tissue-specific transport systems (e.g., systems $B^{o,+}$, $N^m$, and $b^{o,+}$ as well as variants of common transport systems). It has been proposed that this arrangement permits both fine regulation of substrate and cell-specific amino acid flows and economy in the number of structures mediating cellular and interorgan amino acid fluxes (96, 97).

### 1. *Common systems for zwitterionic amino acids*

The zwitterionic amino acid transport systems A, ASC, and L are present in almost all cell types. Systems A and ASC mediate symport of amino acid with small side chain with sodium, and system L mediates uniport of amino acids with bulky side chains (i.e., branched and aromatic groups). System L has a high exchange property (i.e., it shows *trans*-stimulation, stimulation by substrates in the *trans*-compartment) and has been postulated to serve in many circumstances to mediate efflux from cells rather than influx into cells (96). Preferred substrates for system A are alanine, serine, and glutamine, and for system ASC alanine, serine, and cysteine (99, 101). In contrast, amino acids with a small, nonbranched side chain are poor substrates for system L, for which the analogs 2-amino*endo*bicyclo-[2,2,1]-heptane-2-carboxylic acid (BCH) and 3-amino*endo*bicyclo-[3,2,1]-octane-3-carboxylic acid (BCO) are model substrates in the absence of sodium. System L has been subdivided into subtypes L1 (substrate affinity in the micromolar range) and L2 (substrate affinity in the millimolar range), which are present at different ages in hepatocytes and hepatoma cell lines (597). Therefore, zwitterionic amino acids with bulky side chains are not cotransported with sodium in many cell types. This is different in epithelial cells, where broad specificity systems (e.g., systems $B^o$, $B^{o,+}$) accumulate these amino acids by coupling the electrochemical gradient of sodium. One criterion for discrimination of system A is the fact that it transports *N*-methylated amino acids (101); in many instances, sodium-dependent transport of alanine inhibitable by the model analog *N*-methylaminoisobutyric acid (MeAIB) or the sodium-dependent transport of MeAIB is used for determining system A transport activity. System A is highly pH sensitive. Intracellular histidyl residues may form part of the pH sensor of the transporter (43, 384). In contrast, system ASC is relatively pH insensitive. Additional differential characteristics of systems A and ASC are that the former is electrogenic and shows the property of *trans*-inhibition (i.e., inhibition by substrates in the *trans*-compartment), and the latter may be electroneutral and shows *trans*-stimulation, probably as a consequence of a high property of exchange. Therefore, whereas system A is considered a true sodium-amino acid cotransporter, system ASC may be an antiporter of amino acids necessarily associated with the movement of sodium in both directions (for review, see Ref. 185).

TABLE 1. *Best-known amino acid transport systems present in the plasma membrane of mammalian cells*

| Amino Acid Transport System | Isolated cDNA |
|---|---|
| *Zwitterionic amino acids* | |
| Sodium dependent | |
| A: serves mainly for small amino acids; highly regulated; tolerates an *N*-methyl group; sensitive to pH changes; *trans*-inhibition associated; widespread | |
| ASC: excludes *N*-methylated amino acids; *trans*-stimulation associated; widespread | ASCT1-2 |
| N: for Gln, Asn, and His; sensitive to pH changes; so far restricted to hepatocytes; variant $N^m$ in muscle | |
| BETA: transports β-Ala, taurine, and GABA; chloride dependent; variants known; widespread | Series GAT-1 to -3 BGT-1, TAUT |
| GLY: transports Gly and sarcosine; chloride dependent; variants known; present in several tissues | GLYT1-2 |
| IMINO: handles proline, hydroxyprolines, and *N*-methylated glycines; interacts with MeAIB; in intestinal brush-border membranes | |
| PHE: handles primarily Phe and Met; in brush-border membranes | |
| $B^o$: broad specificity for most zwitterionic amino acids, including branched aromatic ones; accepts BCH but not MeAIB; in brush-border membranes; most probably identical to system NBB (renamed B) | $ATB^o$ |
| Sodium independent | |
| L: mainly for bulky side chain amino acids; *trans*-stimulated; bicyclic amino acids as model substrates; variants described; widespread | |
| *Cationic amino acids* | |
| Sodium dependent | |
| $B^{o,+}$: broad specificity for zwitterionic and dibasic amino acids; accepts BCH but not with MeAIB; in blastocyts, *Xenopus* oocytes and probably also in brush-border membranes | |
| Sodium independent | |
| $b^+$: cation preferring; does not interact with homoserine even in presence of sodium; variants known; in mouse conceptuses | |
| $y^+$: handles cationic and zwitterionic amino acids with sodium; variants known; sensitive to *N*-ethylmaleimide; widespread | CAT-1 to -4 |
| $y^+L$: handles cationic amino acids and zwitterionic amino acids with high affinity only with sodium; insensitive to *N*-ethylmaleimide; in erythrocytes and placenta | 4F2hc |
| $b^{o,+}$: like $B^{o,+}$ but limited by positions of branching; not inhibited by BCH; in blastocysts and in brush-border membranes | rBAT |
| *Anionic amino acids* | |
| $X^-_{AG}$: similarly reactive with L-Glu and D- and L-Asp; potassium dependent; widespread | EAAT1 to -5 |
| $x^-_C$: cystine competes and exchanges with Glu; in heptocytes and fibroblasts; electroneutral | |

For anionic amino acids, a capital X is used when sodium dependent. MeAIB, methylaminoisobutyric acid; BCH, *z*-amino*endo*bicyclo-[2,2,1]-heptane-2-carboxylic acid.

Transporters ASCT1–2 from the superfamily of sodium- and potassium-dependent transporters of anionic and zwitterionic amino acids may represent transporter variants of system ASC (see sect. II). The molecular identity of systems A and L is unknown.

An important distinguishing feature of system A is that in many cell types its activity is highly regulated. This includes upregulation during cell-cycle progression and cell growth in many cell types, and hormonal control (insulin, glucagon, catecholamines, glucocorticoids, and growth factors and mitogens) through a wide variety of mechanisms. Thus glucagon and epidermal growth factor short-term stimulate system A in hepatocytes, whereas insulin upregulates system A in a gene transcription-dependent manner in hepatocytes and through a rapid mechanism in skeletal muscle. This is independent of protein synthesis and the electrochemical gradient of sodium, suggesting direct stimulation of preexisting system A transporters or recruitment of these to the plasma membrane. Paradoxically, situations associated with insulin deficiency or insulin resistance (e.g., diabetes, starvation, pregnancy) are associated with upregulation of system A activity in both hepatocytes and skeletal muscle. Two additional long-term maximum velocity ($V_{max}$) regulation processes of system A have been demonstrated only in culture or incubated cells: adaptative regulation (i.e., repression and derepression of system A in the presence or absence of amino acids) and upregulation by hyperosmolarity. In both types of regulation, there is indirect evidence for the presence of system A regulatory proteins. For a detailed description of the putative mechanisms involved in the regulation of system A, the reader is directed to excellent recent reviews (185, 201, 350, 414) and to specific articles on insulin action in skeletal muscle (188–190, 561). The complexity of the regulation of system A emphasizes the importance of this transport activity in maintaining the accumulation of small side-chain zwitterionic amino acids as a source for precursor molecules,

energy, and perhaps even as osmolytes. Unfortunately, the lack of structural information on the system A transporter (see sect. IB1) prevents further understanding of the molecular mechanisms underlying system A regulation.

### 2. *Tissue-specific systems for zwitterionic amino acids*

Additional sodium-dependent zwitterionic transport systems of restricted distribution have been described (Table 1). Transport of L-glutamine, L-histidine, and L-asparagine in hepatocytes has been demonstrated to occur via a sodium-dependent transport system named N (276). A system with similar properties to system N was defined in skeletal muscle and termed $N^m$ (222). System Gly, specific for glycine and sarcosine, occurs in several cell types (134). Transporters GLYT1–2, from the superfamily of sodium- and chloride-dependent transporters of neurotransmitters, may represent variants of system Gly (see sect. II). A transport system for β-alanine, taurine, and GABA (system BETA) has been characterized in several tissues and with differences in substrate affinity and specificity (369). Transporters GAT1–3, BGT-1, and TAUT, which belong to the superfamily of sodium- and chloride-dependent transporters of neurotransmitters, may be considered variants of system BETA (see sect. II).

Several zwitterionic transport systems seem to be specific to the apical pole of epithelial cells. In intestinal brush-border membrane vesicles, a sodium-dependent transport system (NBB, which stands for neutral brush border) serving for neutral amino acids is present. This system was renamed B for consistency with other broad-specificity systems (e.g., $B^{o,+}$, $b^{o,+}$, $b^+$; see below) (337). More recently, in bovine renal brush-border membranes, a sodium-dependent system for neutral amino acids was described that was termed $B^o$ (329). Most probably the transport systems B (NBB) and $B^o$ represent the same transport agency distributed in epithelial cells, as suggested after the cloning of the putative transporter for system $B^o$ ($ATB^o$, from the superfamily of sodium- and potassium-dependent transporters for anionic and zwitterionic amino acids; see sect. II). This broad-specificity system is thought to be responsible (together with the dipeptide and tripeptide transport systems; for review, see Refs. 122, 299) for the bulk of renal reabsorption and intestinal absorption of zwitterionic amino acids. Therefore, system $B^o$ and the $ATB^o$ cDNA could represent the transport activity and the corresponding transcript that are altered in Hartnup disease (304), an inherited hyperaminoaciduria of neutral amino acids (see sect. III). Additional transport systems (see Table 1) seem to be specific to brush-border membranes. System IMINO, which catalyzes sodium-dependent transport of proline and *N*-methylated glycines and is inhibited by MeAIB, has been detected in kidney and intestine and in other epithelia (192, 376, 514). The proline transporter PROT, from the superfamily of sodium- and chloride-dependent transporters of neurotransmitters, might represent a brain-specific high-affinity [Michaelis constant ($K_m$) in the low micromolar range] variant of system IMINO; this is not yet clear (see sect. II). The broad-specificity (cationic and zwitterionic amino acids) transport systems $B^{o,+}$ and $b^{o,+}$ are described in section IA3, together with cationic amino acid transport systems.

### 3. *Cationic amino acid transport systems*

Five transport systems that mediate the uptake of cationic amino acids are known (Table 1). One corresponds to the widespread classical system $y^+$, whereas the other four were discovered in the late 1980s and early 1990s (systems $y^+L$, $b^+$, $b^{o,+}$, and $B^{o,+}$) and at present have been described only in specific tissues. The activity of all these systems can be distinguished by their affinity for the cationic amino acids, by their dependence on sodium, and by their capacity to share transport with zwitterionic amino acids (for a short review, see Ref. 105). System $y^+$ catalyzes high-affinity ($K_m$ in the micromolar range) sodium-independent transport of cationic amino acids and the transport of zwitterionic amino acids with low affinity ($K_m$ in the large millimolar range; affinity increases with chain length) only in the presence of sodium; this system is electrogenic and accumulates its substrates by coupling with the cell plasma membrane potential (98, 455, 601). System $y^+L$ was discovered in human erythrocytes (127) and has also been described in placenta (135, 146). It is possible that system $y^+L$ is widely distributed among different tissues; thus it has also been detected in human fibroblasts (D. Torrents and M. Palacín, unpublished data). This system transports cationic amino acids with high affinity ($K_m$ in the micromolar range) with no need for sodium in the external medium, but it transports both small and large zwitterionic amino acids with high affinity ($K_m$ in the micromolar range) in the presence of external sodium; in the absence of sodium, transport of zwitterionic amino acids is of very low affinity. In addition to this, system $y^+$ and $y^+L$ activities could be discriminated, at least in erythrocytes and placenta, by *N*-ethylmaleimide (NEM) treatment, the former being sensitive and the latter resistant. Systems $y^+$ and $y^+L$ show very high capacity for *trans*-stimulation (i.e., exchange). It is thought that exchange via system $y^+$ allows equilibration of cationic amino acids across the plasma membrane, whereas heteroexchange between cationic and zwitterionic amino acids plus sodium via system $y^+L$ catalyzes the efflux of cationic amino acids against the membrane potential, the driving force being provided by the sodium ion concentration gradient (14, 90). Systems $y^+$ and $y^+L$ have been suggested to be candidate transport activities

affected in the inherited disease lysinuric protein intolerance (LPI) (for review, see Ref. 497). This is discussed in section III. The cDNA for up to five potential $y^+$ transporters have been isolated (CAT-1, CAT-2, the splice variant CAT-2a, CAT-3, and possibly the recently identified CAT-4), which form the cationic amino acid transporter family (see sect. II). Several groups described expression of system $y^+L$ transport activity in oocytes by the 4F2hc surface antigen, which shows homology with another protein, rBAT, also related to broad-specificity amino acid transport. Because 4F2hc and rBAT are less hydrophobic than typical transporter proteins and form disulfide-bound heterodimers with unidentified proteins, it has been suggested that 4F2hc may represent a putative subunit of system $y^+L$ transporter; this ascription is not yet clear (see sect. II).

Systems $B^{0,+}$, $b^{0,+}$, and $b^+$ were discovered in mouse blastocysts (576–578; for review, see Ref. 573). Among the systems that form the series of transport activities for cationic amino acids, the embryonic sodium-independent systems $b^+$ (subtypes $b1^+$ and $b2^+$, which differ in the embryonic stage expression and sensitivity to cationic amino acid inhibition) show the narrowest specificity, serving only for cationic amino acids (576). Systems $B^{0,+}$ and $b^{0,+}$ show very similar broad specificity with high affinity ($K_m$ in the micromolar range) for cationic and small and large zwitterionic amino acids. As a distinguishing feature, the former is sodium dependent and inhibitable by BCH and BCO, and the latter prefers bulky $\alpha,\beta$-unbranched zwitterionic amino acids. More probably, both systems have a wide distribution on epithelial cells. In fact, system $b^{0,+}$ (or a variant, $b^{0,+}$-like) has been detected in renal epithelial cells and in Caco-2 cells (374, 557). Expression of rBAT, a protein homologous to the cell surface antigen 4F2hc, is needed for system $b^{0,+}$-like transport activity; it is believed that rBAT acts as a subunit of this transporter (see sect. II). Mutations in rBAT/system $b^{0,+}$-like transport activity cause cystinuria type I (for reviews, see Refs. 170, 408, 409), an inherited hyperaminoaciduria due to defective renal reabsorption and intestinal absorption of cationic amino acids and cystine (for review, see Ref. 487). The role of rBAT in cystinuria is discussed in section III.

#### 4. *Anionic amino acid transport systems*

L-Glutamate and L-aspartate are accumulated in many cells (e.g., neurons and glial cells, hepatocytes, enterocytes, fibroblasts, and placental trophoblasts) by the high-affinity ($K_m$ in the micromolar range) sodium- and potassium-dependent system $X^-_{AG}$ (165) (for review, see Ref. 185). This system shows identical affinity for the D- and L-stereoisomers of aspartate (165). Variants of this transport systems occur in neural tissues (100, 147). It is believed that the five glutamate transporters EAAT1–5 from the superfamily of sodium- and potassium-dependent transporters of anionic and zwitterionic amino acids represent variants of system $X^-_{AG}$ (see sect. II).

Several cell types (e.g., hepatocytes, fibroblasts, and embryonic cells) transport L-glutamate (specifically anionic amino acids with 3 or more carbon atoms in the side chain) and L-cystine (as tripolar ion) via the sodium-independent antiport system $x^-_C$ (28, 533). This system has an apparent $K_m$ in the 100–200 $\mu$M range, is insensitive to membrane potential, and presents *trans*-stimulation (for review, see Ref. 185). Bannai's group (27) proposed that this system participates in a glutamine-cystine cycle that helps cells to resist oxidative stress; glutamine, entering the cell via systems ASC and A, is converted to glutamate, which is exchanged for cystine via the oxidative stress-induced system $x^-_C$; accumulated cystine then nourishes glutathione synthesis, which protects cells against oxidative insult (27, 29, 596; for review, see Ref. 228).

### B. Strategies Used to Identify Mammalian Amino Acid Transporters as Yet Uncloned

As described in section IA, the present explosion of cloned cDNA related to plasma amino acid transport in mammals is revealing an intriguing range of structural diversity within amino acid transporter proteins. This diversity is already even more pronounced than that shown by the sodium-dependent glucose transport (for review, see Ref. 608) and the facilitated glucose transporter isoforms (for review, see Refs. 381, 556). The lack of high-affinity inhibitors for mammalian amino acid carriers and their low abundance in plasma membranes complicate their structural identification and isolation. Because of this, there are many amino acid transport systems not yet identified at a molecular level (see Table 1). Among these systems, there are the highly regulated system A and the well-characterized systems L, N, and $x^-_C$. In this section, we focus on the strategies used to identify these four transporters and also speculate, in some cases, about why some strategies have failed.

#### 1. *System A*

One of the goals of several laboratories has been to reconstitute and purify system A transporter. Kilberg's group (195) reported the solubilization, reconstitution, and partial purification of system A (70-fold over plasma membrane vesicles). They then used this protein fraction to immunize mice for the generation of monoclonal antibodies. Some of these antibodies specifically coprecipitate fodrin and system A transport activity. Because the protein ankyrin often binds directly to integral membrane proteins and fodrin, the authors tested whether an antibody against ankyrin could immunoprecipitate system A transport activity, and it did. McGivan's group (437) par-

tially purified system A activity from rat liver with concanavalin A-affinity chromatography. This demonstrated that either system A or a protein bound to the carrier is a glycoprotein. McCormick and Johnstone (348) purified system A transport activity from Ehrlich ascites with a 30-fold enrichment. Three major peaks were eluted from the system A-purified Ehrlich cell preparation: high-molecular-mass aggregates, a low-molecular-mass band (~40 kDa), and the most conspicuous band of 120–130 kDa. Interestingly, polyclonal antibodies against the 120- to 130-kDa purified fraction immunoprecipitated system A transport activity. More recently, $NH_2$-terminal sequence analysis of the 120- to 130-kDa peptide revealed a sequence similar to that of the $\alpha_3$-subunit of the $\alpha_3\beta_1$-integrin (349). Further purification of these extracts using lectin columns resulted in the separation of most of the $\alpha_3\beta_1$-integrin from the system A activity, indicating that this integrin is not essential for amino acid transport. Moreover, the fact that transfection of $\alpha_3$-integrin into K562 or RD cells increased system A transport activity provides evidence that this protein could modulate this transporter. In summary, from these studies of reconstitution, one may conclude that several distinct proteins contribute to the entire system A transport activity. Probably in the near future the microsequencing of some of the proteins present in these purified extracts will result in the isolation of all the components necessary for system A function.

Another strategy used to identify system A is the functional expression in *Xenopus laevis* oocytes. Expression of system A has been claimed (409, 546) based on the following (for review, see Ref. 277). *1*) The effect of glucagon on system A in vivo was maintained after mRNA extraction and injection into the oocyte; glucagon is known to stimulate system A transport activity in liver, at least in part, through mRNA and protein synthesis-dependent mechanisms. *2*) The apparent substrate affinities reported by these authors were in the same range as those described for the transport of the substrates tested via system A. *3*) The *cis*-inhibition of the transport of L-alanine induced by MeAIB suggested that at least part of this expressed activity was due to system A. *4*) The expressed transport activity, in contrast to the endogenous uptake, was inhibited by an extracellular pH of 6.5. *5*) Messenger RNA from the Chinese hamster ovary (CHO) cell line alar-H3.9, which overexpresses system A activity (371, 372), resulted in higher transport rates than mRNA from the parental cell line CHO-K1. More recently, Lin et al. (313) presented evidence that mRNA of differing sizes (2.2 and 4.2 kb) from two cell lines (GF-14 cells, Ehrlich cells) increase the expression of system A transport upon injection into *Xenopus* oocytes. However, only the synthesis of the 2.2-kb transcript is raised by insulin, which is consistent with the idea that there are variants of system A transporter (see below). Expression cloning of this transport activity has not yet been achieved, possibly due to the high background (i.e., basal oocyte endogenous activity), and perhaps because the system A transporter would need the expression of different proteins that form part of the whole transporter or are upregulators of its activity (e.g., as shown by the adaptative or osmotic regulation of system A; see above, for review see Ref. 350). In the same line of functional expression of system A transport activity, Lin et al. (312) restored normal growth of a mutated yeast cell line incapable of growth in minimal medium with proline by transfection with a cDNA (E51) from mouse Ehrlich cells. This cDNA is 90% homologous to $\gamma$-actin. Similarly, this cDNA increases sodium-dependent amino acid uptake when expressed in oocytes and in a mutated mammalian lymphocyte cell line (GF-17), deficient in system A transport activity. This suggests that the $\gamma$-actin-like protein coded for by E51 cDNA may play a significant regulatory role in sodium-dependent amino acid transport. In summary, reconstitution-purification and functional expression studies suggest that a multiplicity of proteins might be involved in the functional expression and modulation of system A transport activity.

Another approach is the development of cell lines that show mutations in amino acid transport activity (reviewed in Refs. 113, 603). In this way, Englesberg's group (371) has isolated constitutive or derepressed mutants for system A activity from CHO-K1 cells by alanine-resistant selection for proline uptake (alar4 mutant) and by a stepwise selection (hydroxyurea treatment and resistance to increased alanine concentration) (alar4-H3.9 mutant). In comparison to the wild type, these mutants showed higher system A activity in isolated plasma membrane vesicles and higher mRNA-induced sodium-dependent aminoisobutyric acid uptake in *Xenopus* oocytes (371, 546). These mutants have increased levels of peptides banding at 62–66 kDa and 29 kDa. Sequencing the $NH_2$ terminus of the 62- to 66-kDa peptide shows between 80 and 100% identity with the mammalian mitochondrial 60-kDa heat-shock protein (HSP60) (235). Whether these proteins are components of system A carrier is at present unknown.

Other approaches involve the chemical modification of specific residues by covalent reagents. Hayes and McGivan (202) identified a 20-kDa protein as a putative component of sodium-dependent alanine transport in liver plasma membrane vesicles. On the other hand, the presence of histidine residues critical for activity in the system A from rat liver (i.e., sensitive to diethyl pyrocarbonate inactivation) has also been demonstrated using this approach (43). Thiol reagents have been used to reveal structural differences between these carriers and between normal and transformed cells. It has been suggested that structural differences occur in system A transporters of transformed cells, based on the much greater sensitivity to NEM inactivation of liposome-reconstituted system A activity from normal hepatocytes than that from hepatoma cell lines (132). Moreover, all these studies should

be critically evaluated, since these specific reagents can modify, with different affinities, a variety of different amino acid residues in proteins. In any case, no further structural information on system A has been achieved with this strategy.

### 2. System L

Using the strategy of functional expression in *Xenopus* oocytes, Oxender's group (521) reported the expression of a sodium-independent L-leucine transport system shared with dibasic amino acids, by injection of mRNA from CHO cells. This suggests that the expressed transport could correspond to that induced by the expression of rBAT (i.e., system $b^{0,+}$) and not to system L. In any case, this ascription is not yet clear, since the data from Oxender's group (521) and rBAT-expressed amino acid transport activity (549) differ in the sensitivity to inhibition by L-tryptophan. More recently, Broër et al. (68) also expressed sodium-independent isoleucine transport activity from mRNA of rat brain in oocytes. The sodium-independent component of isoleucine transport was inhibited by leucine, phenylalanine, and BCH, consistent with the expression of a system L-like transporter. However, the isolated cDNA responsible for this activity was rat 4F2hc, which also expresses cationic amino acid transport in oocytes (69). As discussed in section II, several groups proposed that 4F2hc expresses a system $y^+$L-like transport activity in oocytes. In our view, expression of system L in oocytes has not been conclusively demonstrated.

Another interesting strategy to assess the structure of this transporter has been developed by Oxender's group (136). It is based on the fact that the transport activity of system L can be derepressed by severe "starvation" for leucine or by increasing the temperature of culture in mutant cell lines with temperature-sensitive leucyl-tRNA synthetase (reviewed in Ref. 603). Oxender's group (136) transformed a temperature-sensitive leucyl-tRNA synthetase mutant CHO cell line (CHO-025C1) with human DNA from a cosmid library. Subsequent selection of transformants for inability to grow above the permissive temperature in the presence of low leucine concentration allowed the isolation of cells with higher (<2-fold) leucine uptake activity. To date, no report has described the rescue of the human DNA sequences responsible for the above-mentioned transformation.

More recently, Segel's group (606) has developed a new strategy to identify the carrier protein(s) responsible for mammalian L-system amino acid transport. In chronic lymphocytic leukemia (CLL), B lymphocytes have markedly disminished L-system transport, which is restored after treatment with 12-*O*-tetradecanoylphorbol 13-acetate (TPA). These authors identified six candidate L-system-related proteins in TPA-treated CLL cells using an L-system photoprobe (iodoazidophenylalanine) and ultrahigh-resolution two-dimensional gel electrophoresis. Two of these six proteins were microsequenced and show sequence similarity to the mitochondrial heat-shock protein (HSP60). This report and the data published by Englesberg's group (235) implicate the family of heat shock proteins in the regulation of some transport processes. How these proteins develop their function in systems A and L transport activity is unknown.

### 3. System N

Kilberg's group (143), with the same approach of aggregation and differential solubility used to purify system A, achieved a 600-fold enrichment for system N amino acid transport activity in reconstituted proteoliposomes (540). They identifed a 100-kDa protein involved in system N amino acid transport activity by generating monoclonal antibodies against the purified fraction that immunoprecipitate system N transport activity (539). These tools may allow the identification of system N transporter.

Rennie's group (551) has reported the expression of rat liver glutamine transporters after injection of rat liver mRNA into *Xenopus* oocytes. They attributed part of the L-glutamine-induced transport activity to system N based on a characteristic feature of this transport system, that is, the toleration of lithium by sodium substitution and the inhibition by L-histidine in lithium medium. By size-fractioning the mRNA, they found three different induced transport activities: one sodium independent induced by 2.8–3.6 kb mRNA, another sodium-dependent, lithium sustitution intolerant induced by 1.9–2.8 kb mRNA, and one induced by a lighter fraction (<1.9 kb) that is sodium or lithium dependent and that could correspond to system N.

### 4. System $x_c^-$

Bannai's group (227), working with manually defolliculated oocytes, has reported the expression of a mouse-macrophage cystine transporter with characteristics of system $x_c^-$, as it was sodium independent and glutamate inhibitable. Fractions of mRNA of 1.5–2.9 kb are responsible for this induction. Although oocytes seem to express an endogenous system $x_c^-$ (574), expression of this system correlates with injection of mRNA from $x_c^-$-rich cells (macrophages stimulated by diethylmaleate in culture), but not from $x_c^-$-poor cells (noncultured macrophages and mouse leukemia L1210 cells). In addition, cystine uptake expressed by diethylmaleate-stimulated macrophage mRNA was, in contrast to the endogenous cystine uptake, pH sensitive, highly temperature sensitive, and inhibitable by glutamate. This line of research may lead to the identification of system $x_c^-$ transporter.

## II. CURRENT KNOWLEDGE OF THE MOLECULAR STRUCTURE OF AMINO ACID TRANSPORT SYSTEMS

In this section, the cDNA clones that have been related to plasma membrane amino acid transport in mam-

mals are discussed from the structural and functional points of view. With regard to the primary structures elucidated to date, it can be summarized that two main types of membrane proteins are involved in amino acid transport: those that present multiple (i.e., 10–14) transmembrane domains and are therefore considered as putative transporters and those that do not fit this general model and are considered as activators or as components of oligomeric transporters. The first group with typical structure of transporters is arranged in families of related cDNA: *1*) the family of sodium-independent cationic amino acid transporters (CAT); *2*) superfamily of sodium- and chloride-dependent neurotransmitter transporters, which includes amino acid transporters; and *3*) the superfamily of sodium-dependent, and in some cases potassium-dependent, anionic or zwitterionic amino acid transporters. The second group corresponds to the family of proteins rBAT and 4F2hc that induce sodium- and chloride-independent amino acid transport with broad specificity (i.e., for dibasic and zwitterionic amino acids) in *X. laevis* oocytes. The members of this family are less hydrophobic than typical transporters and show heteroligomeric structure.

Another protein related to amino acid transport, whose primary structure was elucidated many years ago, is the anion exchanger band 3 (290). Although its function as an anion exchanger is well accepted, it has been shown to be associated with the transport of some amino acids (e.g., glycine, taurine, and β-alanine), especially under conditions of hyposmotic stress; in response to swelling, erythrocytes recover their initial volume by releasing organic osmolytes via a pathway with a pharmacology similar to that of band 3 (114, 203, 308). This amino acid transport has the properties of a volume-sensitive size-limited anion channel (171). Interestingly, expression of trout band 3 in oocytes resulted in anion-exchange activity but also in chloride channel activity and taurine transport (150). At present, it is not known whether band 3 is involved in the amino acid channel formation or in its regulation. The role of band 3 in amino acid transport is outside the scope of this review. This and the molecular biology of band 3 have recently been reviewed (10, 380, 574).

### A. Cationic Amino Acid Transporters

Four homologous human and rodent genes defining a family of cationic amino acid transporters (CAT-1, -2, -3, and -4) have been, or are in the process of being, identified (Table 2). First, expression in oocytes revealed the ecotropic murine leukemia virus receptor (9) (now named CAT-1) as a putative cationic amino acid transporter (281, 590). Second, full-length cDNA cloned from a previously identified murine T-lymphoma cell line cDNA (Tea, for "T early activation" gene; Ref. 334) showed significant homology with CAT-1 and cationic amino acid transport expression in oocytes (106, 108, 242, 448). These cDNA, now named CAT-2 and CAT-2a, represent splice variants (the "high-affinity" or "T-cell" variant CAT-2 and the "low-affinity" or "liver" variant CAT-2a) (see Table 2) of a single gene (336). It has been suggested that the three putative proteins (CAT-1, CAT-2, and CAT-2a variants) may contain 14 transmembrane domains (TM) (9, 106) (Figs. 1 and 2, see below). Very recently, with strategies based on sequence homology with CAT-1, the mouse and rat counterparts (95% amino acid sequence identity between them) of a new brain-specific cationic amino acid transporter, CAT-3, have been isolated (219, 229). Very recently, Sebastio and co-workers (484, 485) identified a human EST sequence (Table 2) with significant homology to the 5′-end of the open reading frame of CAT-1 and CAT-2/2a cDNA (Fig. 1). Screening of the full-length human CAT-4 cDNA [we renamed HCAT-3 (485) as CAT-4 after the reported cloning of rat and mouse CAT-3 (219, 229)] has been completed, and the putative protein shows 34–38% identity with human CAT-1, -2, and -3 (G. Sebastio, personal communication). At present, there are no reported data on the transport activity associated with CAT-4 expression. Screening, performed by us (DBEST, December 1996), for additional expressed sequence tag sequences homologous to CAT transporters indicative of additional members of the family was negative.

Figure 1 compares the amino acid sequences of the putative human CAT-1 and CAT-2a proteins, the mouse CAT-3 protein, and the putative $NH_2$-terminal fragment of the human CAT-4 transporter. Two potential *N*-glycosylation sites, conserved in all known sequences, are located in the extracellular loop EL3 in the 14-TM model (Figs. 1 and 2). The known amino acid sequences of CAT-2 and CAT-2a (98% identity between the murine counterparts; see Fig. 2) are ~60% identical to that of CAT-1 (106, 448). The rat and mouse CAT-3 show 53–58% amino acid sequence identity with the isolated CAT-1, CAT-2, and CAT-2a cDNA (219). Two regions of extensive amino acid sequence identity (7E80%) of ~150 and 200 amino acid residues, comprising the first three transmembrane domains and transmembrane domains VI–X, are present in the CAT-1, -2, and -3 proteins (334; see Figs. 1 and 2). Murine CAT-2 and CAT-2a differ only in a 41- to 42-amino acid segment located in this highly conserved region (intracellular loop IL4 between TM domains VIII and IX of the 14-TM model) (Fig. 2). Because a single genomic fragment contains both exons, the isoforms result from mutually exclusive alternate splicing of the primary trancript (unpublished data from MacLeod and co-workers quoted in Ref. 336). This amino acid sequence region has a role in substrate binding, as demonstrated by the expression of CAT-2/CAT-2a chimeric transporters (backbone and the 42-amino acid domain) (108).

The CAT transporters are homologous to a family of transporters specific for amino acids, polyamines, and

TABLE 2. *Human cationic amino acid transporters*

| Transporters (Gene Name) | Accession Numbers (Origin of Human Clones) | Origin of First Clone and Other Names | Human Chromosome | Protein Amino Acid Length | Other Clones in Mammals |
|---|---|---|---|---|---|
| CAT-1 (SLC7A1) | X59155 (Hut78 T-cells) (619) | NIH 3T3 fibroblasts (mCAT-1) (9) (REC-1, EcoR, ERR, MLV-R ATRC1, y1+, H13) (105) | 13q12-q14 (7) | 629 | Rat (433, 610) |
| CAT-2 (SLC7A2) | D29990 (intestine) (218) | Murine SL12 T-lymphoma cells and macrophages (Tea, mCAT-2) murine liver (mCAT-2) (106, 108, 242) | 8p21.3-p22 (218) | | Murine (267) |
| | | Variants: CAT-2(B) (Tea, mCAT-2, mCAT-2B and mCAT-2$\beta$) | | 658 | |
| | | CAT-2A (mCAT-2, mCAT-2$\alpha$ and y2+) | | 657 | |
| CAT-3 (not shown in GDB) | U70859 (229) (mouse brain) | Mouse brain (CAT-3) (229) | | 619 | Rat (219) |
| CAT-4 (?) (not shown in GDB) | EST H05853 (484, 485) | | 22q11.2 (484, 485) | ? | |

Accession numbers for human cationic amino acid transporter (CAT)-1, CAT-2, and CAT-2a and for the murine CAT-3 cDNA and one EST sequence corresponding to human CAT-4 are indicated. Human CAT-4 is tentatively included since the known structure of this cDNA shows significant homology with other CAT transporters (G. Sebastio, personal communication). GDB, gene data bank; m, murine. Reference numbers are given in parentheses.

choline (APC family) that catalyze solute uniport, solute/cation symport, or solute/solute antiport in yeast, fungi, and eubacteria (448). Marked sequence divergence of these proteins was observed mainly in the hydrophilic $NH_2$ terminals that precede the first transmembrane helices and in the COOH-terminal regions (448). Southern blot studies revealed that all vertebrates examined hybridize to the probes of CAT-1 and CAT-2, indicating a high conservation of these proteins among vertebrates (448). Thus the human CAT-1 protein (7, 619) and the rat CAT-1 protein (433, 610) are 86 and 95% identical, respectively, to the mouse CAT-1, and the human analogs of CAT-2 and CAT-2a proteins are ~90% identical to the murine counterparts (218; unpublished data quoted in Ref. 105).

The chromosomal location of the human *CAT* genes is showed in Table 2. The possible involvement of *CAT* genes in LPI, a human inherited hyperaminoaciduria that seems to result from an impairment of a system $y^+$-like activity (497), is discussed in section III.

Two excellent recent reviews described functional and structural data as well as available data on the regulation of the expression of CAT-1 and CAT-2/2a transporters (105, 336).

### *1. Tissue expression*

The tissue distribution of *CAT* genes has been examined by Northern blot analysis (for mCAT-1; Refs. 9, 242, 281; for hCAT-4, G. Sebastio, personal communication) and by RT-PCR (specific detection of mCAT-2 and mCAT-2a; Refs. 151, 336). Tissue distribution and transcript size of these genes are indicated in Table 3. Semi-quantitative data for the murine genes were summarized by MacLeod and Kakuda (336); all tissues or cell types examined express at least one of the *mCAT* genes, and in some tissues, both genes (*CAT-1* and *CAT-2*) are expressed. Liver is the only tissue that expresses only mCAT-2a and not mCAT-1 or mCAT-2. Kidney, small intestine, resident macrophages and quiescent splenocytes, and T cells only express the *mCAT-1* gene but neither of the two mCAT-2 splice variants. Upon activation, these cell types express the mCAT-2 variant. The rat and mouse *CAT-3* gene is expressed specifically in brain, as a transcript of ~3.4 kb (219, 229). The human *CAT-4* gene is expressed mainly in pancreas, skeletal muscle, heart, and placenta, and brain, lung, liver, and kidney show a faint band in Northern analysis (Sebastio, personal communication).

The tissue and subcellular distribution of CAT transporter isoforms is less known than their transcript distributions. Expression of mCAT-1 protein has been studied by exploiting its function as a viral receptor (infectivity or viral glycoprotein gp70 binding assay; Refs. 108, 281, 590, 610) and by using anti-mCAT-1 antisera (106, 108, 605). Recently, approaches to the detection of mCAT-1 based on its function as a viral receptor have been validated in null knockout CAT-1 mice (419); primary embryo fibroblasts from these mice were completely resistant to ecotropic retrovirus infection (i.e., mCAT-1 is the sole receptor for ecotropic murine leukemia virus). The lack of constitutive expression of CAT-1 in human, murine, and rat liver has been demonstrated by virus infectability studies (610) and immunofluorescence studies (605). These strategies served to demonstrate the induction of surface expression of CAT-1 in the murine liver after partial hepatectomy and after insulin and dexamethasone treatment (610).

Antibodies directed against the COOH terminus of

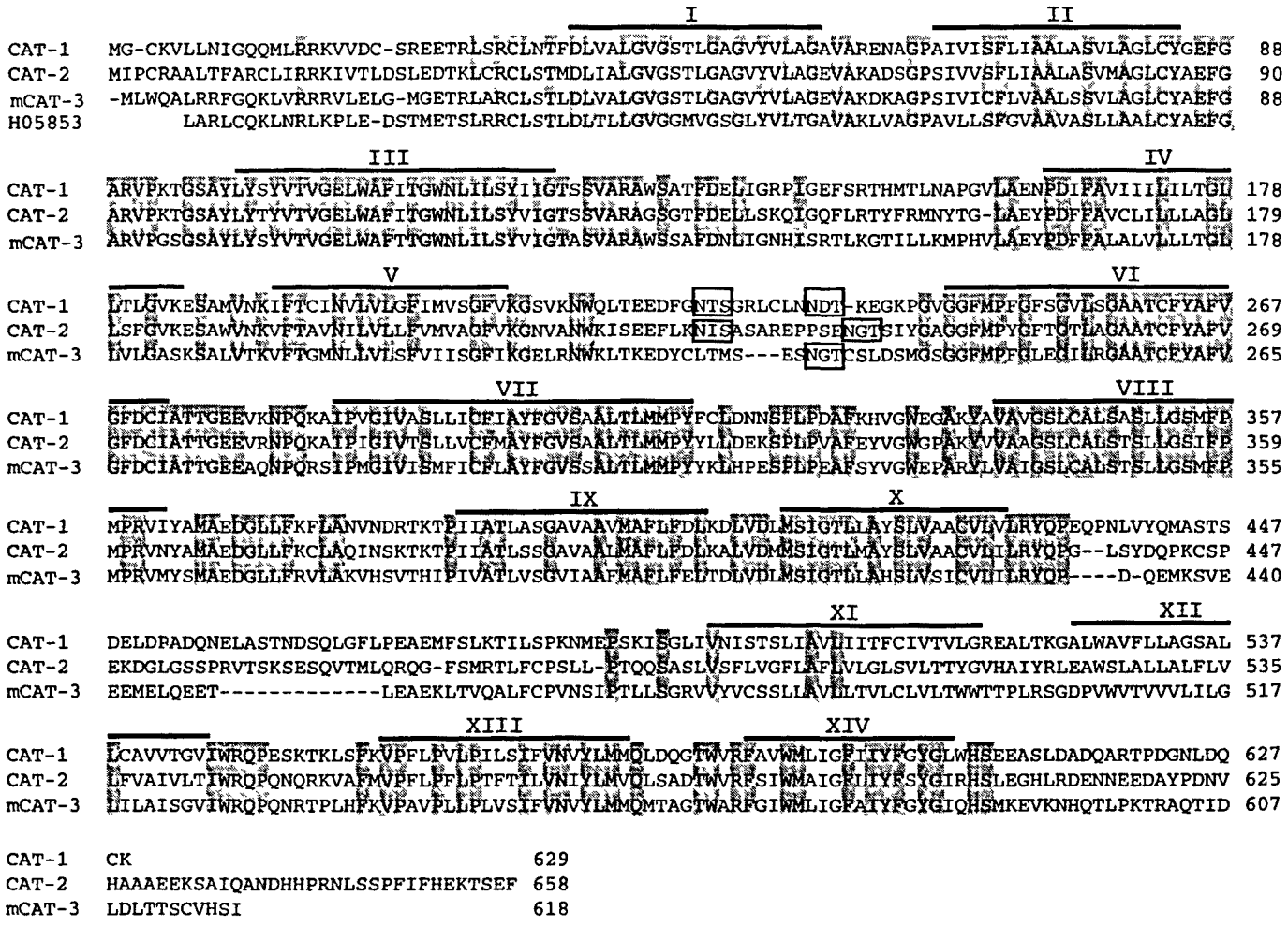


FIG 1 Amino acid sequence comparison of human cationic amino acid transporters (CAT) HO5853 sequence corresponds to best EST sequence in database DBEST that showed homology with human CAT-1 and CAT-2, and rat CAT-3, and that served for human CAT-4 cloning (G. Sebastio, personal communication) Amino acid residues present in all CAT transporter sequences known to date are indicated by gray boxes Straight lines over sequences indicate putative transmembrane (TM) domains (I-XIV) Between TM V and TM VI, two potential *N*-glycosylation sites are conserved (open boxes). Dash lines indicate gaps for sequence alignment, which corresponds to that reported by Closs (105)

CAT-2a, which do not distinguish between CAT-2 and CAT-2a, detected a peptide band of 70–80 kDa in liver (106). Very recently, MacLeod's and Closs' groups obtained antibodies capable of distinguishing between CAT-2 and CAT-2a. This is not an easy task, since the main difference between the two mCAT-2 splice variants is an eight-amino acid segment with five substitutions (see Fig. 2), but full reports on this issue have not yet appeared (C. MacLeod and E. Closs, personal communication). Therefore, confirmation, at the protein level, of the tissue distribution and regulation of the expression of the CAT-2 isoforms is expected to be reported soon. No antibodies have been reported against the rodent CAT-3 or the human CAT-4 proteins.

The specific tissue distribution and regulation of the expression of the different CAT transporter isoforms (see sect. II*A5*) suggests a high level of regulation of the expression of the corresponding gene promoters and splice variants (336). MacLeods's (151) group has addressed this question for the m*CAT-2* gene. The promoter region of m*CAT-2* is extremely complex, with several 5′-untranslated regions (UTR) expanded in a genomic region of 19 kb from the first 5′-coding exon. For more detailed information, the reader is directed to the review by MacLeod and Kakuda (336). MacLeod's lab (151) described five exon 1 isoforms (1a, 1b, 1b/1c, 1c, and 1d) that splice into a common sequence 16 bp 5′ of the AUG start methionine codon (151). Kavanaugh et al. (267) described from a liver clone a putative complex additional 5′-UTR (named 1e) of 515 bp, with six initiation and termination codons that precede the translation start codon, which is subjected to posttranscriptional regulation. Promoter 1a (at the far end of the complex promoter region)

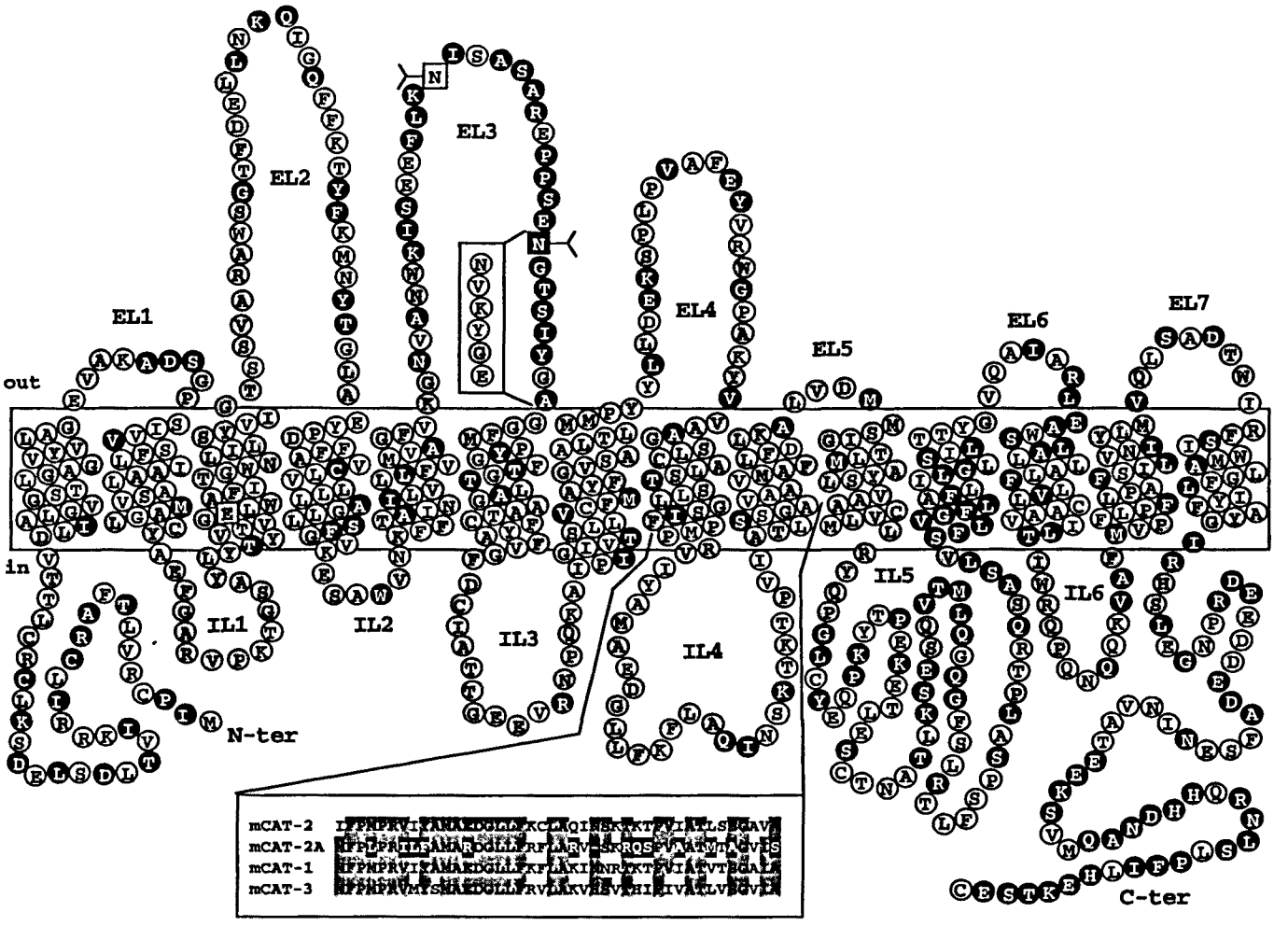


FIG. 2. Fourteen TM transmembrane topology model for murine mCAT-2 transporter. Extracellular (EL) and intracellular (IL) loops are numbered. Amino acid residues conserved in all known CAT transporters are indicated in gray circles, and residues that are specific for known CAT-2 and CAT-2a transporters are indicated in white over a black circle. At *bottom*, 41- to 42-amino acid segment corresponding to splice variant exon of mCAT-2 and mCAT-2a transporters are compared with homologous mCAT-1 and mCAT-3 regions (residues present in at least 3 of sequences are contained in gray boxes, and those specific for low-affinity CAT-2a isoform are in white on black boxes). In EL3 loop, amino acid sequence that binds viral envelope glycoprotein gp70, present in murine and rat CAT-1, is boxed. Three residues, a Glu in TM I|I and 2 glycosylated (Y) Asn residues in EL3, are marked by squares, indicating homologous residues that have been analyzed by site-directed mutagenesis studies of mCAT-1 sequence. Human *CAT-1* gene structure has been published (619), and it has been reported that mouse *CAT-1* gene contains 8 coding exons (419). To our knowledge, gene structure of *CAT-2* has not been reported.

predominates over the others in every cell type and tissue examined (336). The promoter of exon 1a is a TATA-less one with staggered initiation, GC rich, and with several SP1 and CAC boxes. Liver (where only the mCAT-2a variant is expressed) and activated macrophages (where only the mCAT-2a variant is expressed) use promoter 1a exclusively (151); this demonstrates that promoter usage does not dictate the splicing events that render the mCAT-2 and mCAT-2a splice variants (336).

Posttranscriptional regulation of *CAT-1* gene expression has been reported in liver regeneration (25), a model that induces system $y^+$/CAT-1 isoform expression (see sect. II*A5*). This study shows that accumulation of *CAT-1* mRNA in the regenerating rat liver is due to posttranscriptional regulation, and there is no increased transcriptional activity (run-on experiments) of the gene; this posttranscriptional regulation is sensitive to cycloheximide. In the rat, *CAT-1* produces two transcripts (7.9 and 3.4 kb in length), which represent alternative polyadenylation signal usage (the long transcript uses a consensus polyadenylation sequence, whereas the shorter uses a noncanonical signal); both transcripts accumulate in the regenerating liver. The specific 3′-UTR of the long transcript contains destabilizing AU-rich sequences that are associated with a shorter half-life (90 and 250 min for the long and short trancripts, respectively); interestingly, the longer transcript accumulates to higher

TABLE 3. *Tissue distribution and transport characteristics of expressed CAT transporters*

| CAT Transporter | Tissue Distribution (Transcript Size) | Expression System | Substrates ($K_m$, $\mu$M) | Cotransported Ligands | *Trans*-Stimulation |
|---|---|---|---|---|---|
| CAT-1 | Widely expressed (absent from liver)[a] (~7 and ~9 kb) | Oocytes,[e] mink fibroblasts (588, 589) | L-Arg, L-Lys, L-Orn (70–200)<br>L-His (~2,000)<br>L-Cys (25) | $Na^+$ dependent, only for aa°(590)<br>Electrogenic (264, 267) | 8-fold (90, 106, 108) |
| CAT-2 | T cell, macrophage, lung, testis[b] (~4.5 and ~8.5 kb) | Oocytes[f] | L-Arg, L-Lys (38–380)<br>L-Orn (175–400)<br>aa° (low affinity) | Electrogenic (267) | 2.9-fold (106, 108, 267) |
| CAT-2a | Liver, muscle, skin[c] (~4.5 and ~8.5 kb) | Oocytes[g] | L-Arg (2,000–5,000)<br>L-Lys, L-Orn (NA) | $Na^+$ dependent, only for aa°(108)<br>Electrogenic (267) | 1.5-fold (108, 242) |
| CAT-3 | Brain specific (219, 229) (~3.3 kb) | COS-7 cells (219), oocytes (229) | L-Arg (~100), L-Lys (~150), L-Orn (NA) | | Yes (229) |
| CAT-4 | Pancreas, skeletal muscle, heart, placenta >> brain, lung, liver, kidney[d] (~2.4 kb) | Not yet reported | ? | ? | ? |

Transcript size of CAT transporters corresponds to mouse tissues for CAT-1, CAT-2, and CAT-2a, to rat brain for CAT-3, and to human tissues for CAT-4. *Trans*-stimulation is expressed as times that efflux to a *trans*-side containing 0 substrate is increased when measured at 100 $\mu$M *trans*-side substrate concentration. Apparent Michaelis constant ($K_m$) values were obtained by different labs expressing murine CAT isoforms in *Xenopus* oocytes. aa°, Zwitterionic amino acids; NA, no data available. References are as follows: a) 9, 107, 242, 281; b) 108, 151, 242, 267, 336; c) 151, 336; d) 106, 484, 485; e) 8, 106, 242, 281, 590; f) 108, 242, 267; g) 106, 108, 268. Other references are given in parentheses.

levels than the shorter transcript. All this suggests that protein factors control the stability of CAT-1 mRNA through the long-specific 3′-UTR and through common sequences for both transcripts. In fact, cycloheximide administered in vivo to control rats upregulates the levels of the long transcript in several tissues but unfortunately not in liver, suggesting tissue-specific regulation of the half-life of CAT-1 transcripts. Similarly, in rat hepatoma FTO2B cells, where *CAT-1* expression decreases with confluency, the relative abundance of the two transcripts also varies with confluency; the shorter transcript decreases faster than the longer (610). All this suggests that the 3′-UTR sequences of *CAT-1* transcripts may be involved in the regulation of polyadenylation and/or stability of the transcripts (25). Unfortunately, in these studies showing differential expression of the two *CAT-1* transcripts, no attempt was made to correlate transcript levels and CAT-1 protein abundance to assess translation efficiency. As an additional regulation mechanism of *CAT-1* gene expression, in analogy with *CAT-2* gene, these authors quoted unpublished results that suggest multiple promoter usage for the rat *CAT-1* gene, but no report or confirmation of this is yet available.

To our knowledge, information on the promoter regulation of *CAT* genes to explain the modulation of *CAT-1* and *CAT-2* expression (see sect. IIA5) has not been reported.

### 2. *Transport properties of CAT transporters*

The characteristics of the amino acid transport acitivities elicited by the murine CAT transporters mCAT-1, mCAT-2, and mCAT-2a have been studied in *Xenopus* oocytes and are summarized in Table 3.

*1*) There is sodium-independent transport of cationic amino acids (e.g., L-arginine, L-lysine, and L-ornithine) with high affinity ($K_m$ in the micromolar range) by mCAT-1 and mCAT-2 (106, 108, 242, 267, 281, 590) and with low affinity ($K_m$ in the millimolar range for L-arginine) by mCAT-2a (106, 267). It is worth mentioning that $K_m$ values for L-ornithine influx are higher than those for L-arginine and L-lysine via mCAT-2, suggesting true differences in the extracellular recognition of these substrates (105). As shown in Table 3, there are discrepancies between labs as to the $K_m$ values of cationic amino acids in mCAT-1 and mCAT-2 transporters. Transport of cationic amino acids via mCAT-1 is voltage dependent; hyperpolarization increases the $V_{max}$ and decreases the apparent $K_m$ for influx (the reverse is true for efflux) (264). Closs (105) argued that differences of oocyte membrane potential in different labs and experimental conditions could underlie the variation reported for $K_m$ values.

*2*) For mCAT-1, mCAT-2, and mCAT-2a (242, 267, 590), the transport expressed has been shown to be electrogenic (positive charge follows the cationic amino acid flux) and stereospecific (i.e., $K_m$ in the millimolar range for D-cationic amino acids).

*3*) mCAT-1, mCAT-2, and mCAT-2a present *trans*-stimulation of arginine uptake, with mCAT-1 being more sensitive to this phenomenon (106, 108). mCAT-2a transport activity is largely independent of *trans*-side substrate (Table 3) (106, 108, 267).

*4*) Electrophysiological studies (242, 590) showed

that mCAT-1 and mCAT-2 transport the zwitterionic amino acids homoserine and cysteine only in the presence of sodium (242, 590). Expression of low-affinity histidine uptake is also elicited by mCAT-1 and mCAT-2; for mCAT-1, it has been shown to be partially dependent on the presence of *cis*-sodium. At low pH, when histidine is protonated, this amino acid becomes a better substrate, demonstrating selectivity of CAT transporters for dibasic amino acids. For mCAT-2a (106), transport of zwitterionic amino acids in the presence of sodium has not been observed, although in these studies transport activity was measured by radioactive amino acid uptake, a less sensitive method than electrophysiological measurements.

At present, there are no data available on the amino acid transport activity expressed by hCAT-4 (but expression of hCAT-4 in oocytes resulted in increased L-arginine uptake; Sebastio, personal communication), and there are two reports on rat and mouse CAT-3 (Table 3). Transient expression of rCAT-3 in COS-7 cells resulted in sodium- and chloride-independent transport of radiolabeled L-arginine with an apparent $K_m$ of ~100 $\mu$M, inhibitable by cationic amino acids and dependent on membrane potential, as expected for a cationic amino acid transporter (219). Expression of mCAT-3 resulted in high-affinity, sodium-independent transport of dibasic amino acid, which shows *trans*-stimulation (229). Therefore, CAT-3 together with CAT-1 and CAT-2 transporters are high-affinity cationic amino acid transporters in contrast to the CAT-2a isoform.

It is worth mentioning that the proposed channel mode of action described for the sodium-dependent amino acid transporters, like members of the superfamilies of neurotransmitters and of excitatory amino acid transporters (see the corresponding sections), has not been described for the CAT transporters. It is interesting that these transporters and the proteins rBAT and 4F2hc, which essentially do not mediate sodium-dependent transport, do not seem to have a channel mode of action (90, 110).

Closs et al. (108) obtained surprising data on the accumulation capacity of mCAT-1, -2 and -2a transporters in oocytes at a nonphysiological extracellular concentration of 10 mM L-arginine. Incubation of oocytes in a high L-arginine concentration (10 mM) for 6 h, assuming an oocyte space distribution of ~180 nl/oocyte (90), leads to 0.6-fold accumulation in mCAT-1-expressing oocytes, 1.4-fold in mCAT-2-expressing oocytes, and 6-fold in mCAT-2a-expressing oocytes. These differences have been interpreted as the consequence of an apparent intracellular substrate affinity of mCAT-2a smaller than that of mCAT-1 and mCAT-2 (105). In our opinion, thermodynamic gradients are unlikely to be the result of substrate affinity differences. The regular oocyte membrane potential (−30 to −50 mV) is valid for an accumulation gradient of a positive charged substrate (i.e., L-arginine) of six- to eightfold. Interestingly, accumulation of 10 mM L-arginine in mCAT-2a-expressing oocytes from a sodium-free medium tends to this value (108). Why do mCAT-1 and mCAT-2 not reach the same accumulation gradient? In the experiments by Closs et al. (108), the membrane potential was not clamped, and therefore, the impact of the high L-arginine flux (10 mM extracellular concentration) was not controlled. Additional work at different extracellular substrate concentrations and at constant membrane potentials is needed to characterize the accumulation capacity of these transporters and the transport mechanisms underlying any possible difference between them.

For the human CAT-1, -2, and -2a counterparts, as for the mouse analogs, oocyte expression showed cationic amino acid transport of high affinity that was sensitive to *trans*-stimulation for hCAT-1 and hCAT-2 and cationic amino acid transport of low-affinity that was only slightly sensitive to *trans*-stimulation for hCAT-2a (unpublished data quoted in Ref. 105).

On the basis of all these characteristics (transport properties and tissue distribution), these cDNA (CAT-1, CAT-2, CAT-2a, and CAT-3) have been attributed to system $y^+$ and its variants (242, 281, 590). In summary, transport activity elicited by mCAT-1, mCAT-2, and rCAT-3 expression is similar but with subtle differences (105, 219): sodium-independent high-affinity transport for cationic amino acids, with a slightly higher apparent affinity for mCAT-1, which is more sensitive to *trans*-stimulation. No data are reported on *trans*-stimulation via CAT-3. The transport properties and tissue distribution of CAT-1, CAT-2, and CAT-3 are consistent with subtle variants of system $y^+$ (reviewed in Refs. 126, 600), the common cationic amino acid transport activity of mammalian cells. Most probably, CAT-2a represents a low-affinity liver variant of $y^+$ activity. White and Christensen (601) described a low-affinity transport of L-arginine in primary hepatocytes not subjected to *trans*-stimulation and concluded that the classical $y^+$ activity was absent or altered in hepatocytes. However, Van Winkle (574) suggested that the transport activities expressed by CAT-1 and CAT-2 could fit those of systems $b^+$. Van Winkle et al. (579) also reassessed mCAT kinetic data, suggesting the presence of both a high- and a low-affinity component for each protein (mainly for mCAT-2a) when expressed in oocytes. At present, it is not clear whether this complex kinetic behavior represents an artifact of the expression model, different conformation or oligomeric states, or interaction with endogenous proteins. A more careful characterization of these amino acid transport activities based on inhibition by amino acids and analogs is needed to clarify this issue. Similarly, cell knockout or antisense experiments, like those reported for system $b^{0,+}$-like in opossum kidney (OK) cells (374), would clarify the contribution of CAT transporters to $y^+/b^+$ transport activity in cells. In this sense, uptake studies in cells derived from the null knockout CAT-1 mice (419) may help to clarify this issue.

*3. Protein structure of CAT transporters*

Structural information on CAT transporters is scarce. All CAT transporters identified lack a characteristic signal peptide, and therefore, the $NH_2$ terminus is considered to be cytoplasmic (see Refs. 105 and 336 for review and Ref. 219 for rCAT-3). Most of the additional information available has been obtained from mCAT-1, and it has been extrapolated to CAT-2 and CAT-3 transporters since they show almost identical hydrophobicity profiles (105, 219). These profiles initially suggested two membrane topology models for CAT transporters: 12 TM (according to MacLeod's and Saier's groups) or 14 TM (according to Cunningham's group) (9, 106, 334, 448). The two models differ in the middle TM domains (TM domains VII and X of the 14-TM model are considered to be intracellular in the 12-TM model; see Fig. 2). The 12-TM model is supported by the fact that CAT transporters belong to the APC transporter superfamily of yeast, fungi, and eubacteria, which presumably contain 12 TM domains (448), whereas the proposed membrane topology of the first 8 TM domains of the homologous yeast and fungi permeases argue in favor of the 14-TM model (105, 508). Mutational analysis showed that the viral binding site of mCAT-1 (see Fig. 2) is located between TM V and VI, confirming the extracellular location of extracellular loop (EL) 3 in both models (8). Evidence in favor of the 14-TM model has been obtained: *1*) antibodies directed against peptides of the EL3 and EL4 loops of mCAT-1 in the 14-TM model immunostained nonpermeabilized cells (605). This confirmed the extracellular location of these protein regions; the 12-TM model predicts an intracellular location for the EL4 protein region. *2*) The glycosylation of CAT transporters has been demonstrated by endoglycosidase F (endo F) treatment of immunodetected CAT-1 (i.e., antiserum raised against the COOH terminus of murine CAT-1) and CAT-2/CAT-2a (i.e., antiserum raised against COOH terminus of murine CAT-2a; a region that is identical to CAT-2) from mammalian cells or expressed in oocytes. These studies showed a broad glycosylated moiety of 3–9 kDa for mCAT-1 and mCAT-2a transporters (106, 280). Mutation in mCAT-1 of the two putative *N*-glycosylation sites Asn-223 and Asn-229 to histidine, conserved in all CAT transporters characterized (Fig. 1), results in a protein with identical SDS-PAGE mobility to the endo F-treated wild-type mCAT-1; mutation of either Asn residue results in an intermediate mobility. The 12-TM model predicts an additional, unconserved extracellular *N*-glycosylation site in mCAT-1 (Asn-373, located in the intracellular IL4 of the 14-TM model). Mutation of Asn-373 to histidine does not affect glycosylation of mCAT-1. These studies (280) demonstrated that Asn-223 and Asn-229 are the glycosylated residues of mCAT-1, and therefore extracellular, like the loop EL3 in the 14-TM model (Fig. 2), and that Asn-373 (in the IL4 loop of the 14-TM model) might not be located extracellularly, which thus favors the 14-TM model.

To our knowledge, extensive studies in search of evidence for the 14-TM model, like those performed with the GABA transporter GAT1 (38), the glycine transporter GLYT1 (401), and glutamate transporters (585, 498), have not been reported.

*4. Structure-function relationship*

Swapping chimeras with the divergent amino acid segment of CAT transporters, mutational analysis and studies related to the interaction with the murine ecotropic leukemia virus provided the core of our knowledge of the structure-function relationship for CAT transporters.

The apparent substrate affinity, maximum transport rate, *trans*-stimulation, and accumulation capacity are distinctive features of mCAT-2 and mCAT-2a (see Table 2, CATS). This suggests that these differential transport capacities are determined by the variant exon coding for the 41- to 42-amino acid residue divergent segment of the two proteins (see Fig. 2). Closs et al. (108) performed elegant studies, in which chimeric transporters with the backbone of mCAT-1 were completed with the divergent domain of mCAT-2 and mCAT-2a, and the backbone of mCAT-2 was completed with the corresponding domain of mCAT-1 (see Fig. 2). The transport characteristics (apparent $K_m$, $V_{max}$, *trans*-stimulation, and accumulation of L-arginine) of these chimeras expressed in oocytes are similar to those of the divergent region. Interestingly, the recently cloned rat CAT-3 expresses high-affinity ($K_m$ ~100 $\mu$M) L-arginine uptake in COS-7 cells, and its divergent domain is more similar to that of CAT-1 and CAT-2 than to that of CAT-2a (219) (see Fig. 2). These data suggest that the divergent protein domain of CAT transporters has an impact on all transport properties, and therefore, it might have a role in substrate recognition, turnover number, and the translocation mechanism. As indicated in Fig. 2, the divergent domain corresponds to the intracellular loop IL4 (including a few amino acid residues of TM domains VIII and IX) in the 14-TM domain model of CAT transporters.

Residues involved in the reported mutational analyses of mCAT-1 are indicated in the homologous position in the mCAT-2 protein model depicted in Figure 2. *N*-glycosylation is not required for transport function of mCAT-1 (280); the unglycosylated mutant (double Asn to His mutation at positions 223 and 229: see Fig. 1) expresses an unaffected transport activity in oocytes. The glutamate residue at position 107 of mCAT-1 is conserved in the TM domain III of all known CAT transporter sequences (see Figs. 1 and 2) and also in the yeast transporters for arginine, histidine, and choline of the APC family (589). This residue is required for transport activity in mCAT-1 protein expressed in mink CCL64 lung fibroblasts

(589). Substitution by aspartate led to a loss of transport activity; interestingly, substitution by the uncharged glutamine residue did not affect transport activity (data by Kim and Cunningham quoted in Ref. 105). All these substitutions led to mCAT-1 protein expressed in the plasma membrane of the transfected cells as demonstrated by its role as a virus receptor (infectivity and viral glycoprotein gp70 binding). All this suggests that the carbon backbone size but not the negative charge of residue glutamate 107 of mCAT-1 determines transport function for the CAT transporters.

Meruelo and co-workers (621) and Cunninngham and co-workers (8) identified by domain swapping and mutational analyses the sequence NVKYGE (amino acid residues 232–237 in mCAT-1) within EL3 (see the corresponding position of this protein segment in Fig. 2) as essential for virus envelope binding and infection; swapping the above-mentioned sequence into the human CAT-1 conferred infectivity and virus binding (8). This sequence is also present in the rat CAT-1 counterpart (610), but not in hCAT-1 or the known CAT-2 proteins (see Figs. 1 and 2). Interestingly, both mCAT-1 and rat CAT-1 serve as a receptor for the virus. Detailed description of the amino acid residues within the EL3 loop required for binding of the viral protein envelope gp70 and permissivity to infection (8, 267) has been reviewed by Closs (105). It is worth mentioning that none of the mutations examined to determine viral interaction with CAT transporters affected their transport activity. In contrast, interaction of mCAT-1 with the virus reduces its transport activity. Coexpression of mCAT-1 and glycoprotein gp70 resulted in a specific reduction of mCAT-1 glycosylation and transport activity; a decrease in transport activity also occurs with the unglycosylated double Asn to His mutant at residues 223 and 229 (280). Binding of glycoprotein gp70 to the transfected mCAT-1 results in noncompetitive inhibition of amino acid import via the murine CAT-1 with no effect on amino acid export (588). The effects of gp70 on transport kinetics led the authors to suggest that gp70 binding represents a steric hindrance that slows the rate-limiting step of the amino acid import cycle, a conformational transition of the empty transporter in which the binding site moves from the inside back to the outside of the cell, and that gp70 has no effect on the rate-limiting step of the amino acid export cycle. A similar mobile carrier hypothesis has been suggested for the two-directional operation of the system $y^+$ (600). The above-mentioned data suggest that amino acid transport and virus receptor functions may be coupled; conformational changes of the transporter may lead to membrane fusion of virus and host cell (105). Interestingly, the transport defective mCAT-1 mutant glu107asp mediates binding of glycoprotein gp70 and virus infection (589). This suggests that transport and receptor function may be uncoupled, but this is still an open question, since conformational changes for the transport-defective mutant have not been ruled out.

### 5. *Physiological role of CAT transporters*

An intriguing question is why there is such a variety of CAT transporters in mammalian cells. Cationic amino acids are needed for protein synthesis, urea synthesis (arginine), and as precursors of bioactive molecules (arginine and ornithine are substrates for the synthesis of urea and nitric oxide as well as polyamines, respectively). Then, what does each CAT transporter isoform contribute to the supply of substrates for these purposes? The contribution of other protein structures to cationic amino acid transport, like rBAT (system $b^{o,+}$-like) and 4F2hc (system $y^+$L-like) are discussed in section II*D*. The nearly ubiquitous CAT-1 isoform most probably corresponds, as discussed before, to the classical system $y^+$, a high-affinity and electrogenic cationic amino acid transport system that allows accumulation of these substrates within the cells for general metabolic purposes. Consistent with this, the null knockout CAT-1 mice are smaller (limited accretion) at birth (419). In this sense, at a physiological extracellular concentration of L-arginine (50 $\mu$M), a high expression level of mCAT-1 in oocytes allows the maintenance of an L-arginine gradient across the plasma membrane of ~19-fold (90).

The known examples of upregulation of CAT-1 transporter expression favor this general role of the classical system $y^+$/CAT-1 isoform. The expression of this gene is enhanced in proliferating cells (e.g., T and B lymphocytes activated by concanavalin A and bacterial lipopolysaccharide, rapidly growing cells infected with Friend leukemia virus, and a variety of tumor cells of different origin) (620). In liver regeneration, CAT-1 expression (both mRNA and protein) is induced a few hours after hepatectomy (25, 610). Recently, Hatzoglou's group (25) showed that *CAT-1* could be considered as a delayed early growth response gene in the regenerating liver that requires protein synthesis for its upregulation. In keeping with this, ecotropic retroviruses infect hepatocytes during fetal development and liver regeneration, but not in adult hepatocytes (198). This supports a role of CAT-1 transporter in accretion, and as discussed by Wu et al. (610), a role of this transporter in the supply of ornithine for polyamine synthesis. Interestingly, the key enzyme in polyamine synthesis, ornithine decarboxylase, peaks during the $G_1$ phase (145), and ornithine levels rise after partial hepatectomy (149). In addition to proliferation, hormone treatment (insulin and dexamethasone) also induces mCAT-1 expression in liver (610). A recent report also links CAT-1 expression with cell proliferation. Perkins et al. (419) reported that the homozygous null knockout CAT-1 mice develop anemia and die after birth. Erythroid maturation is defec-

tive in these mice because of a specific defect in cell proliferation and/or differentiation. In addition, this suggests that CAT-1 transporter is the main contributor to the cationic amino acid supply to erythroid progenitor cells. The specific contribution of CAT-1 transporter to the intracellular accumulation of cationic amino acids in those cells that express additional CAT isoforms (e.g., in brain, heart, skeletal muscle, uterus, ovary, testis, and placenta) is difficult to assess by indirect determinations, like transcripts and protein levels (see below). Specific knockout and antisense experiments are needed to delineate the contribution of each CAT transporter to the macroscopic amino acid flux through the plasma membrane of the cells.

The low-affinity high-capacity transport properties, the accumulation capacity through the plasma membrane at high extracellular substrate concentrations, and the exclusive expression of CAT-2a isoform mRNA, but not CAT-1 (both protein and mRNA) or CAT-2 (mRNA) isoforms, in liver have been envisaged as constituting a kinetic barrier between the hepatic urea cycle and extracellular arginine (105). Furthermore, on the basis of the low intracellular concentration of arginine in liver, it is unlikely that this amino acid is released through the activity of CAT-2. All this is consistent with the lack of activity of the classical high-affinity system $y^+$ in the hepatocyte plasma membranes, which protects extracellular L-arginine from hydrolysis by hepatic arginase (600, 601). The hepatocyte CAT-2a transporter would allow rapid accumulation of cationic amino acids only at high plasma concentrations, leaving sufficient substrates in circulation for cells expressing the high-affinity CAT isoforms (105). In keeping with this, expression of CAT-1 isoform occurs in liver when the urea-cycle enzymes are downregulated (e.g., liver regeneration, insulin treatment, low-protein diet) (610). Interestingly, stress conditions (partial hepatectomy, surgical trauma, and fasting) upregulate mCAT-2a in skeletal muscle (K. D. Finley, quoted in Ref. 336); the CAT-2/-2a isoforms are prevalent in this tissue (242). Some of these stress situations have a muscle proteolytic state in common (309, 324). The possible physiological role of CAT-2a upregulation induced by stress conditions such as fasting in skeletal muscle is far from understood. MacLeod and Kakuda (336) suggested that this is a mechanism to prevent depletion of those amino acids from the tissue with active proteolysis. In this regard, it should be mentioned that the rate of release of lysine or arginine in the rat perfused hindquarter preparation is not modified in response to 48 h of fasting (464). Brief starvation in humans has been reported to enhance the release of lysine, but not of arginine, from skeletal muscle (429). Studies should be performed to determine the role of CAT-1, CAT-2a, and CAT-4 in the metabolism of cationic amino acids in skeletal muscle.

Ashcroft and co-workers (504) studied the transport mechanisms involved in the stimulation of insulin secretion by L-arginine in mouse pancreatic $\beta$-cells. This work suggests that L-arginine raises the intracellular concentration of $Ca^{2+}$ and stimulates insulin secretion as a consequence of its electrogenic transport into this cells. The expression of mCAT-2 and mCAT-2a in $\beta$-cells was demonstrated by RT-PCR. L-Arginine produced a dose-dependent increase in the intracellular concentration of calcium, which suggests that the low-affinity mCAT-2a is the cationic amino acid transporter responsible for the secretagogue action of this amino acid. Specific mCAT-2a knockout experiments in $\beta$-cells or in the whole animal are needed to demonstrate the role of mCAT-2a in the insulin secretagogue action of L-arginine.

The CAT-1 mRNA is constitutively expressed in mature resting and activated T cells and splenocytes and resident macrophages (242, 336). Activation of these cells mainly induces the CAT-2 transporter isoform. SL12 thymoma cell clones, a model system of thymocyte differentiation, show developmental regulation of mCAT-2 during thymocyte maturation (602). The m*CAT-2* gene is downregulated in normal and mature thymocytes until it is activated by mitogens or antigens (151, 242, 334). Peripheral blood lymphocytes and quiescent splenocytes exhibit little transport of lysine via systems $y^+$ and $y^+L$ (64, 127). Upon activation, T cells rapidly increase system $y^+$ transport activity and mCAT-2 mRNA levels in parallel (64). In addition, a transient increase in mCAT-1 expression has been reported (336). Human CAT-1 antisense experiments in phytohemagglutinin-induced lymphocytes reduce the induced system $y^+$ transport activity only partially (88). Combined experiments with antisense sequences of CAT-2 and CAT-1 have not been addressed.

The release of nitric oxide is an important mediator of macrophage function (389, 536). Activation of macrophages by bacterial lipopolysaccharide (LPS) and interferon-$\gamma$ (IFN-$\gamma$) produces the parallel induction of the expression of CAT-2 (108) and the nitric oxide type II synthase (inducible nitric oxide synthase or NOS II), and nitric oxide production (129, 519, 612). Unpublished data from MacLeod's lab showed specific induction of mCAT-2 but not of mCAT-2a after activation of macrophages (quoted in Ref. 336). Nitric oxide synthase II uses L-arginine as a substrate (373), and its activity is dependent on extracellular L-arginine (55, 211, 230, 611). In parallel with macrophage activation, there is an increase in arginine transport rate (55, 473), due to system $y^+$ (36). More recently, concomitant induction of NOS II and CAT-2 transcripts (>20-fold) (no CAT-1 or CAT-2a transcripts) and nitric oxide production (>30-fold) and high-affinity $y^+$ activity (3- to 4-fold) has been observed in brain astrocytes treated with LPS/IFN-$\gamma$ (512). Interestingly, actinomycin D blocks the increase in system $y^+$ activity and nitric oxide production due to LPS/IFN-$\gamma$. This indicates that the contribution of CAT-1 to arginine uptake for nitric

oxide production is negligible compared with that of CAT-2. Similar to macrophages and astrocytes, vascular smooth muscle cells respond to cytokine (interleukin-1$\beta$ and tumor necrosis factor-$\alpha$) treatment by parallel increase in mCAT-2 and NOS II mRNA levels, without any effect on mCAT-1 mRNA levels (167). In contrast, angiotensin II increases mCAT-1 mRNA levels in vascular smooth muscle cells without induction of the nitric oxide secretion pathway (323). No attempt was made in any of these studies to corroborate changes in CAT-2 and CAT-1 expression at the protein level. All this suggests that CAT-2 transporter accounts for this increased uptake. Knockout experiments are needed to elucidate the participation of CAT-2 and CAT-1 isoforms in the supply of arginine for nitric oxide synthesis by NOS II. If this hypothesis is verified, the mechanism by which arginine supplies nitric oxide synthesis by NOS II will be the induction of a specific $y^+$ isoform (with transport characteristics very similar to the widespread $y^+$ isoform) but through the induction of its specific gene promoter. In addition, whether differential transport properties or specific location in plasma membrane domains of CAT-1 and CAT-2 isoforms channel arginine for NOS II has not been addressed. An interesting experiment would be to induce NOS II activity in the context of knockout of *CAT-2* gene and overexpression of *CAT-1* gene.

### B. Superfamily of Sodium- and Chloride-Dependent Neurotransmitter Transporters

The cloning of rat and human brain GABA transporters (GAT1) in 1990 (184, 391) and the human norepinephrine transporter (NET) in 1991 (405) was the starting point for the isolation of related cDNA that constitute the sodium- and chloride-dependent neurotransmitter transporter superfamily (for review, see Refs. 54, 253, 390, 565). Rat brain GABA transporter was purified and microsequenced by Kanner's group (439), and then related oligonucleotide probes were used, in a collaborative effort between Nelson's, Lester's, and Kanner's groups, to isolate rat GAT1 from a rat brain cDNA library (184). Amara's group (405) isolated the NET cDNA from the human neuroblastoma cell line SK-N-SH by expression cloning, after accumulation of the norepinephrine analog [$^{125}$I]iodobenzylguanidine in COS-1 cells (405). In 1992, Burg and Handler and coworkers (614) reported the isolation of the canine betaine transporter (BGT-1) cDNA, which was obtained by expression cloning in oocytes from a size-fractionated cDNA library constructed from MDCK cells maintained in hypertonic medium; mRNA from MDCK cells maintained in hypertonic medium showed increased induction of betaine uptake in oocytes (452). Different strategies based on homology with these previous and the on-coming cDNA sequences from different cDNA sources resulted in the cloning of the rest of transporters of this superfamily (for references for the amino acid transporters, see Table 4).

The members of this superfamily have a common membrane topology prognosis of 12 TM domains, and as a general characteristic that defines this superfamily, the transport activity of these carriers has been found to be sodium and chloride dependent. Substitution of sodium by lithium is not tolerated, and substitution of chloride by other anions ranked the potency order as follows: chloride $\geq Br^- > NO_3^- >$ gluconate $>$ acetate (reviewed in Refs. 44, 260, 302, 465). These transporters (15 putative cDNA have been identified without considering species counterparts) share a high level of homology (30–65%). Homologous transporters have been identified in insects, worms, and yeast (13, 318; reviewed in Ref. 390). On the basis of substrate specificity and extensive amino acid sequence identity, this superfamily has been divided into two major subfamilies (reviewed in Refs. 253, 390, 565). The first major subfamily corresponds to the sodium- and chloride-dependent neurotransmitter transporters, which comprises three minor subfamilies: *1*) biogenic monoamine transporters, which include dopamine, norepinephrine, and serotonin transporters that show an amino acid sequence identity between 40 and 47% with the members of the other subfamilies (53, 213, 279, 405, 494, 567, 570; for review, see Refs. 54, 253, 390, 565) and two subfamilies for amino acid transporters; *2*) GABA and taurine transporters (see Tables 4 and 5), also including creatine transporters (2 have been isolated, one of which corresponds to the previously identified choline transporter as revealed by expression studies and cellular distribution; Refs. 34, 172, 186, 346, 388, 480, 509), with an amino acid sequence identity that ranges between 49 and 69%; and *3*) glycine and proline transporters that show a similar level of homology with each other and with the rest of the superfamily (amino acid sequence identity ranges from 43 to 48%). The second major subfamily comprises three "orphan transporters" with structural characteristics that differ from the previous major subfamily (large second and fourth putative extracellular domains with a canonical *N*-glycosylation site; Refs. 139, 317, 345, 566; for review, see Ref. 565).

In the present review, only the amino acid transporters of this superfamily are considered. Excellent reviews concerning the monoamine, creatine, and orphan transporters are available (11, 22, 54, 302, 565). Because of the high level of confusion with different names for the same transporter cloned from different species (e.g., see different names for the GABA transporters in rat and mouse in Table 4), in the present review we use the nomenclature based on the rat GABA transporter cDNA (see Table 4). In this section, attention is paid to tissue distribution, transport characteristics, protein structure with relation to transport function, and the physiological role of these transporters in both neural and peripheral tissues. The

TABLE 4. *Sodium- and chloride-dependent amino acid transporters within the superfamily of neurotransmitter transporters*

| Transporters (Gene Name) | Accession Numbers (Origin of Human Clones) | Origin of First Clone and Other Names | Human Chromosome | Protein Amino Acid Length |
|---|---|---|---|---|
| GAT-1 (SLC6A1) | X54673 (brain) (391) | Rat brain (GAT-1) (184)<br>Mouse GABAT (318), rat GAT-A (103) | 3p24-p25 (220) | 599 |
| GAT-2 (human not available) | M95762 (rat brain) (60) | Rat brain (GAT-2) (60)<br>Mouse GAT3 (315) | | 602 |
| GAT-3 (not shown in GDB) | S75989 (fetal brain) (57) | Rat brain (GAT-3, GAT-B) (60, 103)<br>Mouse GAT4 (315) | (?) | 632 |
| BGT-1 (not shown in GDB) | L42300 (brain) (59)<br>U27699 (kidney) (446) | MDCK cells (BGT-1) (614)<br>Mouse GAT2 (322) | 12p13 (446) | 614 |
| TAUT (SLC6A6) | Z18956 (thyroid cells) (232)<br>U16120 (placental cells) (445)<br>U09220 (retinal epithelium) (368) | MDCK cells, rat, and mouse brain (TAUT, Tau) (316, 503, 562) | 3p24-p26 (445) | 620 |
| GLYT1 (SLC6A9) | P48067 (brain) (282) | Rat and mouse brain (GLYT, GLYT1) (183, 319, 502)<br>Rat GLYT2 (62)<br>GLYT 1a, 1b & 1c variants (2, 62, 282, 314) | 1p31 3-p32 (282) | 633 (1a)<br>638 (1b)<br>692 (1c) |
| rGLYT2 (human not available) | L21672 (rat brain) (314) | Rat brain (GLYT2) (314) | | 799 |
| PROT (SLC6A7) | Not available (brain) (489) | Rat brain (PROT) (155) | 5q31-q32 (489) | 636 |

*Human transporters with accession numbers for their cDNA are indicated when available Human GAT-2 and GLYT2 cDNA have not been isolated, in their place, rat cDNA are indicated For GLYT1, protein length is indicated for each variant (1a, 1b, and 1c) GDB, Gene Data Bank, r, rat Reference numbers are given in parentheses*

amino acid transporters of this superfamily of neurotransmitter transporters do not necessarily have a role in neurotransmission, since, for example, the GABA transporter (GAT-2), the betaine/GABA transporter (BGT-1), the taurine transporter (TAUT), and the glycine transporter GLYT1 are expressed in nonneural tissues (see Table 5).

### *1. Tissue expression*

The tissue distribution of GAT-1 was monitored by immunocytochemistry before the "cloning era" of these transporters (442). For the rest of the amino acid transporters of this superfamily, the tissue distribution and the transcript size were initially studied by Northern blot (see Table 5) and in situ hybridization analysis. All these transporters are expressed in the central nervous system (CNS), and some of them are also expressed in peripheral tissues. The GABA transporters GAT-1 and GAT-3, the glycine transporter GLYT2, and the proline transporter PROT seem to be specific to the CNS (57, 103, 155, 184, 240, 314, 315, 391, 489).

A) GABA TRANSPORTERS. Several studies address the distribution of the four GABA transporters (GAT-1, -2, and -3 and BGT-1) in the CNS, including a recent review by Borden (56). The three high-affinity ($K_m$ values from 1 to 20 $\mu M$) GABA transporters GAT-1, -2, and -3 are expressed in brain and retina (60, 65). Antibodies raised to mouse and rat GAT-1 showed a relatively even distribution of this GABA transporter in all parts of the brain, in parallel with the distribution of GABA (330, 442). This transporter is present mainly in the neuropil, but also in processes of glial cells in the cerebral cortex, cerebellum, hippocampus, and retina (364, 375, 442, 450). Similarly, both in neuronal and type 2 astrocyte cultures, most of GABA transport (~75%) shows a pharmacological profile specific for GAT-1 (e.g., inhibition by the GAT-1-selective ligand NNC-711) and in parallel GAT-1 transcript levels are abundant (61). The distribution pattern of GAT-1 makes it a good candidate for the GABA transporter that functions in the GABAergic synapses (see review in Ref. 240). Thus immunofluorescence, electron microscopy, and confocal immunolocalization of GAT-1 in rat hippocampus, retina, and cerebellum correlate with its involvement in the termination of the action of GABA by its uptake from the extracellular space into GABAergic axon terminals and astrocytes, where it could also play the additional role of regulating the extracellular concentration of GABA (216, 375, 450). In addition, there is generally good correlation between GAT-1 (mRNA and protein) and glutamic acid decarboxylase-like immunoreactivity (GAD67; i.e., the enzyme responsible for GABA synthesis) in striatum and cerebral cortex (24, 364, 525). However, the expression of GAT-1 is not restricted to neurons involved in GABAergic synapses. Thus, in cerebral cortex, the GAT-1 uptake system (mRNA and protein) is more extensive than the GABA synthesizing system (364, 525) in the cerebellar cortex, GAT-1 and GAD67 mRNA do not correlate in Purkinje cells (447), and in the rat spinal motor neurons, there is expression of GAT-1 mRNA but not GAD67 (506). All these results support the hypothesis that GAT-1 plays its presynaptic role in GABAergic synapses but, in addition, may have postsynaptic roles, and

TABLE 5. *Tissue distribution and transport characteristics of expressed $Na^+$- and $Cl^-$-dependent amino acid transporters*

| Transporter | Tissue Distribution (Transcript Size) | Expression System | Substrates ($K_m$, $\mu$M) | Pharmacology ($K_i$, $\mu$M) | Cotransported Ligands |
|---|---|---|---|---|---|
| GAT-1 | CNS[a] (4.2–4.4 kb) | Oocytes[h]<br>COS-7 cells (60)<br>HeLa cells[i]<br>HEK 293 cells (81, 82) | GABA (<10)<br>Betaine (>>500)<br>β-Ala (>2,000) | NIP (<10), ACHC (~100)<br>L-DABA (<30) | GABA, $2Na^+$, $Cl^-$ (265, 273) |
| GAT-2 | Peripheral tissues and CNS[b] (2.2–2.4 kb) | Oocytes (315)<br>COS-7 cells (60) | GABA (~20)<br>β-Ala (~30)<br>Taurine (~500) | NIP (>500), ACHC (>500)<br>L-DABA (>100), betaine (>>500), β-Ala (~100) | $Na^+$, $Cl^-$ (60) |
| GAT-3 | CNS[c] (4.7–5.0 kb) | Oocytes (315)<br>COS-7 cells (60)<br>LLC-$PK_1$ cells (102)<br>Intestine cells (103) | GABA (~1)<br>β-Ala* (~100)<br>Taurine (~1,500) | NIP (50), ACHC (~800)<br>L-DABA (~100)<br>Betaine (>>500)<br>β-Ala* (<10) | GABA, >1$Na^+$, $Cl^-$ (102) |
| BGT-1 | Peripheral tissues and CNS[d] (3.0–3.4 kb and others) | Oocytes (614)<br>COS-7 cells (59)<br>9HTEo cells (446)<br>LM(tk-) cells (59)<br>MDCK cells (423) | GABA (<100)<br>Betaine (~400)<br>L-Proline (~900) | NIP (>2,000), ACHC (~2,000)<br>L-DABA* (≥2,000)<br>Betaine* (~200)<br>β-Ala (~2,000) | GABA, $2Na^+$, $Cl^-$ (194) |
| TAUT | Peripheral tissues and CNS[e] (6.2–7.5 kb and others) | Oocytes[j]<br>COS-7 cells[k]<br>HeLa cells (445) | Taurine (<10)<br>β-Ala (~60) | Hypotaurine (<10)<br>L-Ala (>250), L-Pro (>>250)<br>GABA* (>2,000)<br>MeAIB (>>2,000) | Tau, $2Na^+$, $Cl^-$ (445) |
| GLYT1 | CNS and peripheral tissues[f] (3.2–3.8 kb) | Oocytes[l]<br>COS-7 cells[m] | Glycine (<50) | Sarcosine (<100)<br>L-Ala, GABA (>1,000)<br>L-Pro (≥1,000) | $Na^+$, $Cl^-$ (183, 282, 319) |
| GLYT2 | CNS (314) (8 kb) | Oocytes (22) | Glycine (~20) | Sarcosine (>1,000)<br>L-Ala, MeAIB (>1,000)<br>β-Ala (>2,000) | Nap, $Cl^-$ (314) |
| PROT | CNS[g] (4 kb) | HeLa cells[n] | L-Pro (<10) | Sarcosine (30), NIP (>>100)<br>L-His, L-Cys (~80) | $Na^+$, $Cl^-$ (489) |

Only range of common transcript size in different species is shown. $K_m$ values are from different labs and obtained by expression in *Xenopus* oocytes. * Substrates or inhibitors with contradictory reports for interaction with corresponding transporter from different labs or species (see text for details). All transporters have been shown to cotransport corresponding substrates plus co-ions, $Na^+$ and $Cl^-$. In addition to biogenic amine transporters of this superfamily, GAT-1 transporter has been shown to have ion leak and ligand-gated channel activity (see text for details); there are no reports on this issue for the rest of the amino acid transporters of this superfamily. NIP, nipecotic acid; ACHC, *cis*-3-aminocyclohexanecarboxylic acid; L-DABA, 2,4-diaminobutyric acid; β-Ala, β-alanine; L-Ala, L-alanine; MeAIB, *N*-methylaminoisobutyric acid; L-pro, L-proline; sarcosine, *N*-methylglycine; L-His, L-histidine; L-Cys, L-cysteine. References are as follows: a) 184, 315, 391; b) 60, 315; c) 60, 103, 315; d) 59, 322, 446, 614; e) 232, 316, 368, 445, 503, 562; f) 2, 62, 183, 282, 319, 502; g) 155, 489; h) 184, 265, 318, 325, 339, 341, 520; i) 37, 261, 273, 288, 410, 451; j) 316, 368, 562; k) 232, 503; l) 183, 319; m) 62, 282, 502; n) 155, 489. Other references are as given in parentheses.

it may regulate the extracellular concentration of GABA in glial cells.

Northern blot analysis and in situ hybridization histochemistry showed a complementary distribution of GAT-3 and GAT-1 (103, 315); GAT-3 has a strong expression in spinal cord, brain stem, thalamus, and hypothalamus and is weakly expressed in cerebellum, hippocampus, cerebral cortex, and striatum, where GAT-1 transcripts are abundant. In many instances, the localization of GAT-3 (mRNA and protein) correlates well with characterized populations of GABAergic neurons and glutamic acid decarboxylase immunoreactivity, as in the medial septum-diagonal band complex, but in others, the distribution is dissimilar, such as in the cerebellum (103) and cerebral cortex (363). The distribution of GAT-3 in brain cells is controversial. Initially, GAT-3 was described predominantly as a neuron transporter (103), but later its presence in astroglial processes was demonstrated by immunocytochemistry (450), and in cerebral cortex it localized exclusively to astrocytic processes (363). Similarly, GAT-3 mRNA is present in neuronal and in type 2 astrocyte cell cultures (61). Recently, in electron microscopic immunolocalization studies in the developing rat brain (i.e., embryonic and early postnatal stages), GAT-1 and GAT-3 protein showed coordinate expression (239): GAT-1 was detected in gray matter and growing axons, and GAT-3 in radial glial cell fascicles oriented perpendicularly to the axons expressing GAT-1. Therefore, at present, it seems that GAT-3 is mainly a glial transporter.

Among the high-affinity GABA transporters, GAT-2 is the only one expressed in peripheral tissues in addition to brain and retina (60, 223, 315). Initial Northern blot analysis revealed that GAT-2 mRNA levels in brain are developmentally regulated, being more abundant in the brains of newborn mice than in the adult or fetal brain (315). Two studies compared the distibution of GAT-2 with the other two high-affinity GABA transporters in retina and brain (216, 223). Immunoreactivity of GAT-2 was

faint throughout the brain but was concentrated in the arachnoid and ependymal cells, a completely different distribution from that of GAT-1 and GAT-3 proteins (see above). Similarly, in the retina, GAT-2 protein localizes to the retinal pigment epithelium layer, nerve fiber layer, and cilliary body epithelium, whereas GAT-1 and GAT-3 localize to amacrine neurons and Muller glial cells, respectively. In rat brain-derived cultures containing O-2A progenitor cells and type 2 astrocytes, GAT-2 mRNA is the second most abundant after GAT-1 transcripts; in contrast, GAT-2 transcripts are not detected in neuronal cultures or type 1 astrocyte cultures (61). These results suggest that GAT-2 may be related to nonneuronal function in brain and retina.

Northern blot analysis showed an even distribution of BGT-1 transcripts in mouse (~5 kb in length) and human brain (≥3 kb and a less conspicuous band of 4.1 kb) (59, 322, 446). BGT-1 is most probably a glial transporter; its transcripts were observed in type 1 and type 2 astrocyte cultures, but not in neuronal cell cultures (61). The presence of BGT-1 mRNA in human and mouse brain (59, 322, 446) suggests that, at least in these species (BGT-1 was not shown in canine brain; Ref. 614), this transporter could participate in brain osmoregulation (59) (see sect. II*B6*). Betaine is present in brain at low concentrations, but levels increased after salt loading (207). Handler's group (537) showed the presence of different 5'-UTR in canine BGT-1 transcripts due to splice variants and the use of three tissue-specific promoters.

The GABA transporters GAT-2 and BGT-1 are expressed in peripheral tissues (59, 60, 315, 322, 446, 614): mouse and rat GAT-2 are expressed in liver and kidney and human and mouse BGT-1 are expressed in kidney medulla and liver. In addition, one report also showed expression of human BGT-1 in placenta, heart, and skeletal muscle (446). In situ hybridization and RT-PCR of microdissected nephron segments revealed that BGT-1 is predominantly expressed in the medullary thick ascending limbs of Henle's loop and the inner medullary collecting ducts (365). In the polarized epithelial cell model MDCK, Handler's group (613) showed that BGT-1 localizes to the basolateral membrane, consistent with its role in protecting cells in the renal medulla from hypertonicity (385, 387). Caplan and co-workers (5, 423) addressed the polarized expression of the four GABA transporters (GAT-1, -2, and -3 and BGT-1) expressed in MDCK and in freshly isolated hippocampal neurons: *1*) GAT-1 localized exclusively to the axons of cultured neurons and to the apical pole of transfected MDCK cells, consistent with its axonal localization in vivo (364, 375, 442, 450). *2*) GAT-3 was expressed in the apical membrane of transfected MDCK cells and in both axons and somatodendritic membranes of hippocampal neuron cultures. *3*) In contrast, expressed GAT-2 and BGT-1 localized to the basolateral membranes of transfected MDCK cells; expression of BGT-1 in hippocampal neurons in culture localized to somatodendritic membranes. These studies are subsidiary to those of Simons and co-workers (130, 131, 221) showing a polarized correlation between axons and the epithelial apical pole, and somatodendritic membranes and epithelial basolateral membranes. Following this line, Caplan and co-workers (5) suggested that GAT-2 may have a basolateral location in kidney and liver and a dendritic location in neurons, but to our knowledge, the subcellular distribution of GAT-2 in epithelia and brain has not been determined. Very recently, Pietrini, Caplan, and co-workers (417), working with MDCK cells BGT-1, rat GAT-1 and human nerve growth factor receptor chimeras, suggested the presence of basolateral sorting information in the cytosolic COOH-terminal domain of MDCK cells BGT-1; a short segment within this domain (residues 565–572), rich in basic residues well conserved in human BGT-1 but not in rat GAT-1, contains information necessary for exit from the endoplasmic reticulum and for the basolateral localization of MDCK cells BGT-1 in these cells.

B) TAURINE, GLYCINE, AND PROLINE TRANSPORTERS. To our knowledge, the tissue distribution of the taurine transporter TAUT has been studied only by Northern blot analysis or RT-PCR. The TAUT transcripts are widespread, and its abundance varies between different studies and species. In general, however, it has been shown to be present in kidney cortex and medulla, small intestinal mucosa, brain, lung, retina, liver, skeletal muscle, heart, placenta, spleen, and pancreas (232, 316, 445, 503, 562). Reverse transcriptase-polymerase chain reaction also showed TAUT mRNA in human ovary, colon, and thyroid (232).

The tissue distribution of the glycine transporters, as revealed by Northern blot analysis, indicates that GLYT1 is expressed in the CNS and peripheral tissues, whereas GLYT2 is specific to the CNS (see Table 5). A recent review by Zafra et al. (622) summarizes the cellular localization studies of glycine transporters at the protein and mRNA levels in brain (2, 62, 183, 237, 314, 328, 502, 623, 625). Both GLYT1 and GLYT2 are mainly expressed in caudal areas, and in addition, GLYT1 has a moderate expression in forebrain areas. The distribution of GLYT2 is consistent with the distribution of the inhibitory glycine receptor (immunocytochemistry and strychnine binding studies) and with neurons with high glycine content (17, 237, 623): high expression in the dorsal and ventral horn of the spinal cord, auditory system, and nuclei of the cranial nerves, and low expression in cerebral hemispheres. The distribution of GLYT1 in caudal areas is more widespread than that of the glycine receptors detected by strychnine binding (623). This indicates first, association of both transporters with the inhibitory glycinergic neurotransmission and a role in the termination of the glycinergic action, and second, additional roles for GLYT1 in nongly-

cinergic regions. Electron microscopic immunolocalization showed a glial (perikarya and processes) location for GLYT1 and an axonal (presynaptic terminals) location for GLYT2 (623). The location of GLYT1 in neurons is at present controversial: some authors did not observe neuronal expression of GLYT1 mRNA (2, 183), whereas others (62, 502, 625) reported in situ hybridization signal in neurons of the spinal cord, brain stem, and cerebellum and also in forebrain regions (cortex, hippocampus, thalamus, hypothalamus, and olfactory bulb). Immunocytochemistry studies failed to detect the neuronal form of the protein clearly (except in the retina; GLYT1 protein was localized in the amacrine neurons, Ref. 623), but they confirmed the glial expression of GLYT1 (238, 623). This controversy might be because of the use of probes with different isoform specificity and antibodies that do not react with the neuronal form of the protein (622). The specific mRNA distribution of GLYT1–1a and 1b/1c (GLYT1–1b probes used in this study do not distinguish between 1b and 1c variants) isoforms has been studied by Borowsky et al. (62): GLYT1–1a is found only in gray matter, whereas GLYT1–1b/1c is found exclusively in fiber tracts. Furthermore, GLYT1–1b/1c is found in all white matter, whereas GLYT1–1a distribution parallels the distribution of mRNA for the strychnine-sensitive and strychnine-insensitive glycine receptor in olfactory bulb, hippocampus, cerebellum, and spinal cord. For the presence of GLYT1 in areas without glycine receptor expression, two explanations have been offered (622): *1*) Smith et al. (502) suggested a role of GLYT1 in modulating glutamatergic transmission through the activity of some *N*-methyl-D-aspartate (NMDA) receptors (see sect. II*B6*), and *2*) association of GLYT1 with non-strychnine-sensitive glycine receptors; in this sense, the mRNA of the $\beta$-subunit of the glycine receptor and GLYT1 show similar distribution (62, 625).

GLYT1 is expressed in peripheral tissues (see Table 5). The GLYT1–1a variant, but not 1b/1c variants, is expressed in rat peripheral tissues: liver, spleen > lung > stomach, uterus > pancreas, kidney (i.e., relative abundance of transcripts) (62). Expression of GLYT1–1a in lung, spleen, liver, and thymus occurs in macrophages (62).

The mRNA coding for the brain-specific high-affinity L-proline transporter PROT was shown to be expressed in subpopulations of putative glutamatergic neurons in the olfactory bulb, cerebral cortex, and hippocampus (155). Western blot studies revealed the presence of PROT in enriched synaptic plasma membrane preparations and its absence from postsynaptic membranes (489, 580). This suggests a presynaptic regulatory role of L-proline or the PROT transporter in specific excitatory pathways in the CNS.

### 2. *Transport characteristics*

A) GENERAL CHARACTERISTICS. The characteristics of the transport activity associated with the expression of the amino acid transporters of this superfamily are summarized in Table 5. Sodium and chloride dependence has been reported for all these transporters (see Table 5).

B) GABA TRANSPORTERS. Of the eight amino acid transporters in this superfamily, only four transporters, GAT-1, -2, and -3 and BGT-1, induce uptake of GABA when expressed in cultured cells or in oocytes; GAT-1 to -3 are high-affinity transporters ($K_m$ values from 1 to 20 $\mu$M), and BGT-1 is a low-affinity GABA transporter (when expressed in oocytes it showed an apparent $K_m$ of <100 $\mu$M for GABA, even lower than that for betaine) (see Table 5). Pharmacological studies helped to distinguish the transport activity of the four GABA transporters (see Table 5). GAT-1 shows the highest sensitivity to *cis*-3-aminocyclohexanecarboxylic acid (ACHC), 2,4-diaminobutyric acid (L-DABA), nipecotic acid (NIP) (also OH-NIP), and guvacine, and it is not inhibited by $\beta$-alanine (60, 103, 117, 273, 315). These are the pharmacological characteristics of the neuronal GABA transport (see references in Refs. 103, 184). In addition, biochemical evidence demonstrated that GAT-1 corresponds to the neuronal high-affinity subtype $GABA_A$ transporter, sensitive to ACHC (for review, see Ref. 260). Lipophilic derivatives of piperidencarboxylic acid [tiagabine, SKF-89976A, CI-966, and NNC-711; the latter with an inhibition constant ($K_i$) of 6 nM] are highly selective for GAT-1 transport activity (58, 102, 103). Interestingly, these inhibitors have anticonvulsant properties (103, 524).

The pharmacologies of GAT-2 and GAT-3 are similar to each other; GAT-3 shows higher sensitivity to NIP (see Table 5) and to a new triarylnipecotic acid derivative, 4(S) (128). The most characteristic BGT-1 inhibitor is betaine (see Table 5). Kilimann and co-workers (187) listed the pharmacological characteristics of the GABA transporters isolated from different species and expressed in different systems and pointed out the dissimilarities in the data reported (e.g., BGT-1 inhibition by L-DABA and betaine, TAUT inhibition by GABA, and interaction of $\beta$-alanine with GAT-3; see Table 5). One of the most relevant dissimilarities is the role of $\beta$-alanine in GAT-3 transport activity: an apparent $K_m$ of ~100 $\mu$M for mouse GAT-4 (i.e., GAT-3) (315), and no transport of $\beta$-alanine up to 500 $\mu$M via rat GAT-B (i.e., GAT-3), but an apparent $K_i$ of ~7 $\mu$M for $\beta$-alanine inhibiting GABA transport (103). More recent studies (102) showed consistent interaction of GAT-3 permanently expressed in LLC-$PK_1$ cells with $\beta$-alanine (i.e., similar apparent $K_m$ and $K_i$ values of ~30 $\mu$M). The reasons for these discrepancies are unknown. Interaction of $\beta$-alanine with GAT-3 is consistent with its presence in glial cells, but not with its expression in neurons (61, 103, 216, 363, 450).

In summary, the pattern of expression in brain and the pharmacological characteristics of the four GABA transporters strongly indicate that GAT-1 corresponds to the most typical neuronal presynaptic GABA transporter,

whereas GAT-2 and GAT-3 characteristics fit the glial transporter activity. In addition, the neuronal expression of GAT-3 and its brain distribution implies a complementary role of GAT-3 and GAT-1 in GABAergic synapses. The β-alanine sensitivity of neuronal GAT-3, a glial characteristic (103), might be explained by this complementary expression of GAT-1 and GAT-3, and the higher expression of GAT-1 in neurons, as described in neuronal cell cultures (61).

C) β-AMINO ACID TRANSPORTERS. Four transporters of this superfamily mediate β-amino acid transport (GAT-2, GAT-3, and TAUT) or are inhibited by β-alanine (BGT-1) (see Table 5). Murine, canine, rat, and human TAUT are highly homologous (~90% identity), have a wide transcript distribution, including kidney and small intestine, and express a very similar transport activity for the sulfur-containing β-amino acids taurine and β-alanine in oocytes (232, 316, 368, 445, 503, 562). Apart from the difference in the length between the mouse (590 amino acid residues; Ref. 316) and the human, rat, and canine proteins (620, 621, or 655 amino acid residues, respectively; Refs. 232, 368, 445, 562), because of different COOH termini, all these transporters could be considered as the counterparts of the same gene for these species. Expression of these transporters in oocytes results in sodium- and chloride-dependent high-affinity transport of taurine ($K_m$, 5–12 μM) and β-alanine ($K_m$, ~50 μM); hypotaurine inhibits transport with a $K_i$ that is probably in the micromolar range, whereas GABA, L-alanine, and MeAIB have no effect at 100 μM (see Table 5). Thus it seems that the taurine/β-alanine transporter is a β-amino acid-specific carrier. A specific system for β-amino acids with high affinity for taurine ($K_m$, 10–14 μM) and similar transport characteristics has been described in luminal plasma membranes from small intestine and renal proximal straight tubules; furthermore, in renal luminal membranes, other transport systems with lower affinity ($K_m$ values in micromolar and millimolar ranges) for taurine have been reported (231, 370, 496). A similar transport activity has been reconstituted from brush-border membranes of human placenta (444). Handler and co-workers (562) proposed that the cloned taurine carrier may correspond to the basolateral transporter described in MDCK cells, since the levels of the carrier mRNA increase after incubation in hypertonic medium. However, this issue is not clear, since the $K_m$ (~50 μM) reported for the basolateral carrier in MDCK cells is higher than that reported for the cloned carrier and for the apical membranes of MDCK cells (~10 μM) (563). Both GAT-2 and GAT-3 encode for high-affinity GABA transporters (see above). These two transporters also carry β-alanine with high affinity ($K_m$ values are ~30 and ~100 μM, respectively) and taurine with a lower affinity ($K_m$ values are ~500 and ~1,500 μM, respectively) when expressed in oocytes. Homology between these two transporters and the taurine transporter is very high (i.e., amino acid sequence identity ranges from 62 to 66%; amino acid residues present in β-amino acid interacting transporters: GAT-2, GAT-3, TAUT, and BGT-1 are idicated in Fig. 3). As for the taurine transporter, GAT-2 and GAT-3 transport activity is inhibited by micromolar concentrations of hypotaurine (562). Therefore, the substrate specificity of GAT-2 and GAT-3 transporters covers GABA and the β-amino acids. As indicated above, GAT-2 and GAT-3 represent tissue/cell-specific isoforms with very similar transport activity: GAT-3 is neural tissue specific, whereas GAT-2 is highly expressed in kidney and liver, and in lower amounts in adult brain.

BGT-1, with high homology (amino acid sequence identity ranges from ~60 to 70%) to the β-amino acid transporters (i.e., TAUT, GAT-2, and GAT-3), encodes for a sodium- and chloride-dependent betaine (fully methylated glycine) and GABA transporter (see sect. II*B2*B). Interestingly, β-alanine interacts weakly with BGT-1 (i.e., 2 mM β-alanine inhibits ~50% of transport). BGT-1 cDNA from mouse, dog, and human most probably represents species counterparts of the same transporter because of their homology (~90% amino acid sequence identity) and similar transport characteristics (see Table 5), in addition to their reported different tissue distribution in brain and peripheral tissues (see above). The murine and human BGT-1 are expressed in kidney, liver, and brain, but the canine transporter is mainly expressed in kidney medulla but not in liver or brain (59, 322, 446, 614). Most probably, the canine BGT-1 transporter represents the major hypertonicity-modulated transporter of the nonperturbing osmolyte betaine that operates in kidney medulla, normally the only hypertonic tissue in mammals (292). As discussed by Yamauchi et al. (614), luminal membranes from small intestine and renal proximal tubules transport betaine in a sodium-dependent manner, which is shared with high-affinity transport of proline. Interestingly, canine BGT-1 transporter expressed in oocytes has a low affinity for proline ($K_m$ in the millimolar range) (614).

In summary, transporters of this superfamily can be grouped according to substrate specificity. From strict GABA transporters to strict β-amino acids (i.e., β-alanine) transporters, the proteins could be ranked as follows (see Table 5): *1*) GAT-1, high affinity and GABA specific; no interaction with β-alanine; neural specific; *2*) BGT-1, inhibition by β-alanine at millimolar concentration; *3*) GAT-2 and the neural-specific GAT-3, substrate affinity in the micromolar range for GABA and β-alanine; and *4*) TAUT transporter, substrate affinity in the micromolar range for β-alanine and taurine and weak, if any, interaction with GABA. The concept of classical system BETA, defined in Ehrlich ascites cells with a low affinity for β-alanine ($K_m$ in millimolar range) (96, 495), might correspond to the variety of different transporter isoforms described here and to carrier isoforms not yet identified. For example, in mammalian kidney, a complex interaction between re-

absorption systems for β-amino acids and GABA has been shown, including shared transport systems for amino acids and GABA as well as more GABA-specific carriers (496). TAUT, BGT-1, GAT-2, and GAT-3 transporters, which show overlapping specificities for β-amino acids and GABA, are expressed in kidney. The challenge is now to relate the function of these transporters with the physiological fluxes of these amino acids in vivo, through the regional and cellular localization of these transporters and the "knockout" of the respective genes.

D) GLYCINE TRANSPORTERS. Two glycine transporter genes, GLYT1 and GLYT2, belong to this superfamily (see Table 5). GLYT1 presents three variants (1a, 1b, 1c) that are transcribed from a single gene (2, 62, 282). The three protein variants differ in their $NH_2$-terminal sequences. Two promoters are responsible for 1a and 1b variants, and 1c isoform is an alternative splicing variant of 1b transcript with a 54-amino acid-long exon toward the $NH_2$ terminus (2) (see Fig. 4*B*). The three variants show no differences in their transport characteristics; in fact, truncated proteins, constructed by elimination of the differential amino acid residues, retain the transport characteristics of the intact proteins, and only their cellular processing is affected (282). GLYT2 (~50% amino acid sequence identity with GLYT1 variants) most probably corresponds to the 100-kDa reconstituted and purified glycine transporter from pig brain (314, 320). GLYT2 is a larger protein than GLYT1 variants, due to a longer $NH_2$ terminus (see Fig. 3). GLYT1 and GLYT2 transport activities can be distinguished by the higher sensitivity of GLYT1 variants to sarcosine (*N*-methylglycine) (see Table 5). Specific high-affinity (apparent $K_m$ values from 20 to 100 μM) transport systems for glycine have been identified in synaptosomes and glial cells (for review, see Ref. 622). The uptake process is electrogenic (inward positive charge flux) with a stoichiometry of 1 glycine, 2 sodium, and 1 chloride (16, 624); these coupling coefficients permit a glycine gradient through the plasma membrane that is strong enough to maintain an extracellular glycine concentration of 0.2 μM (23). The characteristics (substrate affinity, sodium and chloride dependence, and pharmacology) of the glycine transport via GLYT1 and GLYT2 in oocytes and mammalian cells are consistent with the neuronal and glial transport activity (622). Because of their brain distribution, GLYT2 most probably represents the neuronal glycine transporter, and GLYT1 the glial transporter, but the presence of GLYT1 transcripts in neurons (see sect. v*B1*) suggests its contribution to neuronal glycine uptake.

The transport characteristics of GLYT1 (sodium-dependent glycine transport inhibited by sarcosine, but not by MeAIB or β-alanine) resemble that of system Gly (274, 572). Notwithstanding, the expressed transport activity of GLYT1 presents a much higher affinity for glycine than the classical transport system (62, 183, 282, 314, 319, 502) and is mainly found in neural tissues with very low levels of mRNA in liver or kidney (2, 62, 183, 282, 319, 502). Thus the encoded protein might correspond to a transporter isoform of the widespread system Gly. GLYT1 gene expression (1a variant; see sect. II*B1*) in kidney, although low, might be responsible for the high-affinity ($K_m$ in the micromolar range) sodium-dependent glycine uptake component in luminal membranes from proximal straight tubules (reviewed in Ref. 483). This can now be tested by immunolocalization of the GLYT1 in kidney. To this end, it is important to assess whether GLYT1 in kidney is expressed in the epithelial cells or in macrophages, as has been reported for lung, spleen, and liver (62).

E) PROLINE TRANSPORTER. The proline transporters (PROT) isolated from a rat and human brain libraries show ~45% identity to GLYT transporters at the amino acid sequence level (155, 489). The protein is encoded by a 4-kb mRNA that is present in the excitatory pathways of rat brain. This pattern of expression suggests that the encoded protein does not represent an ubiquitous transporter that might have a general metabolic role but rather supports a specific role for L-proline or this transporter in excitatory amino acid neurotransmission (see sect. II*B6*). The transporter expresses sodium- and chloride-dependent uptake of L-proline with very high affinity ($K_m$ is ~10 μM) in HeLa cells (155, 489). The expressed sodium-dependent uptake of proline is sensitive to sarcosine, norleucine, phenylalanine, histidine, and cysteine, with $K_i$ ranging from 30 to 90 μM. Therefore, in common with GLYT transporters, PROT transporters tolerate *N*-methyl derivatives, since both show high-affinity interaction with sarcosine (*N*-methylglycine). This high-affinity L-proline transport is unique to nervous tissue; in contrast, a lower affinity, sodium-dependent L-proline transport has also been described in neural tissues and renal, intestinal, and choroid plexus brush-border membrane vesicles through various systems (e.g., IMINO, $B^{0,A}$) (reviewed in Refs. 483, 513, 505).

### *3. Mechanisms of transport and uncoupled ion fluxes*

The transport characteristics of the first member of this superfamily of transporters to be discovered, GAT-1, have been studied more extensively than the other members (see Table 5). As discussed above, GAT-1 corresponds to the neuronal high-affinity ACHC-sensitive GABA transporter present in synaptosomes and synaptic plasma membranes (260, 273). The transport of GABA by GAT-1 in different expression systems, including permanent expression in mammalian cells, showed the following characteristics (for references, see Table 4): *1*) a single high-affinity ($K_m$ of ~4 μM) component of transport, in full agreement with values obtained in synaptic plasma membranes (250) and reconstituted systems (439); *2*) absolute requirement of sodium, but not of


FIG. 3. Amino acid sequence comparisons of sodium- and chloride-dependent amino acid transporters. Sequences multialigned correspond to human transporters but for rat GAT-2 and GLYT2. Horizontal lines over sequences indicate roughly position of theoretical (i.e., hydrophobicity plots) TM domains I-XII. Potential *N*-glycosylation sites are indicated by open boxes between TM domains III and IV. Gray boxes indicate amino acid residues present in all mammalian amino acid transporters (negative or positive charged residues are considered together) of this superfamily, in 4 GABA transporters (GAT-1, GAT-2, GAT-3, and BGT-1), in $\beta$-alanine-interacting transporters (GAT-2, GAT-3, BGT-1, and TAUT), or in GABA, betaine, and taurine transporter subfamily. Finally specific amino acid residues for glycine and proline subfamily of transporters are shown in white inside black boxes. For all amino acid sequence identity shown here, all mammalian cDNA clones indicated in Table 4 are considered. Dash lines indicate gaps for sequence multialignment obtained with Clustal Multiple Sequence Alignment from Baylor College of Medicine.

chloride; capacitive charge movement and transport-associated current studies indicate that chloride facilitates the binding of sodium and that this limits the overall transport rate at saturating GABA concentrations (339, 325); and *3*) exchange mechanism of transport (i.e., efflux of GABA is *trans*-stimulated by external GABA). This represents a part of the translocation cycle of the transporter (257, 393). Stable expression in mammalian cells revealed unique properties for GAT-3 (102), a $K_m$ values for chloride of 78 mM, which is severalfold higher than that for GAT-1, and the $K_m$ for GABA depends on the chloride concentration (i.e., a decrease in chloride concentration results in an increase in the apparent $K_m$ for GABA).

Stoichiometry of the coupled ions and GABA via cloned GAT-1 was first deduced from the corresponding Hill equations. GAT-1 permanently expressed in mouse $LtK^-$ cells (273) shows a sodium concentration dependence with sigmoidal behavior, whereas the dependence of GABA and chloride concentrations was hyperbolic. This allowed a proposed stoichiometry of cotransport of 1 GABA, > 1 (probably 2) sodium, 1 chloride, in accor-

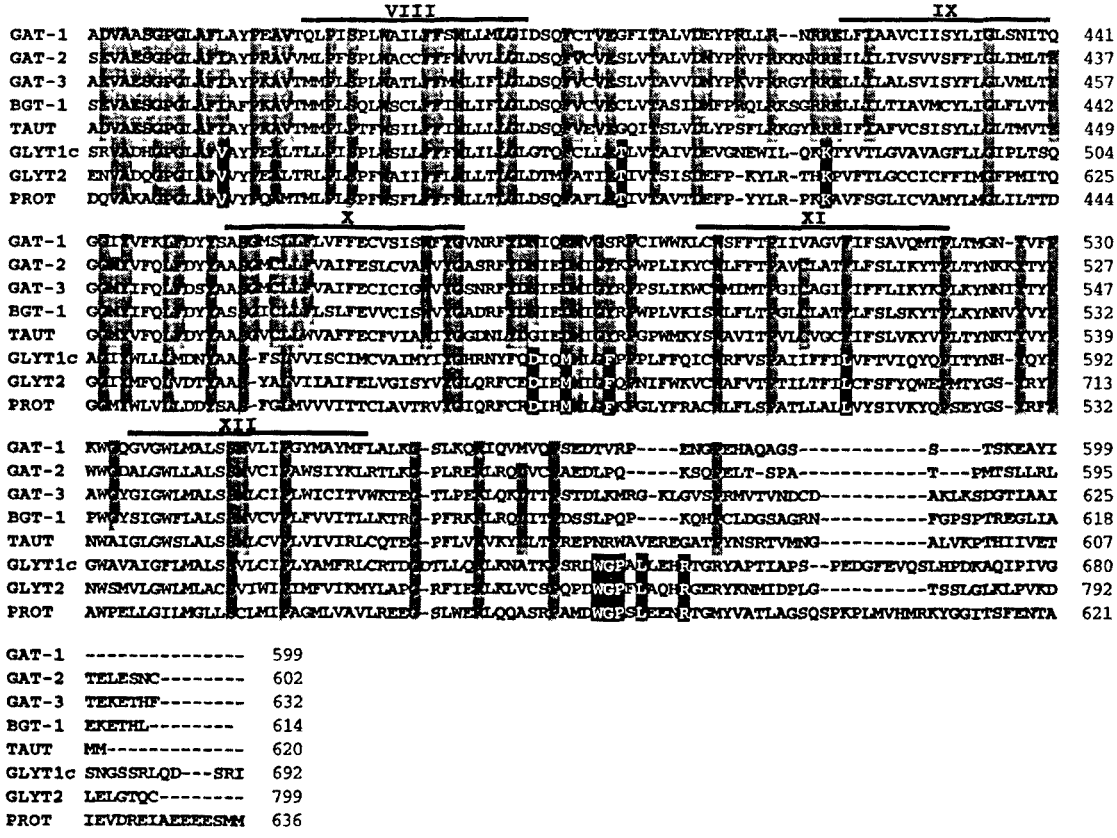

FIG. 3—*Continued*

dance with data obtained previously with synaptic plasma membrane vesicles and the purified transporter (257, 272, 440). Thus direct measurements of $^{22}Na^+$, $^{36}Cl^-$, and [$^3$H]GABA fluxes using proteoliposomes into which a partial purified preparation of the neuronal high-affinity ACHC-sensitive GABA transporter (most probably GAT-1; see above) was reconstituted yielded the following stoichiometry (272): 1 GABA $\geq$ 2 sodium, 1 chloride. This stoichiometry suggests that GABA transport through GAT-1 is electrogenic (i.e., external GABA induces positive inward current). Expression of rat GAT-1 in oocytes resulted in electrogenic uptake of GABA, with an apparent affinity constant of ~5 $\mu$M for GABA and Hill coefficients of 0.7 for chloride and 1.7 for sodium (265). Concentration dependence studies of capacitive charge movements support the interaction of two sodium with GAT-1 (339). Surprisingly, correlation of induced currents and radiolabeled GABA uptake gave a ratio of one positive charge flux per molecule of GABA transported; this indicates a stoichiometry of 1 GABA, 2 sodium, and 1 chloride (265, 341). Similarly, kinetics of GABA uptake induced by rat GAT-1 transfected in HeLa cells gave Hill coefficients compatible with this stoichiometry (451). This fits with the proposed stoichiometry for the rat GAT-3, canine BGT-1, and human dopamine transporter DAT (507, 102), but not with other transporters of this superfamily; a stoichiometry of 1 serotonin, 1 sodium, and 1 chloride for the rat serotonin transporter SERT (180) and 1 norepinephrine, 1 sodium, and 1 chloride for the human transporter NET (161, 181). Therefore, as discussed below for the sodium- and potassium-dependent transporters of glutamate and zwitterionic amino acids, the stoichiometry of the coupled ions does not appear to be conserved between the members of the superfamily of sodium- and chloride-dependent neurotransmitter transporters.

The transport stoichiometry of the neurotransmitters and co-ions just described leads to electrogenic transport. However, the conducting properties of these transporters go well beyond this (301, 507). The expression of these transporters displays several conducting states that resemble single-channel openings and that occur both in the presence of substrate (substrate-gated channel activity) and in its absence (leakage) (301, 507). Uncoupling between transport flux and substrate-evoked current in steady state has been observed for rat SERT, human DAT, human NET, and rat GAT-1 (160, 161, 340, 451). Several recent reviews address this issue (301, 507, 609). This is similar to the uncoupled chloride channel mode of action of several transporters of the superfamily of sodium- and chloride-dependent gluta-

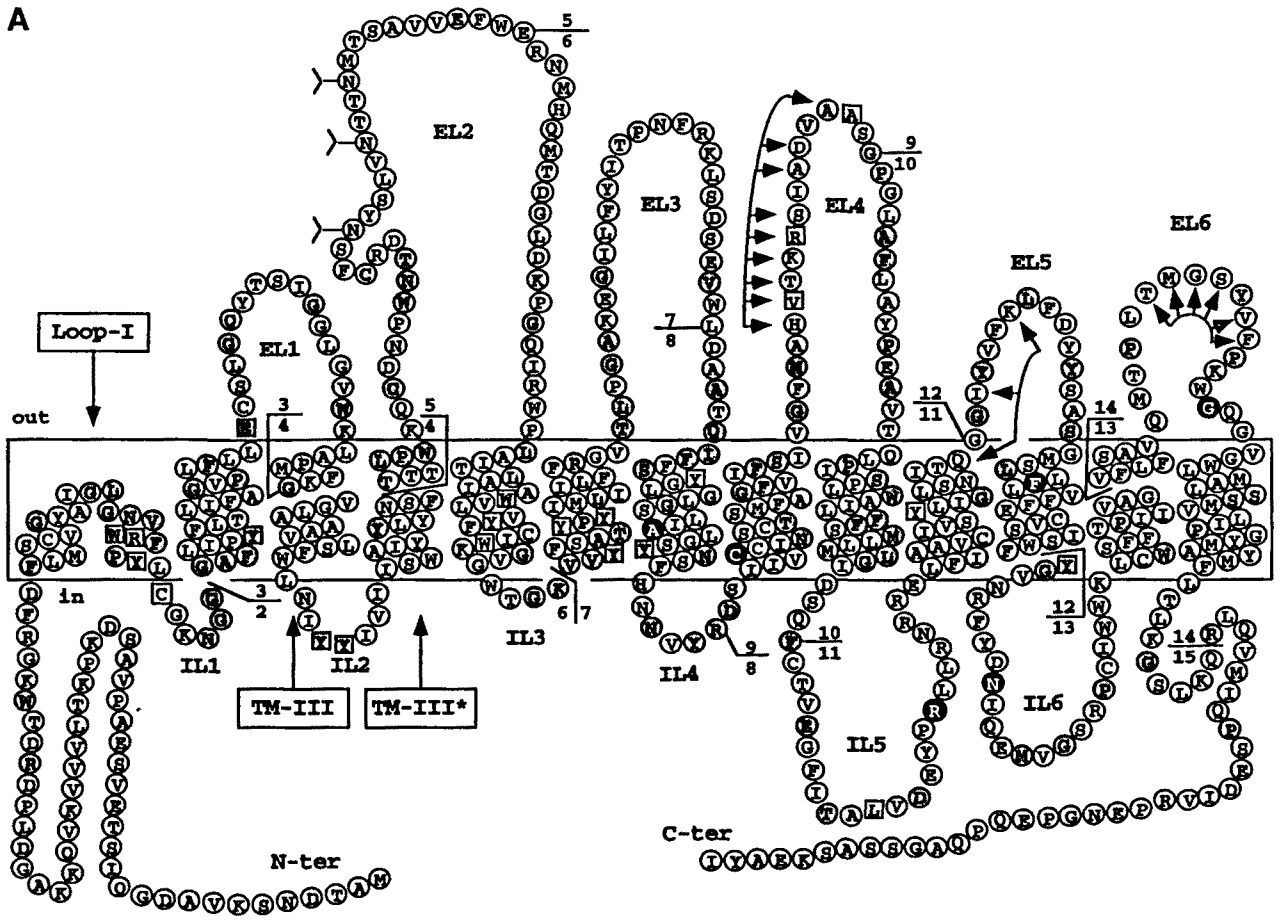


FIG. 4A. new 12-TM domain membrane topology model for rat GAT-1 transporter. This model has been recently proposed by Kanners and co-workers (38), and it is in full agreement with that proposed by Aragón, Giménez, and co-workers (401) for GLYT1 transporter (see Fig. 4B). Notice that hydrophobic domain I corresponds to a "reentrant" membrane loop. Hydrophobic external (EL) and internal (IL) loops are numbered. A 44-amino acid hydrophobic stretch, from Leu-118 to Trp-161, is proposed to contain TM domain III, IL2 loop, and new TM domain III*; sequence within TM domain III* is only tentative. Amino acid residues conserved in all mammalian amino acid transporters of this superfamily are indicated in gray circles, whereas only 6 specific amino acid residues for GABA transporters (GAT-1, -2, -3, and BGT-1) are indicated in white over a black circle. Amino acid residues within squares are those subjected to site-mutagenesis studies (see text for details). Amino acid sequences indicated by arrows connected with a line in EL4 and EL5 are corresponding ones cross-mutated between mouse GABA transporters and proposed to be involved in substrate specificity and affinity in Reference 542 (see text for details). Y, three putative *N*-glycosylation sites in EL2. Exon-intron boundaries of mouse GAT-1 transporter gene (318; corrected in Ref. 390) within putative rat protein sequence are indicated, and exons are numbered. Exon 1 is an untranslated sequence (318). In general, position of exon-intron boundaries is conserved between transporters of this superfamily (390) (see Fig. 4B for murine GLYT1 transporter gene).

mate and zwitterionic amino acid transporters (see sect. IIC), but the charge-carrying ions responsible for these uncoupled currents have not been identified (507). Comparisons of the transport flux and the currents associated with the expression of the biogenic amine transporters (SERT, NET, and DAT) and the GAT-1 GABA transporter revealed ratios greater than the proposed stoichiometries (discrepancies ranged from a factor of 3 to >100), but the apparent Hill coefficients for sodium and chloride for the activation of the substrate-induced currents is consistent with the uptake studies and with the proposed stoichiometry (for review, see Refs. 301, 507). Thus, for rat SERT expressed in oocytes, a ratio of charge flux to serotonin molecule of 5–12 positive charge flux was found, whereas the proposed transport stoichiometry (1 serotonin, 1 sodium, 1 chloride) predicted a ratio of 1 positive charge flux/serotonin molecule (340). Electrophysiological studies with rat GAT-1 permanently transfected in HEK 293 cells showed that the stoichiometry between GABA and co-ions flux was not fixed (e.g., outward and inward currents require different ions on each side of the membrane) (81). DeFelice and co-workers (451) reported that the sodium-dependent GABA-induced currents due to GAT-1 expression

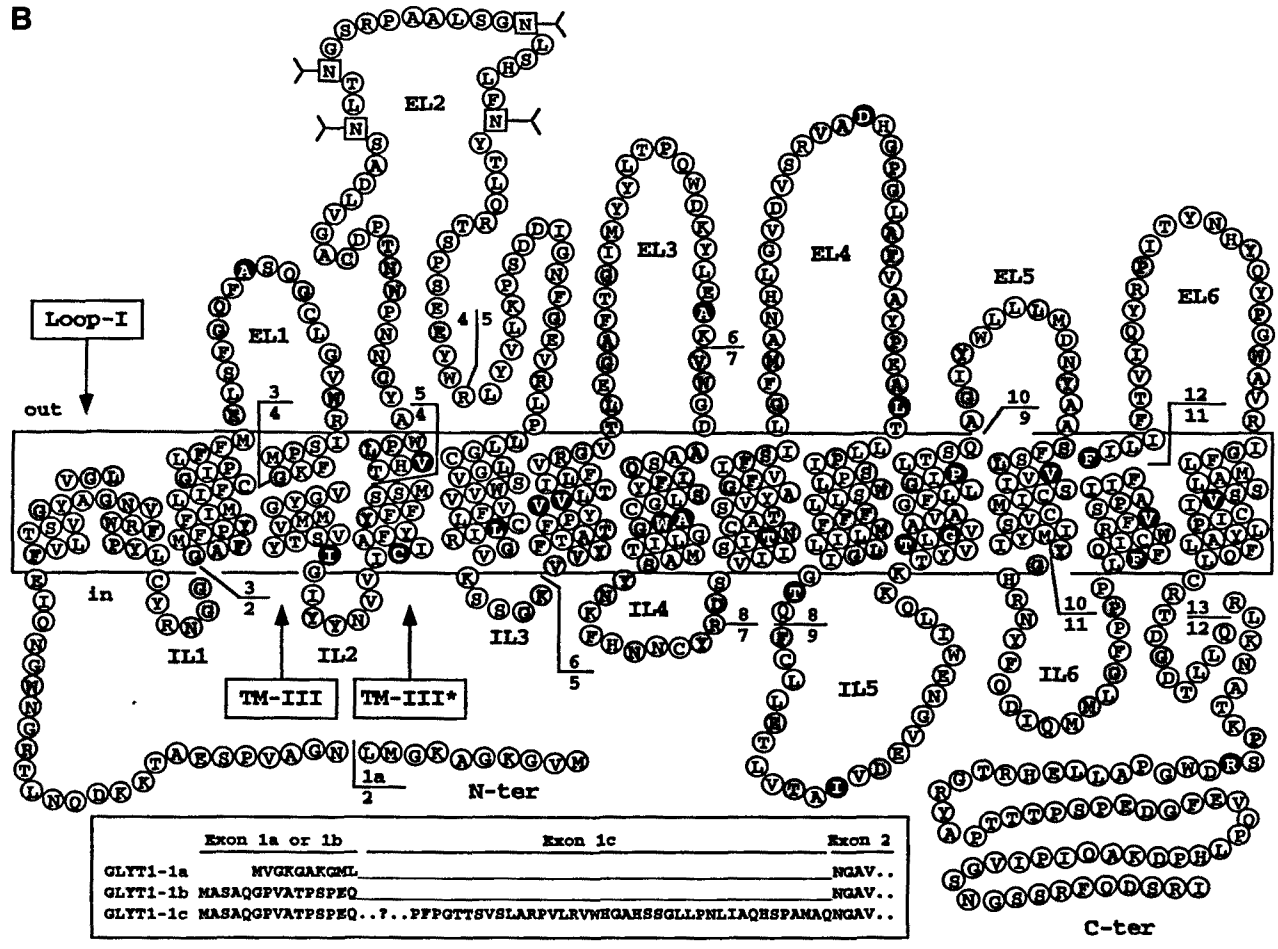


FIG. 4*B*. new 12 TM domain membrane topology for mouse GLYT1a transporter. This model has been proposed by Aragón, Giménez, and co-workers (401) for rat GLYT1 transporter and is in full agreement with model proposed by Kanner and co-workers (38) for rat GAT-1. See Fig. 4*A* for description of model. Amino acid residues conserved in all mammalian amino acid transporters of this superfamily are indicated by gray circles, whereas those specific for glycine transporters are indicated in white over a black circle. *N*-glycosylation sites (Y) used for rat GLYT1 are indicated by a square (see text for details). Murine exon-intron boundaries within putative protein sequence are indicated, and exons are numbered. *Inset*: alignment of $NH_2$ terminals of 3 mouse GLYT1 variants (1a, 1b, and 1c). At present, full-length murine exon 1c is unknown (2), but human one has been reported (282).

in HeLa cells do not show saturation of the current-voltage curve, as fixed stoichiometry would predict, but it shows saturation of the current-external GABA concentration curve at a fixed voltage; these data suggest that saturable binding of external GABA gates a channel through the GAT-1 transporter or an associated channel. Mager et al. (341) estimated that GAT-1 is expressed in oocytes at a plasma membrane density of $10^4$ transporters/$\mu m^2$, and with a transport turnover rate of $\sim 10\ s^{-1}$ (at 300 $\mu$M GABA, 96 mM NaCl, −80 mV and 22°C). To explain the maximal currents due to the expression of GAT-1 in HeLa cells on the basis of the 1 GABA, 2 sodium, 1 chloride-coupled model, either the density of transporters at the cell surface or the turnover rate is >10-fold higher than the values estimated in oocytes (451). In summary, all this suggests substrate-activated conduction, which is not thermodynamically coupled to transport. It is at present unknown, as for the members of the superfamily of sodium- and potassium-dependent glutamate and zwitterionic amino acids (see sect. II*C*), whether the substrate-gated channel occurs through the transporter itself or via interaction with an extrinsic channel protein. Fluctuation analysis indicates that the substrate-gated channel current events (−0.2 to −0.5 pA at −80 to −100 mV), associated with the expression of human NET and rat serotonin transporter (SERT) in HEK 293 cells and oocytes, respectively, are brief (~1 ms) and have an extremely low open probability ($10^{-3}$ to $10^{-6}$); interestingly, the probability of opening increases with substrate concentration (160, 507). This is interpreted, at least for several members of the superfamily of neurotransmitter transporters (SERT, NET, DAT, and

GAT-1), as indicating that these transporters show brief channel openings whose probabilities depend on the concentration of the substrate and co-ions (e.g., 1 opening/350–700 transport cycles; Ref. 301). The channel openings would account for the macroscopic current that exceeds the charge flux expected from transport flux and substrate/co-ion stoichiometry (301, 507).

Transporters of this superfamily produce cation-permeable channel activity in the absence of substrate. This channel mode of action is due to the expression of the corresponding transporter, since it is absent in the nontransfected cells or in uninjected oocytes and shows the same pharmacological sensitivity as the transporters (507). Constitutive transporter leak currents (i.e., flux of driving ions down their electrochemical gradient in the absence of substrate) have been detected for the expressed human NET, rat SERT, human DAT, and rat GAT-1 (81, 82, 161, 340, 520). Similarly, other sodium-dependent cotransporters show leak currents, like the glutamate transporters EAAT1 and EAAT3 (see sect. II*C*), and the sodium/glucose cotransporter SGLT1 (reviewed in Ref. 609). Interestingly, for many of these transporters (rat GAT-1, rat SERT, and human DAT), the ion selectivity of the leak conductance is similar but not identical to the cotransporter activity (alkali metal cations like sodium, potassium, or lithium produce the leak conductance, whereas potassium and lithium do not couple the transport of the corresponding substrates; reviewed in Ref. 507). This raises the question as to whether the leak conductance and the translocation of the co-ions use the same permeation pathway. In any case, the leak pathway depends on the presence of substrate: application of substrate inhibits this conductance associated with the expressed rat GAT-1, rat SERT, and human DAT (82, 340, 507). Patch-clamp studies by Cammack and Schwartz (82) in HEK 293 cells, which permanently express rat GAT-1, suggest that there are two distinct subpopulations of GAT-1 transporters: *1*) the vast majority of the transporters act as normal c-transporters that yield only small currents, and *2*) a small "channel-like" population produces leak conductance in bursts (~1 pA at −50 mV) and is sensitive to the GABA GAT-1-specific inhibitor SKF-89976A. For these authors, the large discrepancy between the number of channels and transporters indicates that they function independently. The question is then, What mechanisms determine whether a protein functions as a channel or as a transporter (82)? Posttranslational modifications, the state of aggregation or interation with other proteins, like cytoskeletal elements, or even silent channels, might be the molecular basis for the channel behavior. Purification and reconstitution of these transporters are clearly needed to demonstrate that they could work intrinsically as channels.

### *4. Protein structure*

Figure 3 shows the alignment of the human amino acid transporters of this superamily, with the exception of rat GAT-2 and rat GLYT2. They show high homology (at least 40%) in their primary structures, with ~150 well-conserved amino acid residues. As general features (see references in Table 4), all these transporters lack a signal peptide, a good prognosis for 12 TM domains, with the $NH_2$ and COOH termini located intracellularly, where most putative phosphorylation sites are located, and one to four putative *N*-glycosylation sites between the theoretical TM domains III and IV. The regions of highest homology are TM domains I, II, and IV–VIII; in contrast, the lowest level of homology occurs in the $NH_2$ and COOH termini (see Fig. 3 and Ref. 12 for review). Regions of extensive homology may be related to general functions for these transporters. In general, there is good conservation of proline, glycine, tyrosine, and tryptophan residues in TM domains (see Fig. 3). Thus every theoretical TM domain has at least one conserved glycine residue; proline residues are conserved in TM domains I, II, V–VIII, XI, and XII; and tyrosine residues are conserved in TM domains I–III, V, and X. Transmembrane domains I and IV present one conserved positive amino acid residue. The structure-function relationship of some of these conserved structural features has been addressed experimentally (see sect. II*B5*).

These transporters are *N*-glycoproteins. The GABA transporter GAT-1 was reconstituted and purified to homogeneity from rat brain (441, 439) and later cloned (184). The transporter was resolved in SDS-PAGE as a polypeptide band of 80 kDa that also dimerizes to an apparent molecular mass of 160 kDa, as revealed by cross-reactivity with polyclonal antibodies (439). The deglycosylated GABA transporter has an electrophoretic mobility compatible with a molecular mass of ~67 kDa, deduced from the cloned GAT-1 transporter (184, 259). Other studies have also demonstrated that GAT-1 is *N*-glycosylated (37, 273, 410, 439). Similarly, *N*-glycosylation has been demonstrated for DAT, SERT, NET, and GLYT1 transporters (70, 307, 357, 358, 400, 468, 415, 547, 637).

Purification to apparent homogeneity of a pig brain glycine transporter showed it to be a glycoprotein (it binds to lectins) with the appearance of a broad band with an average size of ~100 kDa in SDS-PAGE (320). Physicochemical characterization of the native glycine transporter indicated a monomeric structure of this size (321). Treatment with peptide *N*-glycosidase F (PNGase F), but not with endoglycosidase F or *O*-glycanase, produced a dramatic electrophoretic mobility change, which shows that ~30% of the transporter mass corresponds to the carbohydrate moiety; neuraminidase produces a slight reduction of its apparent mass (395). The size of the deglycosylated and glycosylated glycine transporter purified from pig brain suggests that it most probably corresponds to the GLYT2 transporter (314, 395). Interaction with succinylated wheat germ agglutinin lectin, but not with concanavalin A-lectin, and the previous glycosidase treat-

ments indicate a tri- to tetra-antenary complex structure with terminal sialyc acid residues for the carbohydrate moiety of the purified GLYT2 transporter (395). With a similar approach, the carbohydrate moiety of the human DAT transporter was shown to lack high-mannose residues (306).

As indicated before, the cloning of the first two members of this superfamily, GAT-1 and NET, suggested a common 12 TM domain model that was extended to the other members of the family (see Fig. 3). This model initially received some experimental confirmation. Site-directed mutagenesis showed that the glycine transporter GLYT1 is heavily glycosylated at four Asn residues within the loop EL2 (see Figs. 3 and 4*B*), demonstrating the extracellular location of this hydrophilic loop (400, 401). *N*-glycosylation within this loop has also been demonstrated for SERT (547), NET (70, 358), and GAT-1 (38) transporters. Immunofluorescence and electron microscopic studies in permeabilized and nonpermeabilized cells expressing GLYT1 and NET (623, 16, 70), and *N*-glycosylation scanning mutagenesis for GAT-1 and GLYT1 (38, 401) confirmed the intracellular location of the $NH_2$ and COOH terminals of these transporters. Similar evidence obtained from experiments using antibodies located the hydrophilic loop of human NET connecting TM domains VIII and IX intracellullarly (357), and those connecting TM domains III and IV and VII and VIII (loops EL2 and EL4 in Fig. 4, *A* and *B*) extracellularly (70). *N*-glycosylation scanning mutagenesis unambiguously showed the extracellular location of loops EL3 and EL6 (see Fig. 4*A*) of GAT-1 (38) and of loop EL3 of rat GLYT1 (401). *N*-glycosylation of loops EL4 and EL5 (see Fig. 4*B*) has been shown for rat GLYT1, but with an impaired transport function (401). For rat GLYT1, all this has been confirmed by in vitro glycosylation reporter fusion; TM domains VI, VIII, and X act as stop transfer signals for the preceeding hydrophobic TM domains V, VII, and IX, which act as membrane anchor signals (401). The extracellular location of the loop EL6 of rat GLYT1 is supported by similar experiments showing that TM domain XII acts as a stop transfer signal when placed after TM domain XI and the loop EL6 (401). In summary, the theoretical model of 12 TM domains between the extracellular loop EL2 and the COOH terminus is supported by strong experimental evidence.

Very recently, two back-to-back reports examined in depth the membrane topology of GAT-1 (38) and GLYT1 (401) and by different strategies reached the same conclusion: the highly conserved theoretical TM domain I is probably immersed in the plasma membrane, but does not span it completely. In addition, a new TM domain III* is proposed. This new 12 TM domain model is depicted in Figure 4, *A* and *B*. Bennet and Kanner (38) show that the previous intracellular loop connecting TM domains II and III (i.e., new loop EL1, see Fig. 4*A*) can be glycosylated in vivo, as well as loop EL2, which contains the naturally occurring *N*-glycosylation sites, whereas loop IL2 is not glycosylated; therefore, two TM domains should be placed in between the TM domains III and III* shown in Figure 4*A*. There is a hydrophobic segment of 44 amino acid residues within these transporters that could accommodate both TM domains (see Fig. 4*A*). In addition, studies with permeant and impermeant methanesulfonate reagents indicate that the cysteine residue 74 (see Fig. 4*A*) should be located intracellularly, as proposed by the new model, and not extracellularly, as proposed by the previous theoretical model; consistent with this, the hydrophilic loop containing cysteine-74 (i.e., the previous EL1) is not glycosylated (38). Aragón and Giménez and coworkers (401) also used *N*-glycosylation scanning mutagenesis to show that the loop connecting the TM domains II and III can be glycosylated in vivo, and must thus be extracellular. These results suggest the model proposed in Figure 4*B* for rat GLYT1, where the TM domain III* should contain a stop transfer signal. Unfortunately, this has not been demonstrated in studies of fusion reporter glycosylation (401). This suggests that the proposed TM domains III and III* constitute a single "reentrant loop" as proposed for the first highly conserved hydrophobic domain. In this sense, it is not easy to conceive two TM domains within the hydrophobic segment of 44 amino acid residues as proposed by Bennet and Kanner (38) (see Fig. 4*A*). Indeed, no clear support for the intracellular location of the hydrophilic loop IL2 has been offered; in fact, the construct of glycosylation reporter fusion of GLYT1 spanning the $NH_2$ terminus to the TM domain III is glycosylated in vitro (401).

At present, the only evidence for the membrane interaction of the reentrant hydrophobic loop I (see Fig. 4*A*) is that alkaline stripping does not release from microsomes a GLYT1 construct having only the COOH terminus, the reentrant domain I, and a small part of the new IL1 loop (401). Reentrant hydrophobic loops (or "pore loops") have been described for receptors and channels (39, 215, 362) and are involved in ion permeation of voltage- or ligand-dependent ion channels (for review, see Ref. 333). This might help us to understand the channel mode of action described for several transporters within this superfamily. In addition, several amino acid residues that are critical for the transport function of the transporters of this superfamily have been described within this hydrophobic domain (see sect. II*B5*). It is therefore important to clarify, by different strategies, the membrane topology of these transporters within their $NH_2$-terminal third.

### 5. *Structure-function relationship*

Site-directed mutagenesis with rat GAT-1 and GLYT1 transporters by Kanner's, and Aragón's and Giménez's groups (16, 37, 50, 271, 288, 331, 410), a cross-mutation study between the external loops of mouse GAT-1, -2,

and -3 and BGT-1 by Nelson and co-workers (542), examination of the role of the carbohydrate moiety for the glycine transporters by Aragon and co-workers (395, 400), and a substrate-protected proteolytic cleavage study of rat GAT-1 by Mabjeesh and Kanner (332) are the bases for our present knowledge of the structure-function relationship of the sodium- and chloride-dependent amino acid transporters. These data are discussed here in the light of the new membrane topology model described for GAT-1 and GLYT1 transporters (see sect. IIA). These studies show that the $NH_2$-terminal third of these proteins may be involved in common transport functions, whereas the external hydrophilic loops affect substrate discrimination.

In a series of studies, Kanner's group (37, 256, 331) identified domains of rat GAT-1 that are not required for its transport function. Papain- or pronase-treated purified rat GABA transporter, which has probably lost the $NH_2$ and COOH termini, nevertheless retains all the transport characteristics of the intact GAT-1 in a reconstituted system (259, 331). In a parallel study, deletion mutants of rat GAT-1, where most of the hydrophilic $NH_2$ and COOH terminals have been eliminated, also retain all the transport characteristics of the intact transporter when expressed in HeLa cells (37). These results demonstrate that neither terminus of the GABA transporter is needed for its transport function. These protein domains might be relevant for other functions, like regulation of the transport function, or interaction with cytoskeleton, as described for other transporters (e.g., erythrocyte anion transporter, sodium/proton exchanger; Refs. 290, 472). These results cannot be generalized to other transporters of this superfamily. In contrast to GAT-1, the COOH terminus of rat GLYT1 is necessary for the correct trafficking of the protein to the plasma membrane (399). Deletion of the first 30 amino acid residues of GLYT1a (i.e., $NH_2$ terminus) does not alter the transport of glycine by the transporter when it is expressed in COS cells. Deletion of the last 34 amino acid residues (i.e., COOH terminus; see Fig. 4*B*) does not impair the transport function of GLYT1a, but longer deletions within the COOH terminus result in a progressive decrease of its transport expression. Immunofluorescence and transport reconstitution studies showed that this impaired transport expression was due to both a defect in trafficking to the plasma membrane and a loss of the intrinsic transport activity of these mutants (399).

Two studies analyzed the role of the hydrophilic loops in the function of the GABA transporters (542, 256). Kanner et al. (256) examined the effect of deletions of randomly picked nonconserved segments, or even deletion of single residues, within the EL4 and IL5 loops of rat GAT-1 (single residues deleted are indicated by a square in Fig. 4*A*). All deletions, of 1–22 residues, produce a loss of transport activity. This could not be explained by a low level of synthesis (i.e., normal [$^{35}$S]methionine labeling) or by a missorting to the plasma membrane (i.e., there is no rescue of transport activity when the transporter is solubilized and reconstituted from HeLa cells expressing the mutants); only the deletion mutant of valine-348 shows a missorting defect, which is partially responsible for the loss of its transport activity. Interestingly, conserved and nonconserved (mutations to glycine) substitutions of these nonconserved residues within the superfamily of transporters in rat GAT-1 retain significant transport activity when expressed in HeLa cells (256). These results suggest that a minimal length of the hydrophilic loops EL4 and IL5 is important for the transporter functional structure (256). In agreement with this, insertion of an Asn residue between valine-348 and threonine-349 ensures significant transport activity (256).

As discussed above (transport characteristics section), GAT-1 transports GABA, whereas GAT-2 and GAT-3 and BGT-1 transport $\beta$-alanine in addition to GABA; all four GABA transporters show different apparent affinity for GABA (see Table 5), and there are specific amino acid residues for the $\beta$-alanine transporters (i.e., GAT-2, GAT-3, BGT-1, and TAUT) between TM domains VII and VIII, IX and X, and XI and XII (see Fig. 3). Nelson and co-workers (542) examined the role of the external loops EL3 to EL6 (see Fig. 4*A*) in substrate selectivity by cross-mutation between the four GABA transporters (GAT-1 to -3 and BGT-1) (i.e., swapping amino acid residues between these transporters) and expressing the mutants in oocytes (542). The most relevant results in this study are as follows.

*1*) Expression of a mutant produced by swapping amino acid residues of the EL4 loop of GAT-3 (also very similar to GAT-2 sequence) into GAT-1 sequence resulted in an apparent affinity change for GABA that mimics GAT-3 transport ($K_m$ values were ~9, ~1, and ~2 $\mu$M for mouse GAT-1, GAT-3, and the cross-mutant GAT-1/GAT-3-EL4 loop/GAT-1, respectively).

*2*) The cross-mutant GAT-1/BGT-1-EL6/GAT-1 has increased affinity for GABA ($K_m$ ~35 $\mu$M) that mimics BGT-1 transport ($K_m$ <100 $\mu$M).

*3*) The cross-mutant GAT-1/GAT-2-EL5/GAT-1 acquired similar $\beta$-alanine sensitivity to that of GAT-2, which is not present in GAT-1. Cross-mutations within the other loops do not confer $\beta$-alanine sensitivity, and swapping amino acid residues of the EL5 loop of GAT-1 into the GAT-2 sequence reduced $\beta$-alanine sensitivity.

*4*) Cross-mutations within the EL3 loop produce no significant changes.

Therefore, this elegant study strongly suggests that the three external loops EL4–6 (see Fig. 4*A*) might form a pocket on the transporters into which the substrates bind (542). Interestingly, a similar conclusion was reached in studies with chimeric biogenic monoamine transporters (71, 169). More recent studies (72) also showed that the protein regions spanning TM domains V–VII and I–III of NTE and DAT are involved in the selective inhibition by antidepressants and psychomotor stimulants.

Four studies by Kanner's group look for critical amino acid residues for the transport activity of rat GAT-1, within charged residues (410) or conserved tryptophan or tyrosine residues located in the theoretical TM domains (50, 288), or conserved negatively charged residues adjacent to putative TM domains (271) (see Fig. 4*A*). Interestingly, the three studies identified amino acid residues that may be critical for the transport function within the first $NH_2$-terminal part of the protein (see Fig. 4*A*), the membrane topology of which has recently been revised (see sect. II*B4*). Of the five charged residues within theoretical TM domains, only Arg-69, located in the highly conserved reentrant loop (38, 401), is critical for the radiolabeled transport of GABA; the arginine residue itself is critical and not merely the associated positive charge (410). The loss of transport function when the Arg-69 mutants are expressed in HeLa cells is due to intrinsic transport defects and not to protein synthesis or missorting effects (410). The role of Arg-69 is unknown, but its positive charge and the fact that it is conserved in all the transporters of this superfamily prompted the authors to suggest that it might be involved in the binding of chloride (410).

The lack of negatively charged residues conserved in the theoretical TM domains of rat GAT-1 that would be critical for the transport function, and therefore candidates for the binding of sodium (410) fostered the study of the role of tryptophan residues that might interact with their *P*-electrons with this co-ion within the putative TM domains (288). Of the 10 conserved tryptophan residues within putative TM domains, only Trp-68, Trp-222 and Trp-230 resulted in impaired transport function when mutated to serine or leucine residues; Trp-230 mutants showed missorting, whereas mutations in the other two tryptophan residues had intrinsic transport activity defects (288). Interestingly, Trp-68, contiguous to the critical residue Arg-69, is conserved in all the transporters of this superfamily, and the GAT-1 transport activity tolerates substitutions of Trp-68 to other aromatic residues. This suggested that these two contiguous residues might interact with the transport co-ions sodium and chloride (288). Moreover, capacitive charge movement studies in oocytes suggest that the Trp68Leu mutant "locks" sodium onto the transporter by preventing (or slowing) the intracellular release of the substrate (339). As in all types of site-directed mutagenesis study, it is also possible that both residues influence the transport function by affecting the transporter structure.

The study of negatively charged residues adjacent to TM domains identified Glu-101, within the newly proposed loop EL1 (see Fig. 4*A*), as being critical for transport function (271). Replacement of Glu-101 by Asp reduced the transport activity of GAT-1 by 99%. Substitutions of Glu-101 do not show the sodium transient currents, which are indicative of conformational changes during the transport cycle. This has led to the proposal that this residue is critical for the transport cycle-associated conformational changes of GAT-1 transporter (271).

Several lines of evidence highlight the relevance of the reentrant hydrophobic loop I and the adjacent protein regions for the transporters of this superfamily (i.e., it might be close to the permeation pore):

*1*) This domain shows high conservation within the transporters of this superfamily and contains the critical Trp-68 and Arg-69 residues.

*2*) Deletion mutations of the $NH_2$ terminus of rat GAT-1 and GLYT1 affecting amino acid residues adjacent to this domain abolish transport function (16, 37).

*3*) The cysteine residue 74, located in the adjacent IL1 loop (see Fig. 4*A*), is partially responsible for the inactivation of rat GAT-1 by (2-aminoethyl)methanethiosulfonate (38).

*4*) *N*-glycosylation scanning mutagenesis within the extracellular loop EL1 (see Fig. 4*A*) resulted in almost complete loss of transport function.

*5*) The glutamate residue 101, conserved in all the transporters of this superfamily and located in this EL1 loop, has been found to be essential for the transport function of GAT-1 (271).

*6*) Moreover, it is noticeable that the biogenic amine transporters have a specific aspartate residue within this domain (Asp-79 in the human DAT sequence; the amino acid transporters of this superfamily have a conserved glycine residue in this position; Gly-63 in rat GAT-1; see Fig. 4*A*), which is critical for the binding of the amine group by human DAT (286).

In section II*B4*, the presence of reentrant hydrophobic domains in channels was discussed. It is thus important to determine whether mutations within these domains (e.g., Arg-69, Trp-68) affect the channel mode of action of these transporters. In other words, do Arg-69, Trp-68, or adjacent domain (e.g., Glu-101) mutants show the characteristic channel mode of activity of rat GAT-1? If, finally, transporters of this family have intrinsic channel-like activity, strategies developed for the study of the conducting pathways of channels will be useful. As discussed by Lester et al. (301), substitution mutants of critical residues in or near the permeation pathway should affect single-channel conductance, open-channel blockade, or ion selectivity. Only upon purification and reconstitution will it be possible to demonstrate the intrinsic channel mode of action of these transporters. Until then, the residues that are critical for transport and channel activities could be interpreted as being involved in the substrate-transporter conformational changes needed to activate an extrinsic channel activity. The study of mutants able to dissociate between transport and channel functions may also reveal the mechanism of the channel mode of action of these transporters. Lester et al. (301) proposed a variation of the "alternating access model" to explain the putative intrinsic channel activity of these

transporters: the transporter is alternatively gated at the intracellular and the extracellular face during a transport cycle, but with low probability, whereas during its channel activity events both gates remain open, allowing a continuous aqueous phase through the transporter. To explain why the ion selectivity does not always coincide between the transport and the channel activities (either for the present transporters, see above and Ref. 507, or for the chloride conductance of the sodium, potassium-glutamate transporters; see sect. IIC) the substrates and co-ions themselves might become part of the ion-selective pathway, as proposed for the glutamate transporters (582).

The critical residues Trp-222 and Trp-230 are located within TM domain IV (see Fig. 4A). Tryptophan-222 is conserved in the amino acid transporters, but not among the monoamine transporters of this family (see Fig. 3 and Ref. 253). This fosters the hypothesis that Trp-222 might be involved in the binding of the amino group of these substrates (288). Further support for this role of Trp-222 has been obtained by substitution mutants of Trp-222 that do not bind radiolabeled tiagabine, a NIP derivative inhibitor of GAT-1 that is not transported (253). As discussed above, the biogenic amine transporters have a specific aspartate residue within the reentrant hydrophobic loop that seems to mediate the binding of the amine substrates (286). Of the 12 conserved tyrosine residues predicted to be located in the membrane according to the theoretical topological model (see Fig. 3), Tyr-140 (located in TM domain III or in the intracellular loop IL2, depending on the topology model; see Figs. 3 and 4A) is the only one that does not tolerate, in rat GAT-1, replacement by either phenylalanine or tryptophan (50). A detailed study on substitution mutants of residue Tyr-140 of rat GAT-1 expressed in HeLa cells or oocytes demonstrated that this residue is a specific determinant on GABA binding (i.e., sodium and chloride binding are unimpaired) (50). Interestingly, this tyrosine residue is conserved throughout this superfamily of transporters (including the transporters for biogenic amines). This allowed the authors (50) to suggest that Tyr-140 may be involved in the binding of the amino group, the moiety which is common to all the substrates of this superfamily of transporters. Until the membrane topology of the transporters of this superfamily is resolved (see sect. IIB4), it is impossible to know which other group might be located close to Tyr-140 (50), but the results discussed here (50, 286, 288) suggest that this residue and Trp-222 (rat GAT-1 sequence) or Asp-79 (human DAT sequence) are determinants of the binding of the amino group of GABA or biogenic amines, respectively. This suggests proximity for these residues within the three-dimensional structure of these transporters. In any case, all these results confirm the relevance of the $NH_2$-terminal third of these transporters for their transport function.

The *N*-glycosylation of the transporters of this superfamily, with the possible exception of the "orphan transporters," occurs within the external loop EL2 (see Figs. 3 and 4, *A* and *B*). Aragón and co-workers (395, 400) analyzed the role of the carbohydrate component of the pig brain purified glycine transporter and the expressed rat GLYT1 glycine transporter. Treatment of the purified and reconstituted pig brain glycine transporter (GLYT2) with PNGase F results in the loss of ~30% of its apparent mass and a substantial decrease in its transport activity (395). These results do not reveal whether the carbohydrate moiety is important for substrate binding or for stabilizing the active conformation of the transporter. This study cannot be extended to other transporters of this family. Indeed, *N*-glycosidase F treatment of the purified and reconstituted GLYT1 glycine transporter expressed in COS cells results in the loss of its carbohydrate moiety without loss of its transport function; *N*-glycosylation does not appear to be essential for the transport activity of GLYT1 (400). On the other hand, the carbohydrate moiety of GLYT1 is indeed necessary for its proper trafficking to the plasma membrane. Progressive disruption of the four naturally occurring *N*-glycosylation sites of GLYT1 in loop EL2 (see Fig. 4*B*) results in a progressive decrease in the transport activity when the mutants are expressed in COS cells; surface biotinylation and immunofluorescence analysis demonstrated missorting to the plasma membrane of the unglycosylated GLYT1 mutants (400). This is consistent with the behavior of nonglycosylated NET mutants, which upon expression in COS cells had reduced protein stability and surface trafficking, which could explain the loss of transport expression. Interestingly, the residual transport activity conserves substrate and antagonist recognition (358), and loop EL2 of SERT (and probably NET) transporter does not appear to participate in substrate or antidepressant binding. Swapping half of this loop of NET into SERT transporter does not alter substrate or drug affinity but slows the transport rate; this suggests that loop EL2 may be involved in the translocation mechanism (511).

The last item to be discussed on the structure-function relationship of these transporters is the evidence in favor of transport cycle-associated conformational changes. An elegant study by Mabjeesh and Kanner (332) provides experimental evidence of this for rat GAT-1 transporter. The GABA transporter from brain membranes or purified and reconstituted into liposomes is cleaved by proteases (pronase and trypsin), and its transport activity is abolished. The presence of GABA, together with the transport co-ions (sodium and chloride) on the same side of the membrane, almost entirely blocked the action of the proteases, both in the proteolysis of the GAT-1 transporter and in its transport function (332). The concentration of GABA necessary for the half-maximal protection, the partial protection by the GAT-1-specific inhibitor ACHC, and the lack of protection by $\beta$-alanine (noninteracting with GAT-1 transporter) (see Table 5) in

addition suggest that the GAT-1 transporter undergoes conformational changes after binding of its substrate and co-ions. Mabjeesh and Kanner (332) propose that the formation of the translocation complex (GABA plus co-ions) induces conformational changes that render the transporter resistant to digestion by these proteases. As for other substrate-protection strategies, it is not possible to distinguish between protection due to steric hindrance by the substrate or conformational changes hiding protein domains. This discussion is relevant, since Lester and co-workers (520) recently developed a new model of ion-coupled cotransport for GAT-1, SERT, and the sodium-glucose cotransporter (SGLT1) based on substrate-substrate interactions that does not require the global conformational changes characteristic of the paradigmatic alternating access model. In any case, the study of the capacitive properties of the GAT-1 transporter also provides some clues to the conformational changes associated with the binding of sodium and GABA (see Ref. 301 for review). The slow component of capacitive currents is associated with sodium binding, and it is compatible both with sodium ions entering the membrane dielectric field and with reorientation of dipoles after sodium binding (i.e., conformational changes) (301). The fast capacitive currents due to stable expression of GAT-1 in HEK 293 cells show an increased current noise in the membrane patch after addition of GABA that increases with frequency (82), suggesting that GABA binding facilitates sodium binding by eliminating barriers to the entry of ions from solution (301). Similarly, jumps in the sodium concentration produce charge movements that reflect the same population of charges that move during voltage-jump relaxations (339). All this suggests that the binding of GABA and sodium induces conformational changes in the transporter (301).

### 6. *Physiological role*

A) TRANSPORTERS FOR NEUROTRANSMITTER AMINO ACIDS. Sodium-dependent transporters located in the presynaptic and glial membranes remove transmitter molecules (e.g., GABA, glycine, biogenic amines, and glutamate) from the synaptic cleft and thus terminate transmission. This has been directly demonstrated for the dopamine transporter in the DAT knockout mouse; in the homozygotic mice, dopamine persists ~100 times longer in the extracellular space (168). γ-Aminobutyric acid is the major CNS inhibitory neurotransmitter, and glycine has this major role in spinal cord and brain stem. As discussed above, three high-affinity GABA transporters are expressed in the CNS, GAT-1, -2, and -3. Biochemical, pharmacological, and immunolocalization studies demonstrated that GAT-1 corresponds to the neuronal subtype $GABA_A$ transporter (see Ref. 260 for review). Therefore, GAT-1 should be resposible for the presynaptic removal of GABA for terminating transmission in the GABAergic synapses. The blockade of GABAergic transmission precipitates epileptic seizures (for review, see Refs. 56, 157). Interestingly, lipophilic derivatives of piperidencarboxylic acid, which have anticonvulsant properties (524), are highly specific inhibitors of GAT-1 transporter (58, 102, 103); most probably, GAT-1 transporter is the site of action of the anticonvulsant drug tiabagine (56). The GAT-1 uptake system is more extensive than the GABA synthesizing system, and it is also expressed in glial cells of the cerebral and cerebellar cortex and spinal cord (364, 375, 447, 506). Then, GAT-1 should play additional roles to its presynaptic function. In this sense, it might contribute to the regulation of the cerebrospinal concentration of GABA. To our knowledge, antisense or knockout experiments on GAT-1 to demonstrate this have not been reported.

The channel mode of action of GAT-1 suggests a role for this transporter in intracellular signaling. Sonders and Amara (507) have recently reviewed the potential physiological role of the GABA transporter-associated electric activity; at present, evidence in favor of this role is less documented than that for the excitatory amino acid transporters (see sect. II*C*). Application of GABA to glial cells elicited depolarization in a sodium-dependent manner, which is therefore more attributable to transporters than to receptors (291). Depolarization caused by the transport of GABA can trigger intracellular signals. In isolated skate retinal horizontal cells, GABA-evoked transport currents (as determined by the pharmacology and ion dependence) depolarize cells and open voltage-sensitive $Ca^{2+}$ channels (200).

The pharmacological characteristics of the GAT-2 and GAT-3 transporter fit the GABA glial transporter activity (see above), but GAT-3 is present in glial and neuronal cells (61, 103, 450). Studies in the developing brain (239) showed a coordinate expression of GAT-1 and GAT-3 that suggested a role for the latter in the termination of GABAergic synapses. In contrast, GABA uptake inhibitors with anticonvulsant properties do not inhibit uptake via GAT-3 (102). Nelson and co-workers (240) noticed that the general pattern of GAT-3 immunoreactivity is similar to that of GLYT1, which suggested a possible role of GAT-3 in neurons with GABA termini known to be apposed to glycine receptors. As discussed above, the localization of GAT-2 in brain, retina, and peripheral tissues points to a nonneuronal function for this transporter.

There is codistribution in brain of the neuronal-specific glycine transporter GLYT2, the inhibitory glycine receptor (immunocytochemistry and strychnine binding), and neurons with high glycine content (17, 237, 623). In contrast, codistribution of GLYT1 and inhibitory glycinergic neurotransmission is not complete (for review, see Ref. 622). First, this suggests participation of both glycine transporters in the termination of glycinergic synapsis. Second, GLYT1 might have additional roles in the CNS. The presence of GLYT1 (mRNA and protein) in neu-

rons is controversial, but its presence in areas without glycine receptor expression suggests additional roles (622). Based on the mRNA distributions, Smith et al. (502) postulated a role for GLYT1 in the modulation of the glutamatergic transmission through NMDA receptors. This receptor requires two coagonists, glutamate and glycine, to activate its channel (234, 287). Administration of glycine or related agonits potentiates NMDA receptor function in several models in vivo (reviewed in Ref. 622). The concentration of glycine needed to restore normal NMDA electric responses is controversial, and this is an important issue in assessing the role of the glycine transport in the modulation of glutamatergic transmission; 0.1 $\mu$M glycine is enough to restore normal NMDA responses, but it is estimated that glycine concentrations in the cerebrospinal fluid are >10 $\mu$M (622). Two findings leave room for a role of glycine transport in NMDA receptor function. First, the affinity of the NMDA receptor for glycine varies in different neurons (432), depends on the type of NR2 subunits within the receptor (584), and increases with extracellular calcium (182). Second, the concentrative glycine transport present in brain synaptic plasma membrane and glial cells, with a cotransport stoichiometry of 1 glycine, 2 sodium, and 1 chloride (16, 624) (to our knowledge the stoichiometry for the expressed GLYT1 transporter has not been reported) is able to maintain a concentration of 0.2 $\mu$M in the synaptic cleft (23). The finding of brain regions with high NMDA receptor expression without glycinergic terminals also points to a role of the glycine transporter in the regulation of glutamatergic synapsis. The GLYT1 transporter might regulate glycine concentration in the synaptic cleft, not only by the uphill uptake of glycine, but also by the efflux of glycine via the transporter working in the opposite direction (622). This is similar to the nonvesicular release of GABA and glutamate (23). Thus, with synaptic depolarization, the intracellular concentration of sodium increases to levels at which the operation of the glycine transporter is reversed (15). Additional studies are needed to demonstrate the role of the GLYT1 transporter in changing the glycine concentration in the synaptic cleft and thus modulating the NMDA glutamate receptor.

Transporters for two other amino acids, taurine and proline, have been identified in brain. The physiological role of taurine and $\beta$-alanine, two substrates of the TAUT transporter, in the CNS remains obscure. As reviewed by Nelson and co-workers (316) and Weinshank and coworkers (503), taurine is one of the most abundant amino acids in brain, with a function that is best understood as an osmoregulator. Because taurine is degraded slowly, uptake is a relevant way to regulate its extracellular concentration; taurine can be released from neurons and glial cells in response to changes in cell volume. Taurine reaches millimolar concentration in excitable tissues that generate oxidants, a decrease in taurine uptake has been implicated in retinitis pigmentosa, and depletion of taurine results in retina degeneration; this supports a role of taurine in neuronal survival (316, 368, 503). Although most animals can synthesize taurine, this is not sufficient and the supply relies on dietary sources (503). This role for taurine transport is consistent with the presence of TAUT transporter in the blood retinal barrier (retinal pigment epithelium) (368) and in the placenta (445). A more precise cellular localization in the brain of the high-affinity TAUT transporter (see sect. *IIB1*) is needed to understand its role in the CNS.

The cloning of PROT transporter, a sodium- and chloride-dependent high-affinity L-proline transporter expressed in CNS, suggested a role for L-proline in neurotransmission. Circumstantial evidence implicates L-proline as a putative synaptic regulatory molecule (see Refs. 155 and 489 for review).

*1*) As for neurotransmitters, high-affinity sodium-dependent uptake of L-proline has been described in rat brain synaptosomes and slices, and L-proline is released from brain slices and synaptosomes by potassium-induced depolarization. In general, the pharmacology (potency of inhibitors) of the L-proline transport of the human PROT expressed in HeLa cells is consistent with the uptake of L-proline in brain slices.

*2*) L-Proline and its high-affinity synaptosomal transport show heterogeneous regional distribution in the CNS.

*3*) There is a synaptosomal L-proline biosynthetic pathway from ornithine.

*4*) L-Proline produces complex electrophysiological actions when iontophoresed onto neurons.

*5*) Intracerebral injections of L-proline are neurotoxic and disrupt memory processes. Interestingly, the neurotoxic effects of L-proline are blocked by antagonists of glutamate receptors.

Transcripts of PROT are concentrated in subpopulations of putative glutamatergic neurons, and the protein is detected in synaptosomes (155, 489), and a specific postsynaptic role of L-proline at glutamate receptors has been suggested (for references, see Ref. 155). In this scenario, several roles have been proposed for the uptake of L-proline via the neuronal PROT transporter (489): *1*) limitation, or modulation, of the extracellular concentration of L-proline to prevent inadequate activation of, or modulate, inhibitory synapses (glutamate and glycine receptor); and *2*) a nutritional role for feeding the neuronal tricarboxylic acid cycle with intermediates or for presynaptic accumulation of L-proline as a precursor of L-glutamate. Recently, a novel nonopioid action of enkephalins has been described (156): enkephalins, which are not PROT transporter substrates, competitively inhibit this transporter. Subcellular localization, design of specific inhibitors (156, 489), and knockout strategies for the PROT transporter should help to elucidate the role of L-proline and its transporter in CNS.

B) OSMOLYTE TRANSPORTERS. Both BGT-1 and TAUT are established osmolyte transporters. Hypertonicity produces loss of cell water; cells shrink within seconds to equalize intra- and extracellular osmolarity. An immediate consequence, within minutes, is the elevation of the intracellular concentration of electrolytes (e.g., $K^+$), which perturbs the function of macromolecules (for review, see Refs. 193, 292, 293). Cells of all phyla have a fundamental response, the accumulation of nonperturbing small organic osmolytes (e.g., betaine, taurine, *myo*-inositol, and sorbitol) (618). This response occurs in mammalian cells within hours or days. Accumulation of compatible osmolytes and keeping intracellular electrolyte levels isotonic is critical for adaptation to hypertonic stress (for references, see Ref. 292). The kidney medulla is the only mammalian tissue that is normally hypertonic, due to the concentration mechanisms of urine; depending on the hydration status of the animal, osmolarity varies, and in humans, it easily surpasses 1,000 mosM (193, 292). As part of the renal mechanisms for water conservation, cells in the medula accumulate betaine, *myo*-inositol, taurine, and sorbitol; induction of transport for the first three osmolytes and synthesis of sorbitol are the mechanisms that produce osmolyte accumulation (386, 387).

In a series of elegant studies, Handler's and Burg's groups demonstrated the role and the mechanisms of regulation of BGT-1 transport activity in the adaptation of renal cells to osmolarity changes (reviewed in Refs. 194, 292, 293).

*1*) Hypertonic media induce betaine accumulation in the canine renal MDCK cells (385).

*2*) The MDCK cells rely on transport as a source of betaine; the transport activity of BGT-1 is the rate-limiting step in the accumulation of betaine (387, 614).

*3*) Addition of betaine at physiological concentration (100 $\mu$M) restores the MDCK cell growth and survival challenged by hypertonicity (563).

*4*) In MDCK cells, hypertonicity induces the parallel and progressive turn-on of BGT-1 transcription, which raises BGT-1 transcripts and transport activity (~6-fold increase); hypotonicity reverses this process (387, 564, 614).

*5*) The BGT-1 transporter seems to play the same role in renal medulla: renal preparations show sodium- and chloride-dependent betaine uptake (292), the increase in medular tonicity due to dehydration results in an increase in BGT-1 transcript levels (quoted in Ref. 292), and intraperitoneal administration of NaCl in rats rapidly increases BGT-1 transcript abundance in renal medulla, mainly in the thick ascending limbs of Henle's loop (365). In these whole animal models, the expected increase in transcriptional activity of *BGT-1* gene has not been reported.

After cloning the complete *BGT-1* gene (537), Handler and co-workers (538) identified the first-known tonicity-responsive sequence element (TonE; TGCAAAAGTCCAG) 50–62 bp upstream of the first exon of the *BGT-1* gene. Electrophoretic mobility-shift assays with TonE-containing DNA and nuclear extracts from MDCK cells revealed the presence of a specific binding protein (TonEBP) (538), whose binding activity is induced by hypertonicity with a similar time course to the transcription of the *BGT-1* gene (292). To our knowledge, the cloning of TonEBP has not been reported. Hypertonicity also results in an increase in transcript abundance of TAUT and SMIT (sodium/inositol) transporters (615, 562) and aldose reductase for the synthesis of sorbitol (499). A tonicity-responsive sequence element has recently been identified in the mouse aldose reductase promoter, and it is similar to the TonE in the BGT-1 promoter (123). The cell tonicity sensor and its signal transduction pathway (e.g., involvement of mitogen-activated protein kinases) to TonE-dependent transcription in mammalian cells is not yet clear (73, 294). Hormones, cumulative substrate uptake, and oxidative stress also produce the swelling/shrinking reaction in a variety of mammalian cells; in addition to renal medulla, osmolytes have been identified in astrocytes, hepatocytes, lens epithelia, and macrophages (for a short review, see Ref. 594). In mouse macrophages (RAW 264.7 cells), as in MDCK cells, BGT-1 transcript abundance and betaine uptake is strongly dependent on extracellular osmolarity (593). In contrast, in H4IIE rat hepatoma cells and primary hepatocytes, taurine is the most prominent osmolyte, and its TAUT transporter is strongly regulated by tonicity (594). To our knowledge, whether the L-proline (PROT) and glycine (GLYT1) transporters, homologous to BGT-1 and TAUT transporters, are regulated by tonicity has not been reported.

### C. Superfamily of Sodium-Dependent Transporters for Anionic and Zwitterionic Amino Acids

This family of transporters comprises five anionic amino acid transporters (EAAT1 to EAAT5; for excitatory amino acid transporter isoforms 1 to 5) and three zwitterionic amino acid transporters (ASCT1, ASCT2, and ATB°; for system ASC transporter isoforms 1 and 2, and for amino acid transporter for system B°) that are sodium dependent (18, 144, 245, 269, 424, 488, 518, 568). The human homologs for all these transporters appear to have been cloned (18–20, 144, 249, 268, 343, 488, 490, 491, 568). Indeed, most probably ASCT2 is the murine counterpart of human ATB° (see below). The cDNA accession numbers, chromosome location, and protein length for the human transporters are shown in Table 6. The simultaneous cloning from different labs resulted in a confusing array of clone names (see Table 6). For clarity, in this review, the nomenclature used by Amara's group (11) has been adopted for the glutamate transporters (i.e., EAAT). On the basis of sequence homology, two subfamilies could be interpreted: *1*) the human EAAT isoforms (the anionic

TABLE 6. *Sodium-dependent transporters for anionic and zwitterionic amino acids*

| Transporter (Gene Name) | Accession Numbers (Origin of Human Clones) | Origin of First Clone and Other Names | Human Chromosome | Protein Amino Acid Length | Clones in Other Mammals |
|---|---|---|---|---|---|
| Glutamate transporters | | | | | |
| EAAT1 (SLC1A3) | L19158 (cerebellum) (490)<br>D26443 (brain) (268)<br>U03504 (motor cortex) (19) | Rat brain (GLAST) (518)<br>GluT-1 (268) | 5p13 (191, 284, 535)<br>5p11-p12 (516) | 542 | Bovine (225)<br>Murine (191) |
| EAAT2 (SLC1A2) | Z32517 (brain) (343)<br>U03505 (motor cortex) (19) | Rat brain (GLT-1) (424)<br>GLTR (343) | 11p12-p13 (310)<br>11p11.2-p13 (534) | 574 | Murine (285, 382, 523) |
| EAAT3 (SLC1A1) | U06469 (kidney and ileum) (249)<br>U03506 (motor cortex) (19)<br>U08989 (brain stem) (490) | Rabbit small intestine (EAAC1) (245)<br>Glutamate transporter III (490) | 9p24 (500) | 524 | Rat (51, 581)<br>Murine (382) |
| EAAT4 (SLC1A6) | U18244 (cerebellum) (144) | Human cerebellum (144) | ? | 564 | |
| EAAT5 | U76362 (retina) (18) | EAAT5 (18) | ? | 560 | |
| Zwitterionic amino acid transporters | | | | | |
| ASCT1 (SLC1A4) | L14595 (motor cortex) (20)<br>L19444 (hippocampus) (488) | Human motor cortex (20)<br>Human hippocampus (SATT) (488) | 2p13-p15 (214) | 532 | |
| mASCT2* | D85044 (mouse testis) (568) | Mouse adipocyte (AAAT) (311) | ? | 553 | |
| $ATB^0$ (SLC1A5) | U53347 (JAR cells) (269) | Human choriocarcinoma (269)<br>Pancreatic islet (236) cell lines | 19q13.3 (236, 269) | 541 | |

Accession numbers for human cDNA are indicated, except for ASCT2. Sequence homology, tissue distribution, mRNA size, and characteristics of associated amino acid transport activity suggest that human $ATB^0$ and mouse ASCT2 may be species counterparts of same transporter. * Mouse ASCT2; human not available.

transporters) show 36–65% amino acid sequence identity between them, and *2*) the human zwitterionic amino acid transporters ASCT1 and $ATB^0$ show 57% between them. Amino acid sequence identity between human $ATB^0$ and mouse ASCT2 is very high (~80%). Amino acid sequence identity between members of the two subfamilies ranges between 39 and 44%. Homologous prokaryotic proteins (26–32% identity) involved in the transport of glutamate and other dicarboxylates (140, 233, 558, 559, 586) are evolutively related to this amino acid transporter superfamily (205, 247, 252).

Three independent labs cloned the first three members of this superfamily almost simultaneously in 1992, using different approaches. Stoffel and co-workers (518), during the isolation of a galactosyltransferase from rat brain, purified a 66-kDa hydrophobic glycoprotein which upon protein microsequencing and oligonucleotide probe cloning resulted in the isolation of GLAST cDNA (EAAT1 in Table 6); the putative protein showed significant homology with prokaryotic glutamate and dicarboxylate transporters, and its expression in oocytes resulted in anionic amino acid transport activity. Kanner and co-workers (120) purified to apparent homogeneity a rat glial 70- to 80-kDa glycoprotein that upon reconstitution showed L-glutamate transport activity; they raised antibodies against the protein (121) and used them to isolate GLT-1 cDNA (EAAT2 in Table 6). Transfection of EAAT2 in HeLa cells resulted in a sodium-dependent glutamate uptake that was thereafter reconstituted in liposomes (424). Finally, Hediger's lab (245) isolated EAAC1 cDNA (EAAT3 in Table 6) from rabbit small intestine by expression cloning in oocytes, after a sodium-dependent L-glutamate uptake expression signal. The other transporters of this superfamily were cloned based on homology with these seminal sequences. The transport properties of EAAT1, -2, and -3 did not fulfill all the pharmacologically distinguishable glutamate uptake activities in the cerebellum and retina (119, 152, 454). This was pursued by Amara's group to isolate EAAT4 cDNA from human cerebellum by using degenerate oligonucleotides from two conserved regions of EAAT1–3 (i.e., one between TM domains III and IV, the other in the hydrophobic long stretch toward the COOH terminus of the proteins; see Fig. 5) as the starting point of a RT-PCR-based cloning strategy. Expression in oocytes confirmed the sodium-dependent L-glutamate transport activity of EAAT4 (144). More recently, the same group isolated EAAT5 from human retina (18), based on a pre-

vious glutamate transporter cDNA isolated from salamander retina by homology strategies (not reported). Independently, two groups cloned human ASCT1, the first zwitterionic amino acid transporter of the family (also named SATT; see Table 6). Amara and co-workers (20), using a degenerated oligonucleotide from a conserved region of the long hydrophobic stretch of EAAT1–3 (see Fig. 5), isolated ASCT1 from motor cortex, and Fremeau et al. (155) isolated SATT from hippocampus taking advantage of a human expressed sequence tag (EST) (1) that showed slight homology with an *Escherichia coli* glutamate/aspartate transporter (586). Both proteins upon expression in HeLa cells or oocytes exhibit sodium-dependent zwitterionic amino acid transport activity with characteristics of system ASC (20, 488). After the corresponding corrections, sequences ASCT1 (accession no. L14595) and SATT (accession no. L19444) are identical. Serendipity again added to our structural knowledge of amino acid transport. While screening a 3T3-L1 adipocyte cDNA library for clones encoding protein tyrosine phosphatase HA2, Liao and Lane (311) isolated a cDNA (AAAT in Table 6) that showed significant homology with the previous members of this family of amino acid transporters. Independently, Kanai's group (144), after a strategy based on RT-PCR amplification using degenerate oligonucleotide from similar conserved regions to those of Amara's group (20), isolated ASCT2 cDNA from mouse testis (568). Expression in oocytes and transfection in 3T3-L1 preadipocytes of ASCT2 and AAAT resulted mainly in sodium-dependent zwitterionic amino acid uptake, also with characteristics of system ASC (311, 568). Finally, a low-stringency screening of a human placental choriocarcinoma cell cDNA library with a human ASCT1 probe (20) allowed Ganapathy and co-workers (269) to isolate ATB° cDNA. Expression in HeLa cells and oocytes showed a sodium-dependent uptake of zwitterionic amino acids with characteristics of system B° (269). This group screened a mouse kidney cDNA library using rat ATB° cDNA as a probe, and all the positive clones obtained turned out to be ASCT2 (V. Ganapathy, personal communication). This, and the homology and the similarities of the amino acid transport associated with the expression of ASCT2 and ATB° (see below) strongly suggest that both cDNA are species counterparts of the same gene. A search in dbEST performed by the authors of the present review (December 1996) found no other EST clones indicative of new members of this superfamily of transporters in mammals.

Since the identification of the first members of this transporter superfamily, several excellent reviews have appeared related to these glutamate transporters (205, 243, 247, 252, 253). The study of the transporters of this superfamily has revealed intringuing concepts, as follows.

*1*) As a general rule, all these transporters show potassium dependence in addition to sodium dependence when expressed in different cell system, with the possible exception of the zwitterionic amino acid transporters ASCT1 (627), ASCT2 (568), and ATB° (269) (see Table 7). The characteristics of their expressed transport activity suggest that EAAT1–5 isoforms are neural and nonneural variants of the anionic amino acid transport system $X^-_{AG}$, and that ASCT1 and ASCT2 might be variants of system ASC transport activity, or that ATB° and ASCT2 correspond to the epithelial system system B°.

*2*) Several labs provide evidence that some of these transporters (EAAT1–5, ASCT-1, and perhaps ATB°) have a substrate (amino acid and sodium)-gated chloride channel mode of action in addition to their amino acid transport mode of action (18, 144, 270, 582, 583, 627; reviewed in Ref. 507).

*3*) The topology of all these transporters in the plasma membrane is difficult to imagine on the basis of hydrophobicity algorithms (6–10 TM domains have been suggested, including $\beta$-sheets TM domains; Refs. 245, 424, 518), and it is still not evident after experimental work, from three different labs, attempting to elucidate this issue for EAAT1, EAAT2, and a prokaryotic glutamate transporter (140, 498, 585).

*4*) Specific antisense experiments, both in vivo and in cell culture, represent the first experimental evidence of the physiological role of EAAT isoforms in brain (458). More recently, Stoffel and co-workers (416) obtained the null knockout EAAT3 mice, and Tanaka and co-workers (544) obtained the null knockout EAAT2 mice.

These aspects as well as structure-function relationship studies on these transporters are discussed in the following sections.

### *1. Tissue expression*

The tissue distribution of the transporters of this superfamily was studied initially by Northern analysis and in situ hybridization. Table 7 shows the mRNA tissue distribution and the mRNA size for these human transporters, except for the mouse ASCT2. Rat EAAT1–2 and rabbit EAAT3 show a similar tissue distribution and transcript size (245, 424, 518); for the rabbit EAAT3, an additional transcript band of 2.5 kb has been reported (245). For the human ASCT1, Shafqat et al. (488) reported two hybridization bands of ~2 kb (2.8 and 2.2 kb) instead of a single band of ~2.5 kb (20).

The human EAAT glutamate transporters have specific tissue distribution. The EAAT2 isoform is specific to the CNS, EAAT5 is mainly, if not solely, expressed in the retina, and EAAT4 is mainly expressed in cerebellum, whereas the other isoforms are also expressed in peripheral tissues (Table 7). Rat EAAT1 is also brain specific (see below). Tissue and subcellular distribution of EAAT1–3

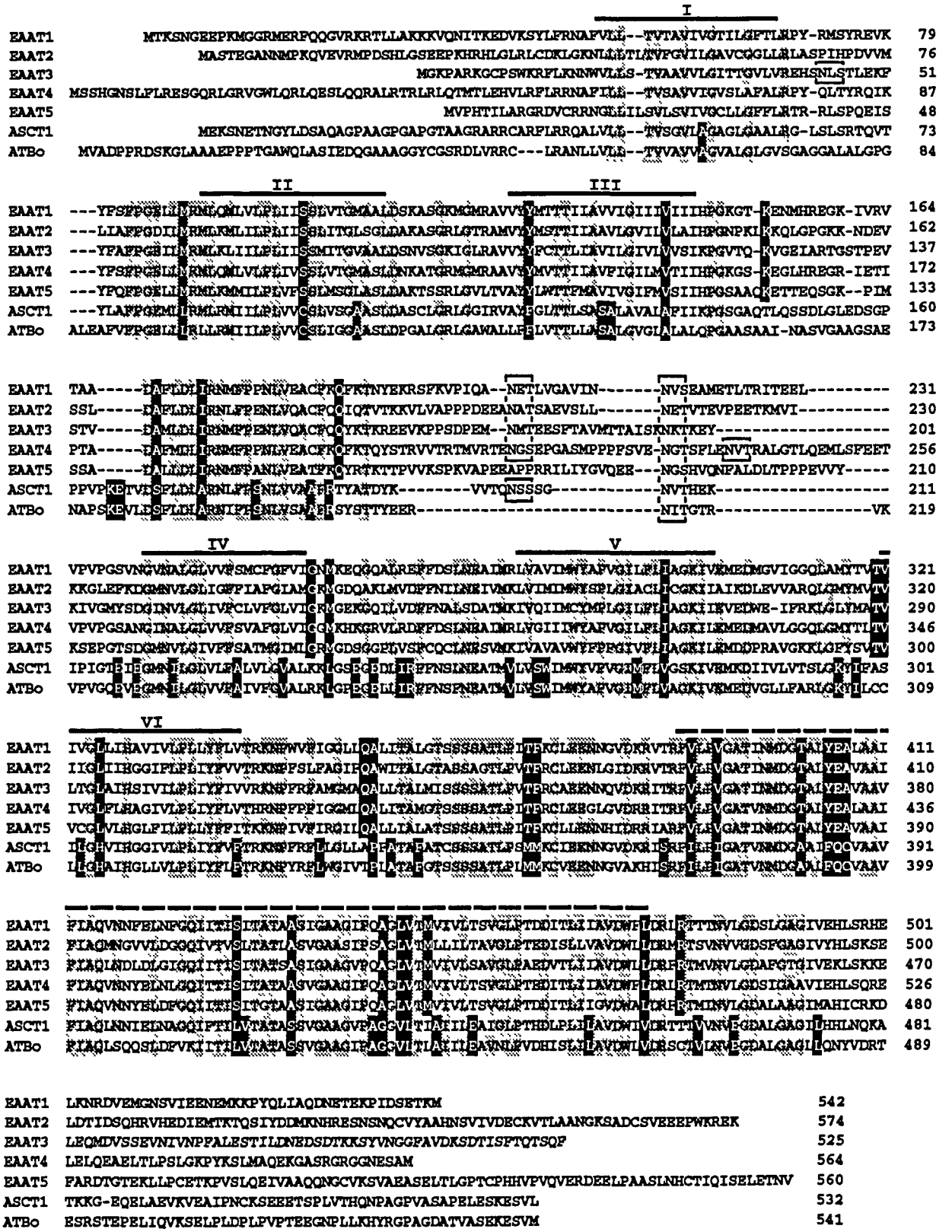


FIG. 5. Amino acid sequence comparison of excitatory amino acid transporter (EAAT) and related zwitterionic amino acid transporters. Alignment of amino acid sequence of 7 human transporters of this superfamily corresponds to that published by Arriza et al. (18) for EAAT1–5 isoforms. Amino acid residues present in at least 6 of listed sequences are indicated by gray boxes. Amino acid residues that are specific to glutamate transporters or zwitterionic amino acid transporters of this superfamily are in white on black boxes. Because of weak homology present in $NH_2$ and COOH termini of these transporters, conserved amino acid residues in those domains are not indicated. Straight lines over sequences indicate putative TM domains (I–VI). Dashed line over sequence delimits highly conserved, long hydrophobic stretch of amino acid residues with a controversial topology. Between TM III and TM IV, 2 or 3 potential *N*-glycosylation sites are conserved (open boxes). Dashes indicate gaps for sequence alignment.

TABLE 7. *Tissue distribution and transport characteristics of expressed EAAT and related zwitterionic amino acid transporters*

| Transporter | Tissue Distribution (Transcript Size) | Expression System | Substrates ($K_m$) | Pharmacology ($K_i$) | Cotransported Ligands | Ion Leak | Ligand-Gated Chloride Channel |
|---|---|---|---|---|---|---|---|
| EAAT1 | Brain (other tissues ?)[a] (~4 kb) | Oocytes[e] COS-7 cells (19) | L-Glu, L-Asp, D-Asp (15–20 μM) PDC (~30 μM) | SOS (~100 μM) DMG (~120 μM) LαAA (>1 mM) KA (>3 mM) | $aa^-$, (3) $Na^+$ (in) $K^+$ (out) (289) Electrogenic (19, 289) | Yes (246, 579) ($Na^+$) | Yes (?) (582) ($E_{rev}$ +9 mV) |
| EAAT2 | Brain[b] (~10 kb) | Oocytes[f] COS-7 cells (19, 285) HeLa cells[g] | L-Glu, L-Asp, D-Asp (10–20 μM) PDC (<10 μM) | KA (<60 μM) DMG (~0.7 mM) SOS (~1.2 mM) LαAA (>1 mM) | $Na^+$ (in), $K^+$ (out)[i] Electrogenic (19) | No (579, 583) | Yes (582, 583) ($E_{rev}$ +60 mV) |
| EAAT3 | Epithelia, brain, and other tissues[c] (~3.5 kb) | Oocytes[h] COS-7 cells (19) | L-Glu, L-Asp, D-Asp* (30–50 μM) PDC (~20 μM) | SOS (~150 μM) DMG (~0.25 mM) LαAA (>1 mM) KA (>3 mM) | $aa^-$, (2/3)† $Na^+$ (in) $K^+$, $OH^-$ (out) (246, 628) Electrogenic (19, 246) | Yes (246) | Yes (?) (582) ($E_{rev}$ +38 mV) |
| EAAT4 | Brain and other tissues[d] (~2.4 kb) | Oocytes (144) | L-Glu, L-Asp, D-Asp (2–3 μM) PDC (~3 μM) Lα-aa (~200 μM) | KA (>5 mM) | $Na^+$ (in) (144) $K^+$ (?) Electrogenic (144) | (?) | Yes (144) ($E_{rev}$ −22 mV) |
| EAAT5 | Retina (~3.5 kb) (other tissues ?) (18) | Oocytes (18) | L-Glu, L-Asp, D-Asp (13–64 μM) | PDC (6 μM) THA (1 μM) | $Na^+$ (in), $K^+$ (?) (18) | Yes (?) (18) | Yes (18) ($E_{rev}$ −20 mV) |
| ASCT1 | Ubiquitous ? (20, 488) (≤5, ≤4, ~2.5 kb) | Oocytes (20) HeLa cells (488, 541) | L-Cys (30 μM), L-Ala L-Ser, L-Thr, L-Val L-Glu | MeAIB (>10 mM) | $Na^+$ (in) (20, 488) $K^+$ (?) (20, 627) Electrogenic (20) | (?) | Yes (627) ($E_{rev}$ −21 mV) |
| ASCT2 (mouse) | Several tissues (311, 568) (no brain or liver) (~2.7 kb) | Oocytes (568) 3T3-L1 cells (311) | L-Ala, L-Ser, L-Cys, and L-Gln (20 μM) Branched aa° L-Glu (1.6 mM) | MeAIB (>1 mM) $aa^+$ (>1 mM) $aa^-$ (~1 mM) | $Na^+$ (in), $K^+$ (?) (568) Electroneutral (568) | (?) | No (?) (568) |
| ATB° | Epithelia and skeletal muscle (269) (no brain or liver) (~2.9 kb) | Oocytes and HeLa cells (269) | aa° | MeAIB (>5 mM) $aa^+$ (>5 mM) $aa^-$ (>5 mM) | $Na^+$ (in), $K^+$ (?) (269) Electrogenic (269) | (?) | Yes (?) (270) ($E_{rev}$ −30 mV) |

Transcript size and tissue distribution correspond to human transporters, except for ASCT2. Apparent $K_m$ values were obtained by different labs expressing corresponding transporters in *Xenopus* oocytes. Pharmacological characteristics of EAAT transporters and all the ligand channel characteristics correspond to those of human counterparts. * Apparent $K_m$ is dependent on membrane voltage (see text). † Two different reports (246, 628) showed different stoichiometry for EAAT3 transporter. Question marks denote either inconsistent data or not tested (see text for details). SOS, L-serine-*O*-sulfate; DMG, *trans*-(dicarboxyl)-2,4-methanoglutamic acid; LαAA, L-α-aminoadipate; KA, kainic acid; PDC, L-*trans*-pyrrolidine-2,4-dicarboxylic acid; THA, threo-β-hydroxyasparate; $aa^+$, dibasic amino acid; $aa^-$, dicarboxylic amino acid; aa°, zwitterionic amino acid. References are as follows: a) 19, 268, 491, 518; b) 19, 343, 382, 424, 523; c) 19, 245, 249, 382, 490; d) 144; e) 19, 115, 116, 225, 268, 289, 518, 543, 571, 582; f) 19, 571, 582,'583; g) 83, 424, 426, 523, 630; h) 19, 245, 246, 249, 581, 582; i) 19, 424, 583. Other references are given in parentheses.

transporters in the CNS has been studied at the protein level (85, 121, 298, 305, 461), largely confirming previous in situ hybridization analyses (205, 245). These studies showed that rat EAAT1 and EAAT2 are present in astroglial cells, whereas EAAT3 is present in neurons. Glial EAAT2 is distributed throughout the brain and spinal cord (most abundant in Bergmann glia in the cerebellar molecular layer); neuronal EAAT3 is also generalized, but it is more prominent in hippocampus than cortex and striatum and less abundant in cerebellum; and glial EAAT1 is most prominent in cerebellum (cerebellum >> hippocampus > cortex > striatum) (85, 298, 461, 581). Ultrastructural analysis revealed that glial EAAT1 is localized to processes that most probably envelop glutamatergic synapses, suggesting a role in synaptic plasticity (461). In contrast, glial EAAT2 localized to cell bodies and processes (461). Neural EAAT3 localized to axons, dendrites, and presynaptic terminals in the deep cerebellar nuclei, but in the cerebellar granule cells it is not expressed presynaptically (461). Astrocyte membranes facing nerve terminals, axons, and spines are higher in EAAT1–2 glutamate transporters than those facing capillaries, pia, or white matter (85). Interestingly, EAAT3 protein is present in, but not restricted to, glutamatergic neurons (e.g., some but not all cortical pyramidal neurons), and it is enriched postsynaptically within GABAergic Purkinje cells in cerebellum (461). This was confirmed by in situ hybridization studies (205, 581), where an additional localization of

EAAT3 to cholinergic α-motor neurons of the spinal cord was shown. These results indicate that neuronal EAAT3 is not the presynaptic glutamate transporter for all glutamatergic synapses and that it is also present in nonglutamatergic neurons. Additional glutamate transporters may be present presynaptically in many glutamatergic neurons. In this sense, the EAAT4 isoform may be a good candidate for those neurons in cerebellum. The presence of neuronal EAAT3 in GABAergic synapsis suggests that it could transport glutamate intracellularly as a precursor for GABA synthesis (461). The general role of EAAT1–3 isoforms in brain in the maintenance of low extracellular glutamate concentration has been addressed by partial and specific knockout of these isoforms (458) and the complete knockout of EAAT3 (416) and EAAT2 (544) (see sect. II*C8*). To our knowledge, human EAAT4 and EAAT5 distribution has been studied only by Northern analysis, showing an almost specific cerebellar and retinal localization, respectively (144). It is worth mentioning that the human EAAT5 has a putative synaptic localization: the COOH terminus of EAAT5 contains a sequence motif (Glu-Ser or Thr-X-Val-COOH) found in synaptic membrane proteins and that interacts in the yeast two-hybrid assay to PDZ (a modular protein-binding motif) domains of the postsynaptic density-95 protein (18).

The peripheral distribution of EAAT1 (brain > heart > skeletal muscle > placenta and lung in human tissues, Ref. 19; specifically expressed in brain for the rat, Ref. 518), EAAT3 (small intestine > kidney > brain > cerebellum, lung, placenta, heart; similar for human and rat tissues, Refs. 19, 245), EAAT4 (cerebellum > > placenta, for human tissues, Ref. 144) and EAAT5 (weak signals in liver and of different transcript size in skeletal muscle and heart from human tissues, Ref. 18) isoforms has been, to our knowledge, only addressed by Northern analysis. It is noticeable that rat EAAT1 seems to be specific to brain (518), whereas peripheral human tissues express this isoform (19). Kanai and Hediger (245) performed in situ hybridization studies with EAAT3 in the small intestine and showed that the transporter is expressed in epithelial cells. This, together with its expression in kidney, suggests a participation of this glutamate transporter in the reabsorption of anionic amino acids (see sect. II*C8*).

The tissue distribution of the zwitterionic amino acid transporters ASCT1, ASCT2, and ATB° has been examined by Northern blot analysis (20, 269, 488, 568). Human ASCT1 transcripts (~5, ~4, and ~2.4 kb; Ref. 20; and ~4.8, ~3.5, ~2.8, and 2.2 kb; Ref. 488) were detected in skeletal muscle, pancreas > brain > placenta > heart, lung, kidney, liver. The mouse ASCT2 transcript (Table 7) shows a complementary tissue distribution: lung, large intestine, kidney > skeletal muscle, testis and white adipose tissue (568). Expression of the two suspected transporter variants of system ASC (ASCT1–2) in liver and placenta is very low. If this low level of expression also occurs at the protein level, to our knowledge not yet studied, different ASCT variants or transporters not related to this superfamily may be responsible for the high system ASC transport activity present in these tissues (488) (see sect. II*C8*). The human ATB° transcript is present in epithelial tissues (placenta, lung > kidney, pancreas), very scarce in skeletal muscle, and absent, according to Northern analysis, in heart, brain, and liver. It has been proposed that ATB° corresponds to the apical (i.e., brush-border membrane) system B° (Ref. 269; see below) and is therefore expected to be expressed in small intestine, where this transport activity has been shown (329, 337, 515). Indeed, rabbit ATB° cDNA has been isolated from jejunum (270). It is worth mentioning that the tissue distribution of ATB° is similar to that of ASCT2, again favoring the hypothesis that both cDNA are species counterpart of the same gene. Immunolocalization studies to demonstrate the presence of ATB° in epithelial brush-border membranes are not yet reported.

### 2. *Transport properties*

The transport properties of the glutamate (EAAT1–5) and zwitterionic amino acid transporters (ASCT1–2 and ATB°) have been studied upon expression in oocytes or transfection into mammalian cells followed by both radioisotopic and electric measurements (see Table 7). Reconstitution studies from the expressed protein have been reported only for the glutamate transporter EAAT2 (424, 426, 630). All these transporters share several transport properties (see Table 7). *1*) The glutamate EAAT transporters are sodium cotransporters and potassium countertransporters. Potassium dependence (countertransport) has been demonstrated for all of these transporters, except EAAT4 and EAAT5, for which it has not been reported (18, 144). *2*) The zwitterionic amino acid transporters (ASCT1, ASCT2, and ATB°) are probably electroneutral sodium-dependent amino acid exchangers that do not interact with potassium (162, 627), but to our knowledge, the putative exchange mechanism of transport for ASCT2 and a role of potassium for ATB° and ASCT2 has not been properly tested. *3*) In addition to their transport mode of action, for EAAT1–5 and ASCT1 cumulative evidence has been obtained that they also have a chloride channel mode of action (144, 582, 583, 627). Very recent data also suggest that this channel activity might be associated with ATB° (270). To our knowledge, this has not been reported or tested for ASCT2, and the only available study shows no electric activity associated with this transporter (568) (see below).

Substrate specificity has been described for the EAAT isoforms and the zwitterionic amino acid transporters of this superfamily (see Table 7). In constrast to these zwitterionic amino acid transporters, EAAT transporters ex-

press high-affinity sodium- and potassium-dependent transport of L-glutamate (micromolar range). In contrast, the interaction of these transporters with zwitterionic amino acids (i.e., either as a substrate or as a *cis*-inhibitor) is of low affinity (millimolar range). All this information is consistent with a large body of accumulated knowledge on the native glutamate transport properties in cells, membrane preparations, synaptosomes, and purified transporters of neural origin (for review, see Refs. 251, 394). Interestingly, these EAAT isoforms do not interact with neurotransmitters that are substrates of the superfamily of sodium- and chloride-dependent transporters of neurotransmitters (e.g., GABA, dopamine, norepinephrine, serotonin) (reviewed in Ref. 252). The five glutamate transporter isoforms are stereospecific for glutamate but do not discriminate the enantiomers of aspartate, a characteristic of sodium-dependent glutamate transport activities in many tissues (185, 262, 483, 505, 513); only for human EAAT5 is the apparent $K_m$ for L-aspartate approximately fivefold lower than that for D-aspartate (18). The five glutamate transporters form a continuum of transport activities with a different tissue-specific distribution, and they are difficult to distinguish with the usual functional criteria, other than by their pharmacology (see below). Their activity corresponds to system $X^-_{AG}$, which represents various transport agencies that carry anionic amino acids, with the described characteristics, into different cells (41). Moreover, as expected for system $X^-_{AG}$ (41), threo-3-hydroxy-DL-aspartate (THA) is a competitive substrate of EAAT1–3 (19, 518). When the five human EAAT isoforms are expressed in oocytes, the highest affinity is shown by EAAT4 [apparent $K_m$ of 2–3 $\mu$M for L-glutamate, L- and D-asparate, and the analog L-*trans*-pyrrolidine-2,4-dicarboxylic acid (PDC)]; the other isoforms showed apparent $K_m$ values for glutamate in the range between 10 and 64 $\mu$M (18, 19). These $K_m$ values (and those shown in Table 7) obtained in oocytes should be interpreted with caution since they depend on the expression system used: human EAAT2 has an apparent $K_m$ for L-glutamate of 18 $\mu$M in oocytes (19), whereas for rat EAAT2 (i.e., GLT1) expressed in HeLa cells, the $K_m$ is 10 $\mu$M, and 2 $\mu$M when it is reconstituted in proteolisosomes (424). This latter value fits the affinity of L-glutamate when assayed in rat brain membrane preparations or in rat brain purified and reconstituted glutamate transporter (120, 255, 263, 425). Endogenous L-glutamate diluting the radiolabeled tracer, membrane lipid composition, posttranslational modifications, or other factors may affect the apparent affinity of these transporters in different expression systems (19, 424). Interestingly, the apparent $K_m$ values determined for rat EAAT1 in oocytes when measured by radiolabeled glutamate (~80 $\mu$M) are higher than those based on measurement of the induced glutamate-dependent current (11 $\mu$M) (289), favoring the impression that endogenous substrate diluting the radiolabeled substrate increases the apparent $K_m$ values in those studies. It is worth mentioning that for human EAAT3, dependence of the apparent $K_m$ on membrane potential has been described (249).

Pharmacological studies helped to distinguish between the transport activity of the five isoforms (see Table 7). Sequence comparisons strongly indicate that human EAAT1–3 corresponds to the rat GLAST1 (96% amino acid sequence identity; Ref. 518), rat GLT1 (95% amino acid sequence identity to the corrected sequence; Refs. 253 and 424), and rabbit EAAC1 (92% amino acid sequence identity; Refs. 245, 249). Because of this, in the present review, they are considered to be counterparts of the glutamate transporter isoforms in different species. In contrast, pharmacological similarities between species are less clear. Interaction of different inhibitors with the transport activity of the human EAAT isoforms is shown in Table 7. Human EAAT1 and EAAT3 show a similar pharmacology, which is different from that of human EAAT2 (19), EAAT4 (144), and EAAT5 (18). Human EAAT2 is the isoform sensitive to dihydrokainic acid (DHK) and kainic acid (KA), insensitive to L-$\alpha$-aminoadipate (L$\alpha$AA), and relatively insensitive to L-serine-*O*-sulfate (SOS); human EAAT1 and EAAT3 are highly sensitive to SOS and insensitive (i.e., $K_i$ >3 mM) to DHK, KA, and L$\alpha$AA; and human EAAT4 is the isoform that is sensitive to L$\alpha$AA and insensitive to DHK and KA ($K_i$ >3 mM). In contrast to the other EAAT isoforms, for which THA and PDC are competitive substrates, for human EAAT5 these analogs act as blockers ($K_i$ ~1–6 $\mu$M) and not as substrates (18). In constrast to the human EAAT transporters, rat GLT-1 (rat EAAT2 counterpart) and rabbit EAAC1 (rabbit EAAT3 counterpart) are very sensitive to L$\alpha$AA ($K_i$ in the micromolar range) (245, 424). These results suggest pharmacological differences between the human and other EAAT isoforms. Brain regional differences in pharmacology have suggested at least four glutamate transporters subtypes (454); this is consistent with the four mammalian brain EAAT transporter isoforms isolated.

The zwitterionic amino acid transporters of this superfamily share as general transport properties high affinity for zwitterionic amino acids and low affinity for L-glutamate and sodium dependence, whereas the potassium dependence is controversial (20, 269, 488, 541, 627). A weak potassium dependence was described initially for ASCT1 (alanine-induced current, Ref. 20) and ASCT2 (alanine uptake, Ref. 568) upon expression in oocytes. To our knowledge, potassium dependence for ATB$^0$ has not been examined. Later on, Zerangue and Kavanaugh (627) stated the contrary, i.e., that alanine transport (both influx and efflux) was independent on the external potassium concentration in oocytes expressing ASCT1 under voltage clamp. One explanation of these dissimilar results, obtained with electric or radiolabeled L-alanine uptake studies, within the same group could be that alanine transport

via ASCT1 is electroneutral, but sodium and the substrate evoked a chloride channel activity associated with ASCT1, which is thermodynamically uncoupled from the amino acid transport (627). It has been suggested that the sodium dependence of ASCT1 is not the result of sodium cotransport, since transport of L-alanine via ASCT1 is electroneutral and potassium independent, and the ligand-evoked chloride current shows a Hill coefficient of 1 for external sodium (627). In contrast, the electroneutral uptake of radiolabeled L-alanine via ASCT1 involves the electroneutral exchange of extracellular and intracellular amino acid substrates (627); influx and efflux of L-alanine gave a 1:1 flux stoichiometry with the substrate specificity of ASCT1. Interestingly, external sodium is needed for this exchange. Very recently, Ganapathy and Leibach (162) reported exchanger transport activity for ATB°, but a full paper is still lacking on this issue. In addition, a substrate-induced current that reverses at −30 to −40 mV has been associated with rabbit ATB° (270). These results offer a new view of the transport mechanisms of these zwitterionic amino acid transporters: *1*) electroneutral exchange of zwitterionic amino acid which is dependent on extracellular sodium; *2*) ligand-evoked chloride currents, which are thermodynamically uncoupled from the amino acid transport, as for the EAAT transporters of this superfamily; and *3*) lack of interaction with potassium. Interestingly, these zwitterionic amino acid transporters do not conserve the glutamate residue identified as crucial for potassium countertransport of the EAAT transporters of this superfamily (see sect. II*C7*). Additional studies are needed to clarify these transport mechanisms.

*1*) Does ASCT1 operate as an obligatory exchanger for a wide range of amino acid and sodium gradients through the plasma membrane? Unfortunately, in the Zerangue and Kavanaugh's study of the amino acid exchanger activity of ASCT1 (627), influx and efflux rates were only compared at a fixed concentration of external L-alanine and sodium; it is therefore possible that this exchange reflects ASCT1 transport near equilibrium and not a real obligatory exchanger mechanism. A similar transport mechanism, but concentrative, was described for system ASC in fibroblasts (76).

*2*) What is the role of sodium in the ASCT1 exchanger mode of action proposed by Zerangue and Kavanaugh (627)? Is the sodium ion really translocated through the membrane, or is its action like that of an allosteric modulator? Uptake measurements of $^{22}Na$ are needed to clarify this issue. Then, if sodium is translocated through ASCT1, what mechanism explains the lack of concentrative transport activity of ASCT1 located along the large sodium electrochemical gradient of the plasma membrane?

*3*) Is the exchange mechanism of transport of ASCT1 and ATB° extensive to ASCT2? It has been reported that mouse ASCT2 shows no electric activity evoked by amino acid substrates and sodium even in the presence of chloride (568). This suggests an electroneutral amino acid exchange mechanism like that of ASCT1, and a not very conspicuous ligand-evoked channel mode of action, but to our knowledge, amino acid exchange via ASCT2 has not been examined. On the other hand, the lack of electric activity of ASCT2 (627) might be a consequence of charge flux compensation between the transport mode of action of the carrier and a yet unknown chloride channel associated activity? If so, what is the electric activity of ASCT2 in a chloride-free system (i.e., extracellular chloride = 0 and chloride-depleted oocytes)?

*4*) Finally, is the ligand-evoked chloride channel activity associated with the glutamate transporters of this superfamily and to ASCT1 extensive to ASCT2 and ATB°? The ligand-evoked current associated with rabbit ATB° reverses at −30 to −40 mV (270). Is this a reflection of an associated ligand-evoked channel activity? If so, its ion selectivity might be different from the channel activity associated with the other members of this superfamily that tends to reverse current at the equilibrium potential of chloride in oocytes (i.e., −23 mV).

Transporters ASCT1 and ASCT2 upon expression in HeLa cells or oocytes have transport properties similar to system ASC (185) (see Table 7), i.e., high-affinity (micromolar range) and sodium-dependent transport for neutral amino acids (including small ones like alanine, serine, and cysteine) and interaction with anionic amino acids at pH <7.4 (i.e., the protonated amino acid species is probably the substrate), and insensitive to inhibition by dibasic amino acid and the analog MeAIB (20, 488, 541, 568). This suggested that these two carriers represent isoform variants of system ASC. Indeed, system ASC showed significant variability in substrate specificity; e.g., threonine is a better substrate than cysteine in rat liver, but the converse is true in the hepatoma cell line HTC (165, 196, 275, 569). Northern analysis showed a very low expression of ASCT1 and no expression of ASCT2 in liver, a tissue with high system ASC activity. This suggests that neither ASCT1 nor ASCT2 represents the liver system ASC transporter. Work by Kilberg's group aiming to identify a liver homolog of ASCT1–2 failed to isolate a new transporter cDNA (M. S. Kilberg, personal communication). System ASC is concentrative, voltage dependent, and electroneutral (185). It is necessary to clarify whether ASCT1 and ASCT2 mediate a concentrative transport (see above) of their substrates before ascribing ASCT1 and ASCT2 transporters to variants of system ASC.

The transport characteristics of ATB° upon expression in HeLa cells and oocytes, as well as the epithelial distribution of ATB° transcripts (269), suggested that this transporter corresponds to the epithelial system B°, the major apical sodium-dependent transport for zwitterionic amino acids with broad specificity (excluding methylated amino acids and dibasic and anionic amino acids) (329, 337, 515). The new view that ATB° and ASCT2 might be

species counterparts of the same transporter with an electroneutral amino acid exchange mechanism of transport (162, 270; V. Ganapathy, personnal communication) compromises the initial expected role of ATB° in the active epithelial uptake of neutral amino acids.

### 3. Stoichiometry

The stoichiometry of glutamate or zwitterionic amino acids and the corresponding coupled ions, as well as the participation of pH-changing ions in the transport cycle, varies among the members of the present superfamily. In general, for many cell types, glutamate uptake is electrogenic and driven by cotransport of sodium and countertransport of potassium with a first-order dependence on external L-glutamate and internal potassium and a sigmoidal dependence on external sodium, which suggests a stoichiometry of 1 glutamate:3 sodium:1 potassium (30, 263). In addition, movement of pH-changing ions (cotransport of $H^+$ or countertransport of $OH^-$) occurs during transport (63, 141, 392). In this instance, the stoichiometry of 1 glutamate:2 sodium:1 potassium:1 $OH^-$ would still be electrogenic. As discussed by Kanner (252), a stoichiometry of 1 glutamate:≥2 sodium is favored by direct experimental evidence obtained by kinetic and thermodynamic methods (141, 510).

The stoichiometry of the cotransported ligands of EAAT transporters has been examined for rat EAAT1 (289) and human and rabbit EAAT3 (246, 628) expressed in oocytes, and the models proposed are different for each. Zerangue and Kavanaugh (628) offered evidence that the neuronal human EAAT3 cotransports one glutamate, one hydrogen, and one sodium and countertransports one potassium, with a glutamate-to-charge ratio of 1:2 (2 positive charges accompany the movement of glutamate and in the same direction), and with this flux-coupling model, a transmembrane gradient of glutamate through the transporter of $10^6$ is predicted. This is based on the following.

*1*) Because of the uncoupled chloride channel activity associated with the expression of human EAAT3 in oocytes (582), this study was conducted in a chloride-free medium and chloride-depleted oocytes, or with oocytes clamped at chloride equilibrium potential (−25 mV) to avoid the contribution of this channel activity to the fluxes coupled to the transport of glutamate.

*2*) Flux of the pH-changing ion is thermodynamically coupled to transport, and it is not the consequence of permeation through the uncoupled chloride channel activity of the transporter (137, 144, 295, 582), because in voltage-clamp conditions uptake of glutamate resulted in intracellular acidification of the oocyte even with an inwardly directed electrochemical gradient for $OH^-$.

*3*) Most likely, hydrogen is cotransported with glutamate as a carboxylate ion pair, instead of the countertransport of $OH^-$, because transport of L-cysteine, a structurally related substrate that is transported as a neutral zwitterion (626), resulted in a clearly lower intracellular acidification than transport of an equivalent amount of glutamate. Interestingly, this is at odds with evidence that countertransport of anions (such as $OH^-$ or $HCO_3^-$) is responsible for the pH-changing activity of glutamate transport in salamander retinal glia cells (63).

*4*) Countertransport of potassium is coupled with glutamate transport because, in chloride-free medium and chloride-depleted oocytes expressing human EAAT3, superfusion of glutamate and sodium produced an inward current, and superfusion with potassium produced an outward current; both currents are inhibited by 5 mM KA, a competitive antagonist of EAAT isoforms (see sect. II*C2*). Changes in the reversal potential caused by altering glutamate and potassium membrane gradients are consistent with the countertransport of potassium and glutamate.

*5*) By applying the changes in the glutamate transport reversal potential due to varying glutamate and ion gradients (i.e., for $Na^+$, $H^+$, or $K^+$) to a zero-flux equation relating the membrane potential to the transmembrane ion gradients, the coupling coefficient for each substrate was similar to 1 glutamate:1 hydrogen:3 sodium:1 potassium.

*6*) Consistent with the previous data, the Hill coefficient for external sodium concentration at a fixed external glutamate concentration (10 $\mu$M) was between two and three, whereas this was not different from one when the external concentrations of glutamate, hydrogen, and potassium were varied.

*7*) This stoichiometry is consistent with a measured inward positive charge transfer of two during uptake of tracer L-glutamate (100 $\mu$M) under voltage clamp.

*8*) Finally, uptake of tritiated 1 $\mu$M L-glutamate in oocytes expressing human EAAT3 reaches a steady state of <10 nM external glutamate concentration, which with an estimated intracellular concentration of anionic aminio acids in oocytes of 12 $\mu$M (626) represents a transmembrane concentration gradient $>10^6$; this value is compatible with cotransport of three sodium per glutamate, but not with two sodium per glutamate.

Surprisingly, Zerangue and Kavanaugh's data (628) on human EAAT3 are different from those previously obtained in rabbit EAAT3-expressing oocytes by Hediger and co-workers (246). Initial studies aiming to elucidate the stoichiometry of rabbit EAAT3 revealed a Hill coefficient for external sodium that is dependent on the external concentration of glutamate, suggesting that the affinity for the sodium sites depends on the glutamate concentration; interestingly, the Hill coefficient was 2 at 200 $\mu$M glutamate and >2 at 10 $\mu$M glutamate (246). This covers the glutamate concentration range studied by Zerangue and Kavanaugh (628). Parallel measurements of $^{22}Na$ and [$^{14}C$]glutamate flux, intracellular pH changes, and substrate-evoked currents gave a stoichiometry of cotransport of one glutamate for two sodium ions, countertrans-

port of one potassium ion, and either cotransport of one hydrogen or countertransport of one hydroxide (246). Unfortunately, these studies were conducted without clamping the oocyte membrane potential. In any case, it will be interesting to determine the accumulation capacity of both EAAT transporters at different glutamate concentrations (this has not been reported for the rabbit counterpart), as well as $^{22}Na$ uptake measurements and determination of ion coupling coefficients at high glutamate concentration (e.g., 200 $\mu$M and up) for the human counterpart.

Consistent with Kavanaugh's stoichiometry for human EAAT3, the glial rat EAAT1 expressed in oocytes showed a Hill coefficient for the kinetics of external sodium and glutamate of approximately three and approximately one, respectively (289). In contrast to human EAAT3, the current associated with glutamate transport via rat EAAT1 was not changed by reducing external pH from 7.4 to 6.0, suggesting that glutamate is transported as an anion (289). These results allowed Stoffel's group (289) to propose a stoichiometry for rat EAAT1 of 1 glutamate, 3 sodium/1 potassium. This is at odds with the increased glutamate transport current obtained by decreasing the external pH in glial cells and in oocytes expressing the neuronal human EAAT3 (48, 628). In contrast, it is in agreement with data in fibroblasts and salamander glial cells (165, 482). This result might reflect the participation of different pH-changing ions for glutamate transporters of glial origin. In fact, studies of electrogenic uptake of glutamate into glial cells gave Hill coefficients between 2 and 3 (31, 482). In this sense, it will be very interesting to know if the stoichiometry and the pH-changing ions for the glial EAAT2 fit the data reported by Attwell and co-workers (63) in salamander retinal glia cells. To our knowledge, these studies have not been reported either for EAAT2, EAAT4, or the retinal EAAT5.

Initial data on the stoichiometry and ion dependence of the zwitterionic amino acid transport via ASCT1 and ASCT2 indicate variability of ion coupling among these transporters. Recent strong data supporting the idea that human ASCT1 is a sodium-dependent zwitterionic amino acid transporter exchanger (with a 1:1 stoichiometry of exchange) might help to clarify this issue (see above; Ref. 627). Because of the lack of precise information on the potassium dependence of ASCT2 and the mechanism of transport of ASCT2 and ATB$^0$, the suggested substrate stoichiometry (568) is at present speculative.

### *4. Mechanism of transport*

The mechanism of substrate translocation has been studied in membrane preparations of neural origin by Kanner's group (for review, see Ref. 252), for the expressed rabbit and human EAAT3, human EAAT2, and human ASCT1 (246, 249, 583, 627). Studies with synaptic plasma membrane vesicles from rat brain demonstrated that influx or efflux of glutamate is coupled to efflux or influx of potassium, respectively (261); the same situation has been demonstrated with salamander retinal glia cells (23, 529). In addition, in the absence of potassium, the glutamate transporter catalyzes exchange of its anionic amino acid substrates (255). This suggested that the glutamate translocation step is distinct from that of potassium. The glutamate transport cycle occurs in two parts: *1*) translocation of sodium and glutamate, and *2*) reorientation of the binding sites upon binding and translocation of potassium (252). When a comparison was made of the ion dependence of net flux with that of exchange, the binding order of the substrates during influx was shown as follows (255, 425): *1*) an ordered binding of the coupled two or three sodium ions before the binding of one glutamate ion to the extracellular face, *2*) translocation of the complex, *3*) release of glutamate and the sodium ions (it is not clear whether the release or binding at cytosolic face is also ordered or random), *4*) binding of potassium on the inside, and *5*) translocation and release of potassium to start a new cycle. If necessary, the glutamate transport-coupled pH-changing ions could be translocated concomitantly with either glutamate (i.e., hydrogen) or potassium (i.e., hydroxide) steps (252). Additional evidence for the translocation of sodium and potassium ions in different steps comes from the recent demonstration that rat EAAT2 Glu404Asp mutant is able to mediate exchange of D-aspartate and sodium but not countertransport of potassium (266). The kinetics of human EAAT2 have been examined upon expression in oocytes by analysis of nonlinear capacitance (i.e., pre-steady-state or transient currents) (583), after the pioneer work of Wright and coworkers (411, 412), who aimed to analyze the conformational changes and kinetic properties of the sodium/glucose cotransporter. Human EAAT2 transient currents are compatible with the free carrier being in voltage-dependent equilibrium with the sodium-transporter complex and to a charge movement due to the binding of sodium to a site of the carrier within the membrane electric field (583). Again, EAAT isoforms show different mechanisms of transport, since these currents are not detectable with rabbit or human EAAT3 expressed in oocytes (see below; Refs. 246, 249). Analysis of the charge movement estimated a glutamate turnover of 4–27 $s^{-1}$ over the voltage range 0 to −140 mV (583). Interestingly, these values are similar to those estimated with reconstituted glutamate transporters from rat brain, which were the basis for the cloning of rat EAAT2 (120). In contrast, these values are smaller than those obtained with salamander retinal glia cells ($>10^3$ $s^{-1}$) (482). Again, this most probably reflects that these cells express EAAT transporters other than EAAT2 (e.g., the EAAT5 isoform).

Hediger and co-workers (246, 249) examined the mechanism of transport for the rabbit and human neu-

ronal EAAT3 glutamate transporters. Expression in oocytes of these two EAAT3 counterparts by two independent labs demonstrated that the reverse mode of action (glutamate efflux; potassium influx) is a true reversal of the overall forward reaction (246, 628); thus both reactions have the same stoichiometry, basic mechanism of transport, and rate-limiting step (246), in agreement with the model proposed by Kanner (252). Pre-steady-state currents, substrate-specific current-voltage relationship, and sodium Hill equation-extracellular glutamate concentration relationship studies with human and rabbit EAAT3 expressed in oocytes (246, 249) allowed Hediger and coworkers to propose that *1*) at low extracellular sodium concentration (less than $K_m$) binding of sodium to the extracellular face of the transporter becomes rate limiting. *2*) At high extracellular sodium concentration (more than $K_m$), the rate-limiting translocation step depends on the extracellular L-glutamate concentration. At low concentration (less than or equal to mean affinity constant; the apparent L-glutamate affinity depends on the membrane voltage, Refs. 249, 246), L-glutamate binding to the extracellular face becomes rate limiting, whereas at high concentration of extracellular glutamate (more than mean affinity constant), the charge translocation step becomes rate limiting (i.e., translocation of the fully loaded carrier, the carrier plus L-glutamate plus 2 sodium ions). These results are consistent with previous studies on the high-affinity L-glutamate transport in renal brush-border membrane vesicles (208). In addition, cooperativity of sodium and glutamate binding for rabbit and human EAAT3 strongly suggests an ordered mechanism of binding: first one sodium binds with low affinity, second glutamate binds, and third the second sodium binds with high affinity. The transport cycle then progresses as in the model of Kanner (252). The authors hypothesize that the sodium leak (i.e., transport of sodium in the absence of glutamate) (see Fig. 6) through EAAT3 is a consequence of the translocation of the carrier with two sodium ions bound (246). All this suggests that the mechanism of the glutamate transport cycle is different for the neuronal and renal EAAT3 transporter (246, 249) and the glial EAAT2 transporter (252). In one aspect, the model proposed by Hediger's group for EAAT3 is in conflict with the suggestion that this carrier transports glutamate as a carboxylate ion pair together with one hydrogen ion, which acts as the pH-changing ion (628). Human and rabbit EAAT3 lack significant current relaxation in response to voltage jumps (246, 249). This suggests that the empty EAAT carrier is electroneutral (i.e., any conformational change of the carrier during the transport process does not involve movement of charge residues within the membrane electric field) and that the translocation complex (i.e., carrier plus glutamate plus 2 $Na^+$) has a positive charge and the relocation complex (i.e., carrier plus $K^+$ plus $OH^-$) is electroneutral. It will be interesting to know the kinetic behavior of EAAT3 using cysteine as a substrate, the strategy used by Zerangue and Kavanaugh (628) to identify hydrogen as the pH-changing ion in EAAT3, and the behavior of EAAT3 (e.g., pre-steady-state currents, potassium-specific current-voltage relationship, and potassium Hill equation) in the reverse mode of action (i.e., absence of glutamate and presence of potassium in the external medium).

### 5. *Ligand-gated chloride channel activity associated with the transporters*

As stated in the introduction to this section, for the human EAAT1–5 isoforms and the human zwitterionic amino acid transporter ASCT1, evidence for a mode of action as a sodium/amino acid-gated chloride channel has been offered by Amara's and Kavanaugh's groups (18, 144, 582, 583, 627; for review, see Ref. 507). In a recent review, Wright et al. (609) argued that this, in addition to a mode of action as water channel of the sodium-glucose SGLT1 cotransporter and water cotransport of SGLT1 and GAT1, and sodium leak by glutamate transporters and SGLT1, GAT1, and NET1, is indicative of the multifunctional (i.e., cotransporters, uniporters, channels, and water transporters) behavior of these cotransporters.

Let us examine the evidence for the sodium/amino acid-gated chloride channel activity of human glutamate EAAT1–5, rat EAAT2, and human ASCT1 transporters (18, 144, 266, 582, 627).

*1*) The initial observation was that the cotransporter-coupled currents were larger than expected for the cotransporter density and turnover number, i.e., the current exceeds the charge movement due to the amino acid transport. In chloride-depleted conditions or at the chloride equilibrium potential (−23 mV in oocytes), the current due to the transport mode of action could be estimated and would represent, at a membrane potential of −60 to −80 mV, only 5% of the total current elicited by glutamate and sodium in oocytes expressing EAAT4 (144) and varies from 50 to 73% in oocytes expressing human EAAT1–3 (582). In chloride-depleted conditions, glutamate did not induce measurable current in oocytes expressing human EAAT5 (18). Thus it appears that currents elicited by glutamate and sodium in EAAT5 are due primarily to the chloride conductance. For human ASCT1, with an electroneutral mode of transport, ~100% of the ligand-evoked current is because of chloride conductance (627).

*2*) In steady-state flux condition measurements, the reversal potential ($E_{rev}$) evoked by the amino acid and sodium due to the expression of the transporters fits with the proportion of chloride currents and the electrogenicity due to the amino acid transport activity (144, 582, 627, 18) (see Table 7): $E_{rev}$ values for EAAT4, EAAT5, and ASCT1 are very close to the chloride equilibrium potential in oocytes, whereas for EAAT1–3, $E_{rev}$ is within a positive

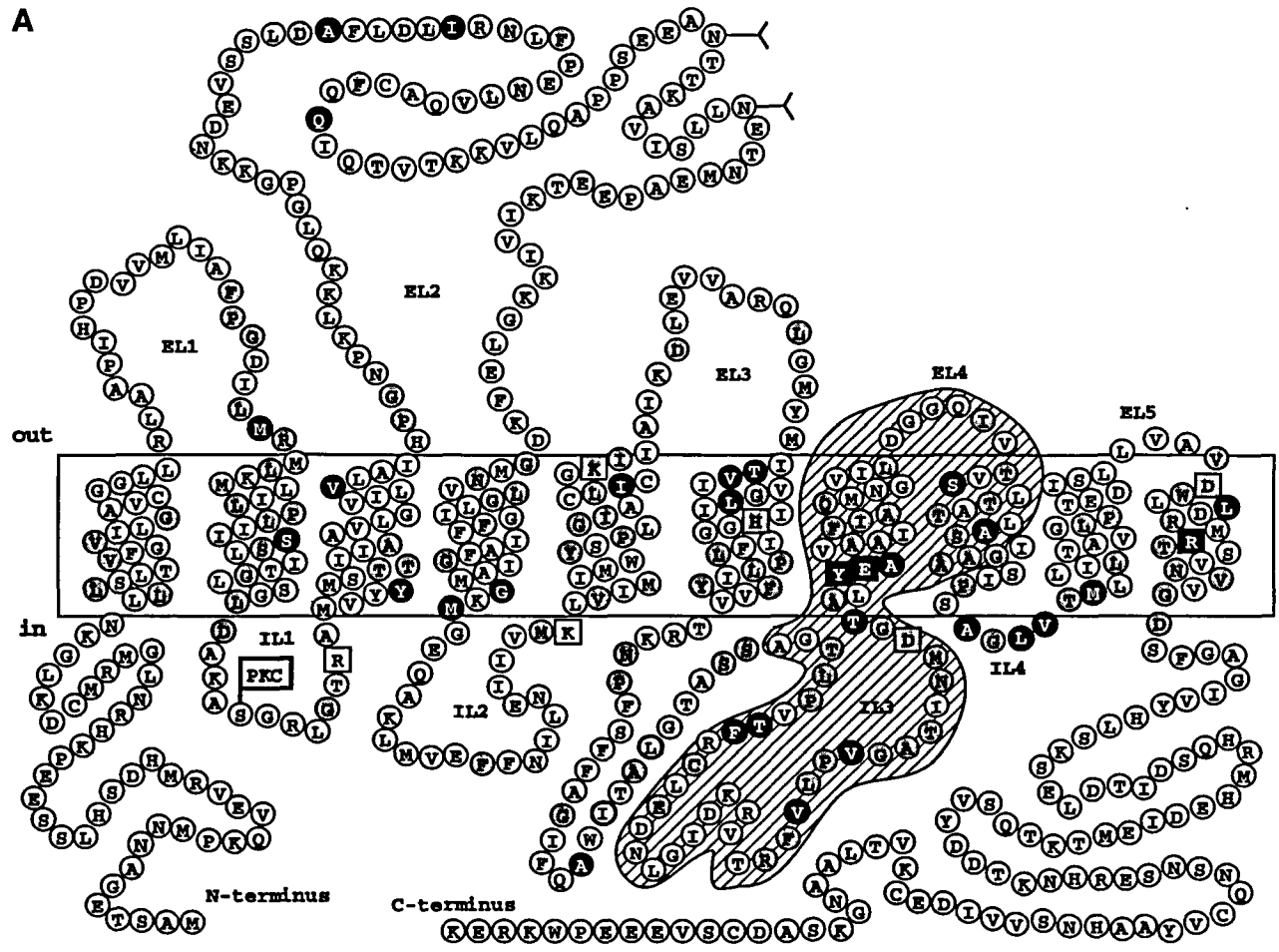


FIG. 6A. 10 TM transmembrane topology model for rat EAAT2 transporter. EL and IL loops are numbered, according to model proposed by Slotboom et al. (498). Amino acid residues conserved in all known transporters of this superfamily are indicated in gray circles, and residues that are specific for EAAT transporters are indicated in white over a black circle. Nine residues (in IL1, IL2, TM V, TM VI, IL3, TM VII, and TM X) and two glycosylated (Y) Asn residues in EL2 are marked by a square, indicating homologous residues that, after analysis by site-directed mutagenesis studies, have been shown to be critical for transport activity (see text for details). Shaded area delimits protein segment involved in kainate binding for human EAAT2 (571). To our knowledge, gene structure of rat *EAAT2* has not been reported. Coding region of human *EAAT2* gene is composed of 10 exons (360; not yet accessible in data bases). Human *EAAT1* gene is composed of 10 exons (accession numbers in NCBI: Z31713, Z31703-Z31710; W. Stoffel, M. Dueker, R. Mueller, and K. Hofmann).

range of membrane potential. The lowest chloride conductance contribution is found with EAAT2, for which current reverses only at +60 mV.

*3*) The chloride current is thermodynamically uncoupled from the amino acid flux via these transporters (18, 144, 582, 627). Thus, for all these transporters, radiolabeled amino acid flux is independent of the chloride current direction and the magnitude of the anion flux when substituting chloride, and for EAAT4 and ASCT1, it is largely or totally independent of the membrane potential.

*4*) The chloride conductance is evoked by sodium and the amino acid substrate (18, 144, 582, 627), and with identical apparent affinities as in the transport mode of action of the corresponding transporters (144, 582, 627); kinetic analysis of the amino acid flux via EAAT5 has not been reported.

*5*) For all these transporters, the sodium/amino acid-evoked chloride conductance exhibits the same chaotropic selectivity sequence: $SCN^- > NO_3^- > I^- > Cl^-$ (144, 582, 627); for human EAAT5, only the partial sequence $NO_3^- > Cl^-$ has been reported (18).

What is the nature of this sodium/amino acid-evoked chloride current? All the data could be interpreted as an intrinsic chloride channel activity of these transporters gated by sodium and the amino acid or, alternatively, as the induction, via direct or indirect interaction, of a silent chloride channel of the oocyte. The ion selectivity of the chloride conductance associated with these transporters

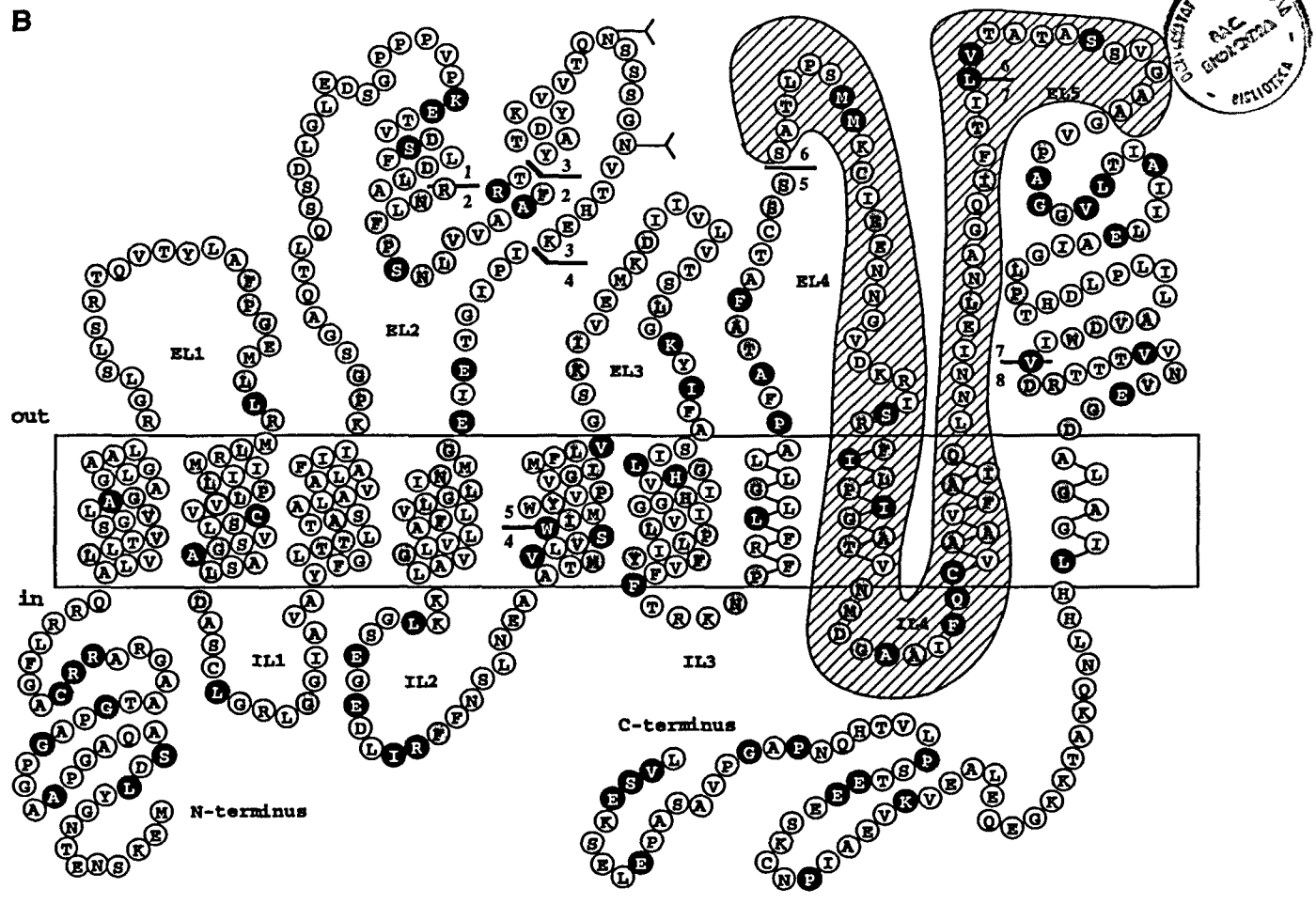


FIG. 6B. 6 TM $\alpha$-helix plus 4 TM $\beta$-sheet transmembrane topology model for human ASCT1 transporter. Amino acid sequence presented corresponds to that of human ASCT1. EL and IL loops are numbered according to model proposed by Wahle and Stoffel (585) for rat EAAT1. Amino acid residues conserved in all known transporters of this superfamily are indicated in gray circles, and residues that are specific for zwitterionic transporters are indicated in white over a black circle. Y, glycosylated residues. Shaded area delimits protein segment homologous to that involved in kainate binding for human EAAT2 (571). Exon boundaries within putative protein sequence are indicated, and exons are numbered (214).

is different from that of the endogenous calcium-dependent chloride channel activity of the oocytes, and it is not inhibited by typical oocyte chloride channel blockers (144, 582). These data indicate that the chloride channel conductance associated with these transporters is not due to activation of known endogenous chloride channels of the oocytes. Interestingly, for EAAT4, the $V_{max}$ of transport for radiolabeled L-glutamate is higher (<2-fold) than that for L-aspartate, whereas the maximum current of the associated chloride channel for L-aspartate is higher (3-fold) than that for L-glutamate (144). This has been interpreted as showing that gating of the channel occurs after binding of the sodium ions and the amino acid, and the different size of L-glutamate and L-aspartate allows a larger chloride flux in the latter case (144, 582).

In our view, however, there is still room for activation of an endogenous silent chloride channel. It is conceivable that an intermediate complex of the amino acid transport cycle activates an endogenous silent chloride channel. In this hypothesis, the identical ion selectivity of this chloride channel activity for many of the transporters of this family would reflect the activity of a single type of channel, and the different magnitude of the chloride channel activity would be due to the activation of a differential number of chloride channels by these transporters. In this instance, the differential chloride current due to L-aspartate and L-glutamate in EAAT4-expressing oocytes might indicate that activation of the chloride channel occurs through interaction with a particular intermediate complex of the transport cycle that would become more represented in the steady-state obtained with L-aspartate than the one obtained with L-glutamate. This transport complex might be the translocating complex (carrier plus sodium/amino acid). Notice that the associated chloride